DEVELOPMENT OF ANALYTICAL METHODS AND REFERENCE MATERIALS FOR CYANOBACTERIAL TOXINS

by

Christie Rose Hollingdale

Submitted in partial fulfilment of the requirements
for the degree of Master of Science

at

Dalhousie University
Halifax, Nova Scotia
May 2013

DALHOUSIE UNIVERSITY

DEPARTMENT OF CHEMISTRY

The undersigned hereby certify that they have read and recommend to the Faculty of Graduate Studies for acceptance a thesis entitled "DEVELOPMENT OF ANALYTICAL METHODS AND REFERENCE MATERIALS FOR CYANOBACTERIAL TOXINS" by Christie Rose Hollingdale in partial fulfilment of the requirements for the degree of Master of Science.

Dated: May 16, 2013

Research Co-Supervisors: _____

_____

Readers: _____

_____

_____

DALHOUSIE UNIVERSITY

DATE: May 16 2013

AUTHOR: Christie Rose Hollingdale

TITLE: DEVELOPMENT OF ANALYTICAL METHODS AND REFERENCE MATERIALS FOR CYANOBACTERIAL TOXINS

DEPARTMENT OR SCHOOL: Department of Chemistry

DEGREE: MSc CONVOCATION: October YEAR: 2013

_____

Signature of Author

TABLE OF CONTENTS

LIST OF TABLES

LIST OF FIGURES

ABSTRACT

Cyanobacterial toxins present a real and growing threat to humans and animals due to the projected increases in algal blooms resulting from increasing global temperature and pollution. Wild animals, livestock, pet animals and humans can be poisoned from contaminated drinking water. With the discovery of cyanobacterial toxins present in nutritional supplements, a new concern looms over consumers with threats of neurotoxin and hepatotoxin related damage from exposure to these products. To this end, work on the development of a freeze dried algal reference material was pursued for future use in environmental and nutritional supplement analysis. The first stage of the project was to prepare needed calibration standards, starting with homoanatoxin-a, a homologue of the highly neurotoxic anatoxin-a compound. The resulting reference material (RM-hATX) had a homoanatoxin-a concentration of 20.2 ± 0.7 μM, and proved to be stable while stored at temperatures of -80°C. Reference samples for dihydro and epoxy analogues of anatoxin-a and homoanatoxin-a were then prepared by semi-synthesis. The second stage of the project was the development of new analytical methods for the anatoxins. A derivatization reaction in which dansyl chloride was coupled with a novel cleanup step produced anatoxin derivatives suitable for liquid chromatography (LC) with mass spectrometry (MS) or fluorescence detection (FLD). Limits of quantitation were 60 ng L^{-1} and 1.6 μg L^{-1} for the developed LC-MS/MS and LC-FLD methods, respectively, with the limit of quantitation significantly better than that of a previously developed method for the underivatized toxins based on HILIC-MS/MS. Quantitative results for anatoxins in various algal samples using all three methods of analysis of were compared and it was found that there were no significant differences between the three methods. Unfortunately, experiments showed that the various toxin analogues did not elicit equimolar responses in either LC-MS/MS or LC-FLD, thus indicating the importance of having individual calibration standards for quantitative analysis. The LC-MS/MS and LC-FLD methods were paired with a previously developed method for the analysis of hepatotoxic microcystins to screen a small number of nutritional supplement samples for cyanobacterial toxins. Microcystins were detected in all five *Aphanizomenon flos-aquae* samples examined. This method involved a fifteen-fold pre-concentration using a solid phase extraction cartridge, which gave a 98% recovery of microcystins. The third phase of the project was the preparation and testing of a preliminary algal matrix reference material as a feasibility study for the eventual production of a CRM. After selecting various algal cultures and samples that could be blended together, a freeze dried algal reference material was prepared and packaged. This material (RM-BGA) was then characterized using several methods including the two new dansylation-based procedures.

LIST OF ABBREVIATIONS USED

ε	molar extinction coefficient
3-Me-Pip	3-methylpiperidine
AcOH	acetic acid
ADDA	3-amino-9-methoxy-2,6,8-trimethyl-10-phenyldeca-4,6-dienoic acid
ADHD	attention deficit hyperactivity disorder
ATX	anatoxin-a
ATXs	anatoxins
BGA	blue-green algae (cyanobacteria)
BMAA	β-methylamino-L-alanine
CE	collision energy
CFIA	Canada food inspection agency
CLND	chemiluminescence nitrogen detector
COSY	correlation spectroscopy
CRM	certified reference material
CYNs	cylindrospermopsins
DNS	dansyl
DNS-Cl	dansyl chloride
DP	declustering potential
DPT	Dietrich provisional tolerance
ELISA	enzyme linked immunosorbent assay
EPI	enhanced product ion
ER	enhanced resolution
ESI	electrospray ionization
FA	formic acid
FAB-MS	fast atom bombardment - mass spectrometry
FLD	fluorescence detection
Fmoc	9-fluorenylmethyl chloroformate
hATX	homoanatoxin-a
HeCd	helium cadmium
HILIC	hydrophilic interaction liquid chromatography
i.d.	internal diameter
i.p	intraperitoneal
IDA	information dependent acquisition
IS	internal standard
ISO	International Organization for Standardization
LC	liquid chromatography
LC-FLD	liquid chromatography – fluorescence detection
LC-MS	liquid chromatography – mass spectrometry
LCT_{50}	lethal concentration and time
LD_{50}	median lethal dose
LLE	liquid-liquid extraction

LOD	limit of detection
LOQ	limit of quantitation
LU	luminescence units
$[M+H]^+$	protonated molecule
MAC	maximum allowable concentration
MCs	microcystins
MeCN	acetonitrile
MeOH	methanol
MHz	megahertz
MRM	multiple reaction monitoring
MS/MS	tandem mass spectrometry
NBD-F	4-fluoro-7-nitro-2,1,3-benzoxadiazole
NMR	nuclear magnetic resonance
NOD	nodularin
NRC	National Research Council
nd	not detected
OR	Oregon regulation
Pip	piperidine
ppm	part per million
PSP	paralytic shellfish poisoning
Pyr	pyrrolidine
qNMR	quantitative nuclear magnetic resonance
RDI	recommended daily intake
RM	Reference Material
RSD	relative standard deviation
SD	standard deviation
SEM	scanning electron microscope
S/N	signal to noise ratio
SR	Switzerland regulation
SRM	selected reaction monitoring
STXs	saxitoxins
TFA	trifluoroacetic acid
TOCOSY	total correlation spectroscopy
UV	ultraviolet

ACKNOWLEDGEMENTS

I am very fortunate to have the assistance of many people throughout my graduate studies. Firstly, I would first like to thank and recognize my Graduate Studies supervisors, Dr. Michael Quilliam and Dr. Robert White for the encouragement, support, guidance and patience extended to me over the past two years. Secondly, I want to thank my supervisory committee, Dr. Alan Doucette and Dr. Stuart Grossert for their advice, support and helpful discussions.

I would also like to thank colleagues and staff at the National Resource Council (NRC) in Halifax who provided practical advice and assistance, including: Krista Thomas for instrumental maintenance and instruction, as well as her continuous support and encouragement throughout my graduate studies; Nancy Lewis for acquiring algal samples that were critical to isolating respective toxins; Marie Tremblay for the preliminary work she performed on dansyl reactions; Dr. Khalida Berki for training on LC-FLD, LC-MS, LC-UV, as well as assisting in all areas during the first four months of my graduate research; Dr. Pearse McCarron and Kelly Reeves for their help in preparation of the freeze dried reference material; Sheila Crain for running NMR for homoanatoxin-a characterization; Bill Hardstaff for his ampouling expertise, which was crucial in the six month stability study for homoanatoxin-a; David O'Neil for scanning electron microscopy; Floyd Toll at the NRC in Ottawa who performed particle size analysis, as well as Sabrina Giddings, Pat Leblanc, Ruth Perez, Elliot Wright, and Elliott Kerrin who

were a wonderful team to work with, and made for an incredible and enjoyable experience at the NRC.

I would like to thank Tara Tovstiga for her partnership in the White lab, as well as the support of family and friends throughout my graduate studies.

Finally, I would like to thank the NRC and the Ontario Ministry of the Environment for funding my graduate research. In addition, I was grateful for funding from Sepracor Canada and Dalhousie Faculty of Graduate Studies, which allowed me to present results from my first year of research at the 95th Canadian Chemistry Conference and Exhibition in Calgary, Alberta. Last, but certainly not least, I would like to thank Dalhousie University Department of Chemistry for the honour of awarding my work the Douglas E. Ryan Prize.

CHAPTER 1 INTRODUCTION

Toxins produced by cyanobacteria present a potential danger lurking in lakes, rivers and drinking water [1]. The toxins of highest concern are neurotoxins, which have been linked to extensive animal deaths [2–4] upon accidental exposure, and hepatotoxins, which have caused both human [5, 6] and animal death. The occurrence of cyanobacterial toxins in water is expected to increase [7], along with resulting deaths. From a public health safety standpoint, proper detection methods are required to screen and quantify water and algae samples. In this thesis, analytical methods for the detection and quantitation of cyanobacterial toxins have been developed and applied to a feasibility study on the development of an algal matrix reference material.

1.1 Cyanobacteria

Cyanobacteria (also known *Cyanophyta* or blue-green algae) are a diverse group of prokaryotes capable of photosynthesis [8]. These gram-negative autotrophs have been found in some of the harshest environments, ranging from sub-zero temperatures to hot springs at temperatures of 70°C [9]. Considered to be some of the most ancient organisms of life, cyanobacteria were responsible for oxygenation of the troposphere, which was of considerable evolutionary significance [10].

Most cyanobacteria possess gas vacuoles that allow cells to float near the surface of water, facilitating access to light for photosynthesis [11]. When eutrophic conditions are present, cyanobacteria can fix nitrogen, forming ammonia [12]. With low levels of dissolved oxygen and high levels of leached phosphorus from sediments, some water

bodies may be naturally eutrophic, while other lakes, rivers and reservoirs become eutrophic due to human actions [7]. Not surprisingly, excessive use of fertilizers and improper disposal of wastes in aquatic environments often results in algal blooms. Studies of North American lakes found that 48% were eutrophic [7]. Indeed, the rise in global temperature, as well as increases in nitrate and ammonia rich conditions have allowed cyanobacteria to reproduce at exponential proportions around the world [13]. A good example of a local incident was in Yarmouth County, Nova Scotia, when in 2011 extensive algal blooms appeared in several lakes contaminated with animal wastes from mink farming [14].

Algal blooms often have a colour and consistency similar to that of pea soup. Sunlight is unable to penetrate the thick mass, and the blooms can choke out life beneath the water's surface. Described as a mix of moldy potatoes and sulfur [5], the unsavory smells accompanying cyanobacteria blooms are displeasing to the eye and nose. Moreover, a study in the Czech Republic found up to 70% of algal blooms are toxic [1]. Very recently, major news networks have reported high levels of cyanobacterial toxins in lakes of every Canadian province [15, 16]. Despite the offensive sight and smells, many humans and animals have been poisoned by the various toxins produced by cyanobacteria [5, 17–22]. The increased frequency of toxic algal blooms is of direct concern to the safety of drinking water, as well as outdoor recreational activities for humans and animals.

As a potential source of protein and nutrients, dry cyanobacteria contain approximately 40% protein by mass, have desirably high fatty acid concentrations [23],

and are possibly a good source of vitamin B_{12}, although reliable data have yet to be published supporting this claim. Cyanobacteria are of interest to the natural health and supplement industries. The high prevalence of toxic cyanobacterial blooms, however, increases the chances that algal nutritional supplements are contaminated with toxins, creating a serious risk to consumers.

Recent findings in a German study found that almost 90% (8/9) of the *Aphanizomenon flos-aquae* (*A. flos-aquae*) supplements tested contained cyanobacterial toxins [24], while a recent Italian study detected cyanobacterial toxins in all 11 supplements tested [25]. This demonstration of widespread toxin contamination of *A. flos-aquae* pills in Italy and Germany demands affirmative action from regulatory agencies, as well as accountability from the natural health and supplement industries.

1.2 Incidents of Cyanobacterial Toxin Poisoning

In 1878, cyanobacterial poisoning of livestock on Lake Alexandria, Australia was documented in *Nature* by Georges Francis [26]. Since this first published account, much progress has been made within the field of cyanobacterial toxins. Despite the large amount of current information, ongoing diligent research is important to discover and characterize new toxins, which present a real concern for the health of humans and livestock.

Cyanobacterial toxins are secondary metabolites that are biosynthesized within the cells of certain species of cyanobacteria [5]. They are produced for three possible reasons [27]:

i. avoidance of consumption by zooplankton and higher level organisms;
ii. protection of the organisms population and domination over other nontoxin-producing cyanobacteria;
iii. using cell signal alleopathy with chemotaxy (movements dependent on chemical signals) to develop trophic relationships with surrounding organisms.

The structures of cyanobacterial toxins range from simple alkaloids to complex cyclic peptides and polycyclic compounds [5] (structural details are given in sections 1.2.2 and 1.2.3). From a human health standpoint, the water soluble toxins pose the greatest threat to drinking and recreational water, while lipid soluble toxins can cause widespread shellfish poisonings that have resulted in human illness and death [5]. Cyanobacterial neurotoxins and hepatotoxins pose the greatest threat to the safety of drinking water. Anatoxins (ATXs) and saxitoxins (STXs) are typical cyanobacterial neurotoxins, while the group of cyanobacterial hepatotoxins includes cylindrospermopsins (CYNs) and microcystins (MCs). Another neurotoxin, β-methylamino-L-alanine (BMAA), has been implicated in the onset of amyotrophic lateral sclerosis (ALS) [28]. While the occurrence of BMAA has been reported in some cyanobacteria [29], there is currently a great deal of debate regarding its wide-spread occurrence [30–34], and more research is required before any conclusion can be drawn.

Paralytic shellfish poisoning (PSP) toxins produced by both marine dinoflagellates and cyanobacteria can accumulate in shellfish. Consumption of contaminated shellfish can result in onset of symptoms and death; notable paralytic shellfish poisonings in humans [5] date back to 1793 [35]. Perhaps the most notable occasion of STX poisoning from cyanobacteria occurred in 1990, when more than 1000 livestock died after drinking from the Darling River in Australia [5]. Poisoning incidents in Canada led to the introduction of the first screening program for PSP toxins in the late 1940s [5]. Currently, acceptable levels of saxitoxin, a PSP toxin and tricyclic guanidinium alkaloid, must not exceed 80 μg per 100 g of raw shellfish soft tissues or 160 μg per 100 g of soft shelled clams and mussels for use as canned food [36].

Cylindrospermopsin, also a tricyclic guanidinium alkaloid, caused a major incident of human poisoning in Queensland, Australia during 1979 when cyanobacteria contaminated drinking water. To prevent further growth of cyanobacteria, the water supply was spiked with copper sulfate. Unfortunately, the resulting cell lysis released toxins into the water supply, and 85 of the 148 people affected required urgent medical care [36].

Animals have been mainly affected by anatoxin-a poisoning. In several instances, poisonings resulting in canine deaths have stemmed from drinking contaminated water or swimming in water bodies containing algal blooms [2]. Death due to anatoxin-a often occurs within one hour of contact, as noted for dogs in California, United States [2], Ontario, Canada [2], France [3] and New Zealand [4]. In each case, death was confirmed

by detection of anatoxin-a within the animals' gastro-intestinal tracts and within the contaminated water bodies [2].

While the sight and smell of cyanobacterial blooms deter humans from drinking water from lakes with blooms and make human poisoning rather rare, the ingestion of cyanobacterial toxins lead to symptoms that can be very similar to viral and bacterial gastrointestinal infections, perhaps accounting for the rarity of confirmed cyanobacterial poisonings [5]. A large portion of a population exhibiting the same symptoms may prompt an investigation, but these investigations are normally focused on the possibility of an infectious disease outbreak. Investigations into poisoning cases are generally conducted only after the initial infectious disease investigation has been closed; at that point the toxins may no longer be present at detectable levels in the water source [5].

Microcystins have been implicated as the cause of sudden human illness [5, 37]. In one particularly regrettable situation at a clinic in Brazil, 76 deaths were recorded after dialysis water contaminated with microcystins caused liver failure in 100 people [5, 6]. The concentration of microcystins in the dialysis water was ~15 $\mu g\ L^{-1}$ [5, 6, 38], whereas the recommended maximum allowable concentration (MAC) of microcystins in drinking water is currently set at 1 $\mu g\ L^{-1}$ by the World Health Organization [7]. Microcystin-LR has an intraperitoneal (i.p.) and intravenous LD_{50} of 36-122 $\mu g\ kg^{-1}$ for mice, and an inhalation toxicity (LCT_{50}) of 180 mg min m^{-3} [38]. This value represents a cumulative exposure – defined as mg of compound per cubic meter multiplied by the exposure time in minutes. The inhalation toxicity is similar to that of organophosphate nerve agents, such as sarin (LCT_{50} = 100 mg min m^{-3}) [39]. Microcystin intoxication presents as

symptoms of weakness, pallor, piloerection, diarrhoea and vomiting. Once ingested, the microcystins quickly target the liver, causing necrosis, blood accumulation and a significant increase in liver weight. Haemorrhagic shock and death occur within a few hours after the subject receives the dose.

1.2.1 The Growing Need for Cyanobacterial Toxin Screening

In addition to the continued monitoring of drinking and recreational waters, the unregulated natural health markets pose a huge risk to human health. Many blue-green algal products are marketed without testing to ensure the safety of consumers. In 2003, a receptionist working for Cell Tech International, a company that packaged and distributed blue green algae harvested from The Upper Lake Klamath, Oregon, died due to liver and kidney failure. Autopsy reports found liver and kidney damage consistent with cyanobacterial toxin poisoning; further analysis of health products found in her home also showed high levels of microcystin toxins [40], and a wrongful death suit was filed against Cell Tech International. Despite the presence of microcystins, the courts ruled that the expert testimony on behalf of the plaintiff was inadmissible and the case was dismissed [40].

Within Canada, health supplements occupy a section of the market that is not under the authority of the Canadian Food Inspection Agency (CFIA). Natural health products and supplements fall under the Natural Health Products Regulation of 2003, which does not require companies to test their products for safety. While many may see blue-green algae as natural, nutritional and safe, the general population is unaware of the risks of consuming toxins. Currently, corn, dried fruit, nuts and shellfish are routinely

tested for toxin content by the CFIA; however, because of the status of algae as a natural health product, no regular testing has been applied to algal products, despite the potential for sickness and death. Health Canada has the authority to remove supplements from the market if they are found to cause illness. Unfortunately, in the case of microcystins and long-term tumor production [5, 27, 41] removal of products from the Canadian market may come too late for some consumers.

Algal health products fall within one of the three species: *A. flos-aquae*, *Spirulina plaensis* and *Chlorella pyrenoidosa*. Supplements composed of *A. flos-aquae* are largely harvested from open environment lakes. The Upper Lake Klamath of Oregon, USA is a hotspot for harvesting algae for nutritional supplements. Due to the open environment, contamination of *A. flos-aquae* with the toxic microcystin producing cyanobacterium *Microcystis aeruginosa* occurs frequently. In one study, 70% of samples from supplements harvested from The Upper Klamath Lake contained microcystin toxins that exceeded the limit of 1 μg microcystin-LR eq g^{-1} set by the Oregon Department of Health and the Oregon Department of Agriculture [25, 42]. Documented *A. flos-aquae* production of anatoxin-a and its homologues have also been cited as another risk factor in harvesting in Upper Lake Klamath [43, 44].

Spirulina plaensis algal supplements have been grown in both open and controlled growth environments. Contamination with other algal cultures [45], or misidentifying the genus [44] has been documented for incidents of *Spirulina* poisoning, in which toxins were detected in health supplements. *Spirulina* grown in controlled environments, however, is generally free of microcystins. In a Health Canada survey of

blue-green algae products available to consumers, only the *Spirulina* supplement was free of microcystins [46]. *Chlorella* supplements are generally grown in controlled environments, which limit their toxin risk. At the point of packaging, however, the dry *Chlorella* product is often mixed with *A. flos-aquae* [24]. For this reason, ingestion of *Chlorella* supplements also risks microcystin and anatoxin-a poisoning. Recent studies finding microcystins in most algal supplements raises concern [24, 25], especially when algal supplements have been marketed to parents for treatment of Attention Deficit Hyperactivity Disorder (ADHD) in children [47]. Toxic effects may be more pronounced in children due to their lower body weight.

Many experts cite the alarmingly high level of toxin-contaminated algae as reason to halt distribution and commercial sale of *A. flos-aquae* products. Based on the depth of research, and the potential for human illness and death, it is the opinion of this author that *A. flos-aquae* products should not be deemed safe for sale, and at the very least, Health Canada should routinely screen and regulate these products.

1.2.2 Anatoxin-a and other ATXs

Anatoxin-a was the first freshwater toxin to be structurally defined (Figure 1.1). In 1977, researchers at the National Research Council of Canada [48] determined that anatoxin-a is a bicyclic compound possessing an α,β-unsaturated ketone, and a secondary amine. Koshinen and Rapoport [49] reported a pKa of 9.4 for anatoxin-a, indicating that it would be found mainly in its protonated form in nature. Cyanobacterial genuses that produce anatoxin-a include *Anabaena*, *Oscillatoria*, *Aphanizomenon*, *Trichodesmium*, *Raphidiopsis*, *Planktothrix*, *Arthrospira*, and *Phormidium* [3, 50–54]. Underscoring the

importance of continual research, the number of algal species found to produce anatoxin-a has doubled in the past few years, which also speaks to the advancement of detection methods in this growing field.

Anatoxin-a is found in nature as the (+)-anatoxin-a enantiomer, whereas much research has been done to investigate the synthesis of both (+)- and (-)-anatoxin-a enantiomers [55] (Figure 1.1). For the remainder of this thesis, unless otherwise specified, all references to anatoxin-a will refer to the natural (+)-anatoxin-a enantiomer.

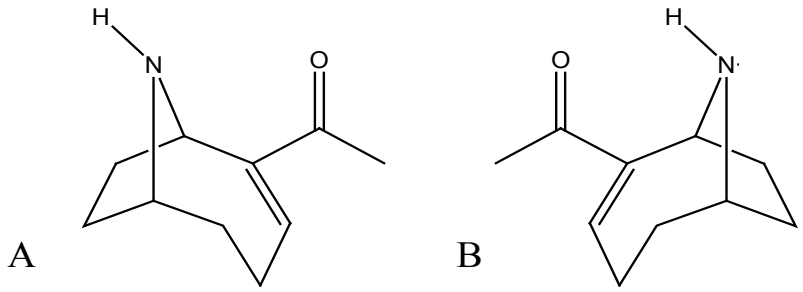

Figure 1.1: Enantiomers of anatoxin-a: a) Structure of natural (+)-anatoxin-a at physiological pH; b) Structure of synthetic (-)-anatoxin-a [49, 55].

Anatoxin-a is an extremely potent neurotoxin that kills mammals within minutes and has often been referred to as Very Fast Death Factor (VFDF) [2, 26, 48]. Anatoxin-a binds to acetylcholine receptors within the brain causing continual stimulation that stops electrical transmission necessary for skeletal muscle activity [56]. At certain levels of anatoxin-a within the body, muscular paralysis is induced along with twitching, gasping, convulsions, and ultimately death due to asphyxiation [56]. Upon exposure of anatoxin-a to mice, death routinely falls within 4-7 minutes; this acute toxicity is induced with as little as 250 $\mu g\ kg^{-1}$ [56].

Another member of the ATX group of toxins is homoanatoxin-a, which possesses an ethyl ketone rather than a methyl ketone (Figure 1.2). Homoanatoxin-a possesses one tenth the toxicity of anatoxin-a, but has still managed to kill animals drinking from lakes [4]. Both homoanatoxin-a and anatoxin-a are modified in the environment by oxidation and reduction mechanisms. While these reaction products have reduced toxicity [57] or are non-toxic [58], the detection of dihydroanatoxin-a, epoxyanatoxin-a, dihydrohomoanatoxin-a and/or epoxyhomoanatoxin-a during routine screening would be useful in alerting the presence of lower, but still toxic, levels of parent toxins, or in forensic investigations to determine the previous presence of parent toxins.

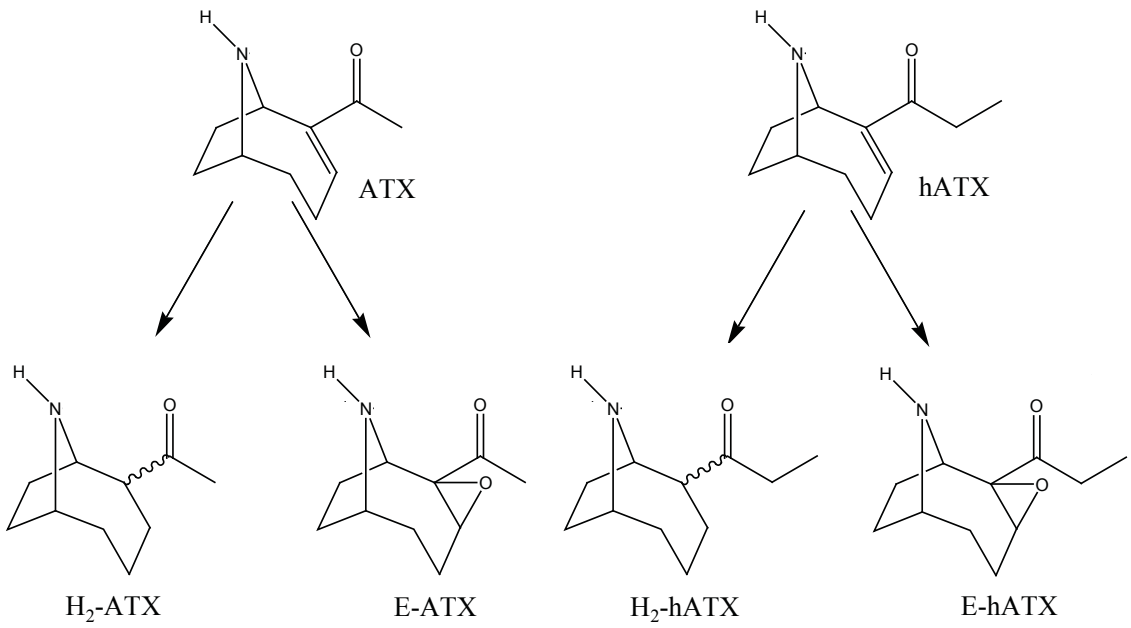

Figure 1.2: The family of ATXs. (TOP): anatoxin-a (ATX) and homoanatoxin-a (hATX). BOTTOM: Oxidation and reduction products; dihydroanatoxin-a (H_2-ATX), epoxyhomoanatoxin-a (E-ATX), dihydrohomoanatoxin-a (H_2-hATX) and epoxyhomoanatoxin-a (E-hATX).

1.2.3 Microcystins

Microcystins are a group of toxins with more than seventy variants that are produced by select freshwater cyanobacteria [59]. They are complex monocyclic heptapeptides, consisting of D-alanine, a variable L-amino acid, D-*erythro*-β-methyl-D-isoaspartic acid, a variable L-amino acid, ADDA (4E,6E-3-amino-9-methoxy-2,6,8-trimethyl-10-phenyldeca-4,6-dienoic acid), D-isoglutamic acid and *N*-methyldehydro-alanine, (Figure 1.3) [5]. Changes in the two variable L-amino acids, as well as changes to other amino acids on the microcystin template give rise to a large number of structurally related toxins (Table 1.1). Microcystin-LR, containing L-leucine and L-arginine, is the most common microcystin. Microcystin-LR was first discovered in 1958 by Bishop and colleagues [60] at the National Research Council of Canada, and initially nicknamed 'Fast Death Factor'. The structure of microcystin-LR was determined in 1984 using fast atom bombardment mass spectrometry (FAB-MS), and nuclear magnetic resonance (NMR) experiments [61]. One microcystin, [Dha7]-LR, has been given the abbreviation 'dmLR' and will be referred to as 'dmLR' for the remainder of the thesis.

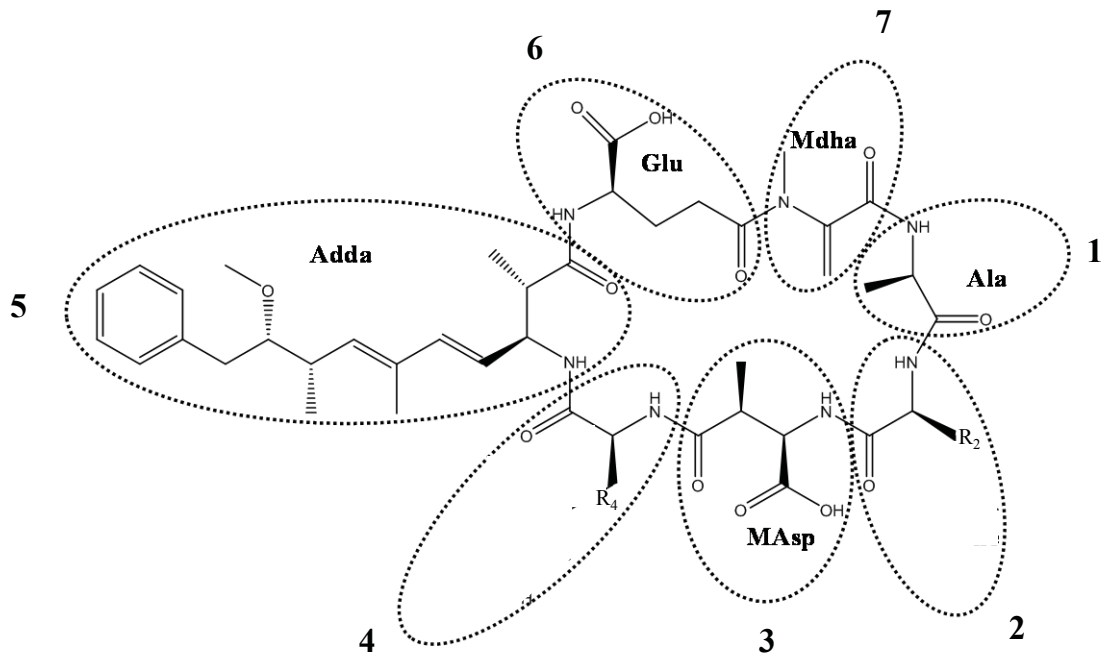

Figure 1.3: Structure of microcystin structure; 1-Ala (alanine), 2-variable L-amino acid (R_2 = variable substituent on the amino acid), 3-MAsp (methyl aspartate), 4-variable L-amino acid (R_4 = variable substituent on the amino acid), 5-ADDA (4E,6E-3-amino-9-methoxy-2,6,8-trimethyl-10-phenyldeca-4,6-dienoic acid), 6-Glu (glutamic acid), 7-Mdha (methyldehydroalanine) [62].

Table 1.1: (Top)Microcystin identification table for all microcystins mentioned in this thesis. Changes in positions 1-7 represent changes to the microcystin template as shown in Figure 1.3. (Bottom) Residue identification defined per compound.

				Position			
Microcystin	**1**	**2**	**3**	**4**	**5**	**6**	**7**
YR		Y		R			
RR		R		R			
LY		L		Y			
LR		L		R			
LA		L		A			
H4yR		H4y		R			
[Leu1]LY	Leu	L		Y			
[Leu1]LR	Leu	L		R			
[Dha7]LR		L		R			Dha
[Asp3]VY		V	Asp	Y			
[Asp3]RY		R	Asp	Y			
[Asp3]RF		R	Asp	F			
[Asp3]LR		L	Asp	R			
[Asp3]LF		L	Asp	F			
[Asp3, Mser7]RY		R	Asp	Y			Mser
[Asp3, Mser7]LY		L	Asp	Y			Mser
[Asp3, DMAdda5]RY		R	Asp	Y	DMAdda		
[Asp3, Dha7]RY		R	Asp	Y			Dha
[Asp3, Dha7]LY		L	Asp	Y			Dha

Residue		**Compound**
R	=	Arginine
A	=	Alanine
Asp	=	Aspartate
Dha	=	Dehydroalanine
L	=	Leucine
Leu	=	Leucine
Mser	=	Methylserine
DMAdda	=	O-demethyl-Adda
F	=	Phenylalanine
Y	=	Tyrosine
V	=	Valine
H4y	=	1,2,3,4-tetrahydrotyrosine

The hepatotoxicity of microcystins results from their ability to inhibit the serine/threonine protein phosphatases PP1 and 2A, which are essential to cellular survival [23, 63]. The activity of many enzymes is regulated by the presence or absence of phosphate groups, and low levels of phosphatase inhibition activity can be fatal [5]. The associated buildup of phosphorylated proteins leads to hepatic hemorrhaging and subsequent death of the organism [38].

Microcystins are a very stable group of toxins, surviving the boiling of drinking water and the low pH present in the stomach [5]. Microcystins have also been linked to tumor production by the strong correlation of increased protein phosphorylation with the production of tumors within the liver [5, 41, 64].

1.2.4 Analysis Methods

Many methods have been reported for the analysis of cyanobacterial toxins, including mouse bioassays, enzyme linked immunosorbent assays (ELISAs), LC with ultraviolet detection (LC-UVD), liquid chromatography-mass spectrometry (LC-MS), and LC with fluorescence detection (LC-FLD). Until recently, mouse bioassays were the preferred method of toxin detection due to their low cost and quick response [51]. While there are benefits to mouse bioassays, they have insufficient sensitivity for regulatory screening and are unable to distinguish among toxins. There is also a general public unease with using mammals for testing purposes [5, 51]. Additionally, the mouse bioassay test is no longer recognized as an official detection method in Europe, which now emphasises chemical testing for toxin monitoring.

The ELISA approach employs antibody/antigen association for specificity, and in competitive binding assays. The required antibodies are generated from animals injected with microcystins linked to a carrier protein [5]. After collection of blood from the animal, the antibodies are precipitated from the serum and redissolved before adding to the well-plate [65]. The antibodies are allowed to incubate, and a sample containing microcystin at an unknown concentration is added to the plate along with microcystins bound to an enzyme (often horseradish peroxidase) and substrate. The enzyme-catalyzed oxidation of the substrate produces a change that is measurable using spectrophotometry [5]. At a high concentration of free microcystin in the sample, a small amount of enzyme-bound microcystin binds to the plate, creating a low response in the assay. Conversely, a low level of microcystin in the sample allows more binding of enzyme-linked microcystin, and a higher intensity response in the assay.

Underivatized anatoxin-a can be detected by LC-UVD due to the α,β-unsaturated ketone (λ_{230}, ε = 12589 [66] (solvent not reported), ε = 10700 [49] in ethanol). Unfortunately LC-UVD methods for anatoxin-a are limited by poor sensitivity and are not often used to monitor ATXs. LC-UVD is a viable method for detection and quantitation of some cyanobacterial toxins and has been used successfully with the microcystins (e.g., microcystin-LR λ_{238}, ε = 30900 [67], 36500 [68], 39800 [69]), which possess more highly absorbing chromophores. Discrepancies within the literature values of extinction coefficients are well known, with current studies aimed to confirm a value. Unfortunately UV detection of microcystins also lacks sensitivity. Other methods such as fluorescence detection are as much as 100-fold more sensitive [51, 70].

The most powerful method for analysis of cyanotoxins is LC-MS [20, 35, 71]. This method offers both high sensitivity and selectivity and the ability to determine multiple toxins in a single analysis. Methods can be very fast, often requiring minimal sample preparation time and the instruments can be automated to analyze hundreds of samples per day.

There have been several efforts made to create methods for LC-MS determination of anatoxin-a. The use of hydrophilic interaction liquid chromatography (HILIC) columns has become increasingly popular [4, 72, 73], however other methods using different columns, such as Synergy Polar-RP [2] columns and C18 columns have also been used [74]. HILIC separation methods have an advantage with anatoxin-a because ion pairing agents are not needed for successful chromatographic separations. The use of ion pairing agents can cause increased background noise and decreased ionization efficiency, which will negatively impact the limits of detection and quantitation for the method [72].

The analysis of anatoxin-a directly by LC-MS does encounter some problems. It has a low molecular weight of 165.2 g mol^{-1}, similar to the molecular weights of amino acids and many other small compounds present in biological samples. One amino acid to note is phenylalanine, which has the same molecular mass as anatoxin-a. Consequently, the quantitation of anatoxin-a in samples containing phenylalanine may have decreased accuracy, and false positives may be obtained when screening samples [66].

The analysis of microcystins with LC-MS allows for selective analysis of the numerous microcystin variants and has been used extensively for microcystin screening

purposes. The fragmentation of the ADDA adduct using selected reaction monitoring (SRM) in LC-MS/MS allows for a characteristic *m*/*z* 135 fragment that is common to all microcystins [75] with many SRM transitions probing the protonated molecule to the *m*/*z* 135 ADDA fragment. Studies examining column optimization of microcystins have found that small particle sizes and fused core particles capable of short run times provide optimal chromatography for LC-MS/MS analysis [76]. Many analysis methods use ion pairing agents such as trifluoroacetic acid (TFA) within mobile phases, however the use of TFA in LC-MS/MS often causes ion suppression and strong source contamination from CF_3COO^- seen in negative ion mode [35].

One advantage for the LC-MS analysis of microcystins is that they possess relatively high molecular masses (within the range of 890–1100 g mol^{-1}), which means they can be detected at *m*/*z* values that are mostly removed from small organic molecules, amino acids and many other co-eluting compounds present in complex samples. There are some challenges however, including the appearance of dominant doubly-charged ions for some microcystins and the extremely complex array of known and unknown microcystins, making the separation, detection and identification of microcystin toxins challenging.

One serious problem when using LC-MS for analyses is that the sample matrix can cause a decrease or in some cases enhancement of the analyte signal. This phenomenon is often observed in complex samples due to the effect of salts and other compounds within the sample [77]. The effect of the matrix on ionization yield is a problem of major concern to quantitation by LC-MS. The use of isotopically labeled

analytes as internal standards is the ideal method for correction of matrix effects, but corrections may also be made using a similar compound with a similar retention time as an internal standard or matrix matched calibration. While LC-MS is the analytical method of choice for many scientists, work in establishing reference materials requires scientists to confirm their results with another method to remove shadows of doubt and to validate data for publication.

LC-FLD can have similar sensitivity to LC-MS and has been a popular method to screen and quantify cyanobacterial toxins [70, 78–81]. Fluorescence detection requires molecules with fluorescent properties, which for most toxins requires derivatization with a fluorescent reagent. Many derivatization reactions have been quite successful; however, while the reagent targets a specific functional group, it is rarely selective for a specific analyte. This can result in overlapping signals and mis-identification of peaks due to incomplete resolution, especially with complex algal samples.

1.3 Derivatization

Derivatization methods have employed several derivatization reagents and a wide range of analytes. This section outlines some of the reagents that have been used specifically for reactions with anatoxin-a.

1.3.1 Derivatization of Anatoxin-a

1.3.1.1 N-Butyl Derivatization

Derivatization of anatoxin-a with n-iodobutane was first investigated by Jefferies et al. [82]. The reaction conditions involve mixing anatoxin-a with K_2CO_3 and

1-iodobutane in acetone and heating at 60˚C for 3 hours to form *N*-butyl-anatoxin-a (Figure 1.4) [82].

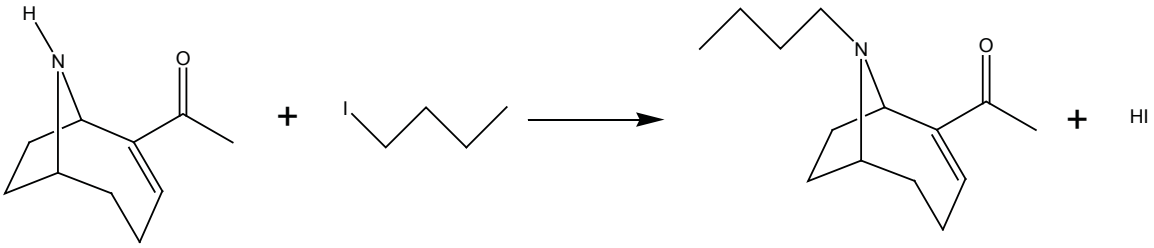

Figure 1.4: Reaction of anatoxin-a and n-iodobutane producing *N*-butyl anatoxin-a.

While the derivatization reagent is simple, the derivatization reaction described is quite lengthy. The high temperature (60˚C) presents a concern; stability studies conducted at the National Research Council in Halifax showed decomposition of anatoxin-a over time at temperatures of 40˚C over short incubation times. With the method outlined by Jefferies et al. [82] LC-MS analysis is possible. Analytical parameters such as limit of detection (LOD) and limit of quantitation (LOQ) for derivatized anatoxin-a, however, were not expressed, and the effectiveness of the analytical method cannot be evaluated from the published information.

1.3.1.2 Fluorenylmethyl chloroformate Derivatization

Takino and colleagues [83] selected 9-fluorenylmethyl chloroformate (Fmoc) as the reagent for the derivatization of anatoxin-a (Figure 1.5). Their method used LC-MS and implemented an online derivatization procedure using a programmable autosampler to carry out the derivatization reaction immediately prior to analysis [83].

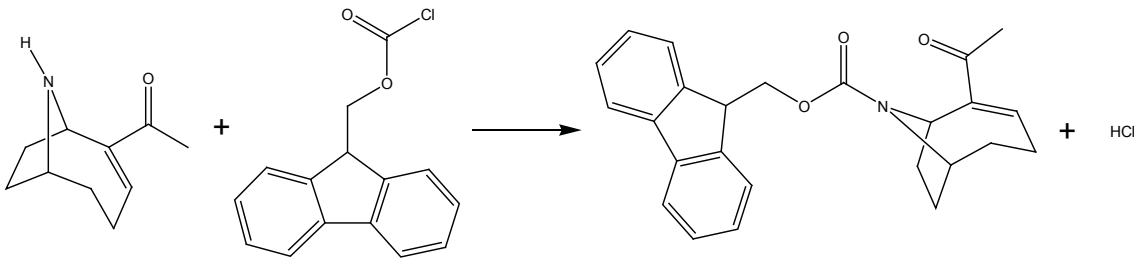

Figure 1.5: Reaction of anatoxin-a and Fmoc producing Fmoc-anatoxin-a.

The Fmoc method has several attractive features, including the simplicity of an online method, reactivity at room temperature, an LOQ of 15.2 ng L^{-1} and an LOD of 2.1 ng L^{-1} [83]. This method, however, will inevitably result in the need for frequent cleaning of the ion source, as the high concentration of derivatization agent needed to obtain complete reaction with toxins in real samples will send excess reagent and salts through the mass spectrometer unless a cleanup method is added. On-line derivatization methods are not common with LC-MS because the highly reactive derivatization reagents will react with the column, stripping silica off the column and reducing column lifetime substantially. Additionally, the results from the LOQ and LOD experiments are problematic because single ion monitoring (SIM) rather than selected reaction monitoring (SRM) was used. In the SIM method Fmoc-anatoxin-a and Fmoc-phenylalanine give the same monitored ion and the method is not selective. Phenylalanine is present in most algal samples and because it also possesses an amine group, it will readily react with Fmoc reagent. No method to distinguish the two was presented within the experiment,

which raises concerns when monitoring water samples. Regardless, this method is unique and presents the attractive prospect of a 'quick and dirty' screening technique.

1.3.1.3 4-Fluoro-7-nitrobenzofurazan Derivatization

A method developed by James et al. [58] uses 4-fluoro-7-nitro-2,1,3-benzoxadiazole (NBD-F) as a derivatization reagent for anatoxin-a using fluorescence detection (Figure 1.6). The method involves evaporating the sample and reconstituting in sodium borate. The derivatization reagent, NBD-F in acetonitrile is added, and the reaction mixture is allowed to sit in the dark at room temperature for 10 minutes. The reaction is then terminated by adding hydrochloric acid, and analyzed using LC-FLD (Figure 1.6). The method provides a LOD of 10 ng L^{-1} and is fairly uncomplicated, raising the molar mass of the derivative to 328 g mol^{-1}, which may also be useful for LC-MS analysis.

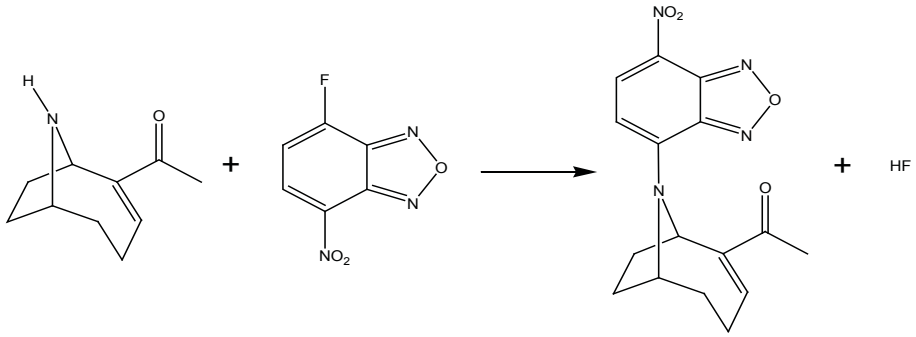

Figure 1.6: Reaction of anatoxin-a with NBD-F producing NBD-anatoxin-a.

1.4 Reference Materials

Reference materials (RMs) are well-characterized standards or samples that are used to assess measurement methods or to perform calibrations. RMs have at least one property that has been verified to uphold the ability to assess, calibrate and quantify [84],

as defined by the International Organization for Standardization (ISO), the authority on development of standards [84, 85]. A certified reference material (CRM) is a reference material that has been certified through validated procedures, assigned a traceable value with an uncertainty, and is complete with an associated certificate issued by the organization producing the product [84, 85]. RMs and CRMs can exist in many different forms for many different purposes, which include [84]:

i. solutions or substances purified for calibration and identification;
ii. matrix matched materials for calibration of specific types of instruments, and/or matrix matched materials required for calibration of a material with a similar matrix;
iii. matrix reference materials that have been certified to represent the matrix of a sample being analyzed; or
iv. reference materials specific to a certain method used, the value, under strict analytical protocol, as defined by the method used by the user.

Reference materials are essential for testing the accuracy of methods used in analytical chemistry. They should be used regularly to verify instrument performance, calibrate instruments, validate methods, assign uncertainty to measurements, or for purposes of quality control, which can include assessing the performance of both the laboratory and the analysis [86]. The use of calibration standards in natural toxins chemistry is required for assurance of instrument optimization and performance, while the matrix CRMs are essential for positive confirmation of toxin presence and the elimination of false negatives and false positives. A good example of this is

phenylalanine and anatoxin-a; without standards, phenylalanine could be misidentified as anatoxin-a based on retention time or molecular weight, creating a false positive.

Due to the difficulty in acquiring or isolating certain toxins, only small amounts may be available for calibration. When working with these rare toxins, relative response factors for analogues may possibly be applied using a 'parent' or closely related CRM. This will allow for limited quantities of precious toxin to be conserved, while allowing for relative error and a concentration based on the closely related analogue. Tests assessing the stability of the toxin over time and its homogeneity between portions would still be required to ensure continued accuracy [87]. The relative response factor may be evaluated based on the ratio of CRM and analyte responses when using instrumental methods, such as LC-UVD, LC-FLD, LC-CLND and LC-MS.

In order to certify an RM to create a CRM, a considerable amount of testing must take place. After the bulk sample has been distributed into sample vials, they must undergo homogeneity testing to assure that the concentration assigned to the batch is representative of the entire batch, with the degree of homogeneity being communicated within the appropriate accompanying certificate. Stability of the RM must also be evaluated in order to estimate the lifetime of the RM, as well as the stability of the material under specific transportation conditions. Characterization of the RM should be carried out using two or more independent reference methods, and stringent uncertainty calculations must be used when assigning the associated uncertainty [85].

The NRC currently holds several cyanobacterial toxin CRMs available for purchase, including cylindrospermopsins, anatoxin-a, and several saxitoxin analogues.

Additionally, three microcystin and one nodularin CRMs are ready to be released for purchase and were also available for use.

1.5 Objectives

Due to the limited number of cyanobacterial toxin RMs available for purchase, the first objective of this work was to produce a homoanatoxin-a reference material for quantitation purposes within this project. An accurate standard was required for the development and evaluation of new analytical methods and would also serve as a feasibility study for a possible project to develop a homoanatoxin-a CRM. As part of this study, the RM was taken through homogeneity and stability studies. Epoxy and dihydro analogues of anatoxin-a and homoanatoxin-a were also prepared to serve as reference standards for the identification and quantification of ATXs in culture and field samples.

After creating the homoanatoxin-a reference material, a second objective was to create and optimize a derivatization method that would be useful for the analysis of ATXs. Derivatization with the dansyl chloride reagent was selected for investigation because the reagent is inexpensive and would facilitate the detection of anatoxins by both LC-MS and LC-FLD. An analysis time of less than 10 minutes was desired to make the LC-MS method viable for high throughput routine screening of field samples. Development of the method required optimization of column performance, mobile phase composition and instrumental parameters to provide a sensitive and selective analysis.

In addition to the development of a LC-MS method, the third objective of the thesis was to develop a method for LC-FLD analysis of dansyl derivatized ATXs. This would provide another method of quantitation with potential as an additional method for

CRM certification purposes. LC-FLD presents certain challenges not experienced in LC-MS, such as the resolution and selectivity needed to separate analytes from natural interferences in samples.

The fourth objective of the thesis was to combine the previous findings to launch a feasibility study of a freeze-dried RM containing anatoxin-a, homoanatoxin-a and several microcystins. Some development of LC-MS and LC-UVD methods for analysis and quantitation of microcystins was also required. Various possible source materials were surveyed and after suitable materials were selected, they were to be blended and packaged as a preliminary RM for testing. Assessment of stability, homogeneity, and quantitation were to be assessed for the ATXs and microcystins contained in the freeze dried RM.

CHAPTER 2 MATERIALS AND METHODS

2.1 Equipment, chemicals and mobile phases

Formic acid (FA; >98% ACS grade) was obtained from EMD (Gibbstown, NJ, USA). All solvents including methanol (MeOH; HPLC grade), acetonitrile (MeCN; HPLC grade) and acetic acid (AcOH; Reagent Plus™ ≥ 99%) were purchased from Caledon (Georgetown, ON, Canada). Deionized water (H_2O) was provided by a Milli-Q water purification system (Millipore Ltd., Billerica, MA, USA). Dansyl chloride (DNS-Cl; 95%), piperidine (pip; ≥99.5%), pyrrolidine (pyr; ≥99.5%), 3-methylpiperidine (3-Me-Pip; 99%) and trifluoroacetic acid (TFA; 99%) were purchased from Sigma-Aldrich (Oakville, ON, Canada). Disodium tetraborate (98%) was supplied by BDH (Toronto, ON, Canada).

The pH of buffers was measured with an ATI Orion PerpHecT Meter (Thermo Orion, Beverly, MA, USA). A Branson 2510 Sonicator was purchased from Emerson Industrial Automation (Danbury, CT, USA). Centrifugations were performed with an IEC Centra MP-4R centrifuge outfitted with an 804S rotor (GMI, Ramsey, MN, USA).

Multiple LC systems were used and listed in Table 2.1. Each LC system was equipped with a solvent reservoir, in-line degasser, binary pump, refrigerated autosampler, and temperature-controlled column oven. LC analyses were performed using four different columns as described in Table 2.2.

Table 2.1: LC Systems used with a description of each system.

LC System	Description	Company
A	Model 1100 LC system	Agilent (Palo Alta, CA, USA)
B	Model 1290 LC system	Agilent (Palo Alta, CA, USA)
C	Model 1100 LC system with 1200 series fraction collector	Agilent (Palo Alta, CA, USA)
D	Accela™ High Speed LC system	Thermo Scientific (Waltham, MA, USA)

Table 2.2: Columns used with LC systems.

Column	Packing	Particle size (μm)	Column length (mm)	Column i.d. (mm)	Company
A	TSK Gel Amide-80®	3	150	2.0	Tosoh Bioscience LLC, (Montgomeryville, PA, USA)
B	Luna C18 (2)	3	150	4.6	Phenomenex (Torrance, CA, USA)
C	Luna C18 (2)	2.5	50	2.0	Phenomenex (Torrance, CA, USA)
D	Poroshell SB C18 (2)	2.7	150	2.1	Agilent (Mississauga, ON, Canada)
E	Luna C18 (2)	3	250	10	Phenomenex (Torrance, CA, USA)
F	Luna C18 (2)	3	150	2.0	Phenomenex (Torrance, CA, USA)

Various detectors were used and listed in Table 2.3. All LC-MS/MS analyses were performed in positive ion mode with an electrospray voltage of 5500 V and a source temperature of 475°C. Nitrogen was used as the nebulizer gas as well as the curtain gas. Dwell times were selected to allow for the collection of at least 15 points across each peak at all times. With HILIC, an MS source temperature of 275°C was used.

Table 2.3: Detectors used for analysis of analytes.

Detector	Description	Company
A	1290 fluorescence detector (model no. G1321A)	Agilent (Mississauga, ON, Canada)
B	1290 ultraviolet detector (model no. G4212A)	Agilent (Mississauga, ON, Canada)
C	1050 Ultraviolet detector	Hewlett Packard (Arcade, NY, USA)
D	API-4000 triple quadrupole mass spectrometer with TurboSpray® interface	AB-SCIEX (Concord, ON, Canada)
E	4000 QTRAP triple quadrupole mass spectrometer with TurboSpray® interface.	AB-SCIEX (Concord, ON, Canada)
F	Scientific Exactive™ mass spectrometer equipped with an Orbitrap mass analyzer	Thermo Fisher (Waltham, MA, USA)
G	Chemiluminescence nitrogen detector (model no. 8060)	Antek (Kitchener, ON, Canada)

Several separation methods were explored using several different mobile phases. The complete list of mobile phases can be found in Table 2.4, with specific LC conditions reported later for each experiment.

Table 2.4: Mobile phases used with LC systems.

Mobile Phase	Phase A	Phase B	Modifier
1	Water + modifier	MeCN	50 mM HCOOH and 2 mM $HCOONH_4$ (pH = 2.3)
2	Water + modifier	MeCN	0.05% TFA
3	12.5% MeOH in water (v/v)		0.05% TFA
4	Water + modifier	MeCN/water (95:5, v/v) + modifier	50 mM HCOOH and 2 mM $HCOONH_4$ (pH=2.3)
5	Water + modifier	MeOH + modifier	0.1% TFA.
6	Water + modifier	MeCN + modifier	0.05% TFA

Peak areas from LC-MS/MS analyses were integrated with the Analyst® instrument control and data processing software, version 1.6.1 (AB SCIEX). Peak areas from LC-FLD, LC-UVD and LC-CLND analyses were integrated using Agilent Chemstation software. Acquisition of accurate mass and data processing was carried out with Xcalibur 2.1 software from Thermo Scientific (Waltham, MA, USA).

Algae were freeze-dried with a Thermo Electron Corporation Micromodulyo Freeze dryer (Nepean, ON, Canada) outfitted with a ThermoSavant VLP 80 ValuPump (Albuquerque, NM, USA) reaching a vacuum of approximately 40 mTorr.

A PM100 planetary ball mill was purchased from Retsch (Newtown, PA, USA) and outfitted with a 500 mL stainless steel grinding jar with 25 stainless steel balls (20 mm diameter). A Turbula® mixer was purchased from WAB (Switzerland). An MB 45 moisture analyzer was purchased from Ohaus (Parsippany, NJ, USA) with a pan handler and aluminum sample pans.

2.2 Algae and reference materials

The National Research Council (NRC) Certified Reference Material Program (CRMP; Halifax, NS, Canada) provided the following calibration standards: CRM-ATX (30 μM), and CRM-microcystin-RR (9.8 μM), CRM-microcystin-LR (10 μM) and CRM-dmLR (9.62 μM). Other standards, microcystin-LA (0.61 μM) and caffeine (USP grade), were purchased from Sigma-Aldrich and quantified with quantitative nuclear magnetic resonance (qNMR) and CLND.

2.3 Homoanatoxin-a reference material and dihydro/epoxy qualitative standards

2.3.1 Homoanatoxin-a extraction, isolation and purification

Biomass (120-160 g) harvested from an *Oscillatoria formosa* culture was divided into two portions and freeze-dried in two separate glass beakers. The lyophilized algal samples were transferred to a 150 mL BD Falcon centrifuge tube (Mississauga, ON, Canada) and were extracted separately in four steps of 100, 50, 40 and 10 mL using an

extraction solvent of H_2O/MeOH/FA (80/20/0.1, v/v). After the addition of each volume, the centrifuge tube was sonicated (5 min, 40 Hz) in a sonication bath at room temperature followed by centrifugation (6300 *g*, 10 min). The supernatants were decanted into separate amber glass jars and analyzed by LC-MS/MS to confirm extraction efficiency. The four extracts were combined and freeze-dried. The resulting powder was redissolved in H_2O (15 mL) and filtered through a Waters Sep-Pack C18 Vac Cartridge (10 g packing, 35 mL volume; Millford, MA, USA), which had been previously conditioned with 0.01% FA. The cartridges were eluted in four steps with 40 mL each: (1) 5% MeOH; (2) 20% MeOH; (3) 50% MeOH; (4) 80% MeOH, all with 0.1% TFA. Each elution was collected in a glass jar. A sample (100-200 µL) of each was filtered (0.45 µm Millipore centrifuge filter; Billerica, MA, USA) for analysis.

Samples were analyzed with HILIC-MS using LC system A, mobile phase #1 with a flow rate of 0.2 mL min^{-1} and column A with a column temperature of 40°C. Sample injection (5 µL) was followed by a 3-s needle wash in 95% MeOH. The HILIC-MS/MS method of Lajeunesse et al. [88] was modified to selectively monitor for the ATXs in a 9.5 min analysis. A gradient elution was used as follows: after a 12 min equilibration with an initial mobile phase (80% B, 20% A), the sample was injected and the percentage of solvent B was decreased linearly to 75% over 9.5 min, then to 70% over 0.5 min, and followed by a hold at 70% for 4 min before returning to initial conditions. Analytes were detected with MS (detector E), using transitions for each anatoxin analogue as shown in Table 2.5.

Table 2.5: LC-MS/MS transitions used for analysis of ATXs with HILIC-MS method. A declustering potential (DP) of 50 and collision energy (CE) of 25 was used.

Analyte	Retention Time (min)	Precursor *m/z*	Product Ion (*m/z*)	
			Quantifier	Qualifier
anatoxin-a	5.0	166	91	131
homoanatoxin-a	4.1	180	145	57
dihydroanatoxin-a	4.7	168	93	56
dihydrohomoanatoxin-a	3.9	182	57	93
Epoxyanatoxin-a	4.5	182	98	93
Epoxyhomoanatoxin-a	3.7	196	141	121

Homoanatoxin-a eluted in fractions 2 and 3, but was recovered (92-97%) from the second fraction. The third fraction was discarded due to slight discolouration. A full scan analysis (50-400 *m/z*) was performed to probe for purity by LC-MS. Determination of purity by LC-UVD analysis used reverse phase chromatography conditions, which involved LC system B, column B, mobile phase #1 at a flow rate of 1.00 mL min^{-1} and a column temperature of 40°C. Sample injection (5-10 µL) was followed by a 3-s needle wash using 95% MeOH. A gradient elution was used as follows: after a 12 min equilibration with an initial mobile phase (95% A, 5% B), the sample was injected and the percentage of solvent B was increased linearly to 25% over 20 min, held for 10 min before returning to initial conditions. Purity was assessed with a UVD (detector B) at 230 nm.

The second fraction from both extract A and B were freeze-dried and redissolved in aqueous 10% MeOH solution (5 mL). The resulting solution was subjected to preparative LC-UVD to isolate homoanatoxin-a. This was performed using LC system C, column E, mobile phase #2 at a flow rate of 4.0 mL min^{-1} and a column temperature of 40°C.

Sample injection (100 µL) was followed by a 3-s needle wash using 95% MeOH. A gradient elution was used as follows: after a 10 min equilibration with an initial mobile phase (95% A, 5% B), the sample was injected and the percentage of solvent B was increased linearly to 25% over 20 min, held for 10 min before returning to initial conditions. The LC was programmed to collect the homoanatoxin flowing from the UVD into 6 mL glass vials. The resulting solutions were combined, freeze-dried and quantified with quantitative nuclear magnetic resonance (qNMR, section 2.3.2).

2.3.2 Homoanatoxin-a quantitation

Fractions of collected from the preparative LC that contained homoanatoxin-a, totalling approximately 250 mL, were pooled and freeze-dried to reduce the volume. The residue was reconstituted in water (~5 mL), and again freeze dried to remove MeOH. One- and two-dimensional (COSY and TOCOSY) NMR spectra were obtained at 700.15 MHz in D_2O using a Bruker Avance II 700 with a 1.7 mm cryoprobe, at 293 K. NMR spectra for quantitation were obtained at 500.132 MHz in H_2O using a Bruker DRX 500 spectrometer with a TX1 probe at 293K. Quantitative NMR (qNMR) was performed using one dimensional proton spectra with H_2O suppression, with NMR tubes tuned and matched. The values of p360 (360^o pulse width) were calibrated and used for setting the value of the pulse width (p1 - use a 90^o pulse to give maximum intensity). The homoanatoxin-a response was calibrated using a caffeine external standard (4.102 mM) run under identical conditions [89].

The LC-UVD-CLND analysis used LC system A, column F, mobile phase #5 at a flow rate of 0.15 mL min^{-1}, detectors C and G, and a column temperature of 30°C.

Sample injection (25 µL) was followed by a 3-s needle wash in 95% MeOH. A gradient elution was used as follows: after a 20 min equilibration with an initial mobile phase (5% B, 95% A), the sample was injected and the percentage of solvent B was increased linearly to 25% over 20 min, with a 10 min hold before returning to initial conditions. The analyte was quantified using two different standards: USP grade caffeine standard and CRM-ATX. The caffeine standard used slightly different chromatography; isocratic conditions (35% B) for 20 min and used a 7.5 µL injection volume. The instrument maintained a pressure setting of 33 psi, vacuum of 30 torr, argon of 50 mL min^{-1}, oxygen of 251 mL min^{-1}, an ozone supply at 24.9 mL min^{-1} and an oven temperature of 1050°C.

The RM solution was prepared by diluting the stock solution from qNMR to 25 mL with aqueous 9% MeOH, 0.01% AcOH. The solution was stored in prewashed and prescored 5 mL amber ampoules from Wheaton (Millville, NJ, USA). Approximately 300 µL of solution was stored in each vial and flame sealed under argon using a Cozzoli ampouling machine (Somerset, NJ, USA). Samples were numbered and labeled in order of fill and sealing.

2.3.3 Characterization

Accurate mass determination of the ampouled sample was performed with the use of an LC System D coupled to an Orbitrap mass analyzer (detector F), using mobile phase #1 with column A. A gradient elution was used as follows: after a 12 min equilibration with an initial mobile phase (80% B, 20% A), the sample was injected and the percentage of solvent B was decreased linearly to 75% over 9.5 min, then to 70% over 0.5 min, and followed by a hold at 70% for 4 min before returning to initial conditions. A flow rate of

0.2 mL min^{-1} was used with a column temperature of 30°C and a 1 µL injection volume. Optimization of the instrument was performed daily using both positive and negative mode. Through optimization, the capillary voltage was set to 35 V, tube lens 130.5 V, and skimmer voltage at 20.7 V using the optimization software ExactiveTune 1.1. Analyses were executed using a "balanced" automatic gain control setting with a 50 ms maximum inject time over the mass range of *m*/*z* 50 to 500. Resolution was set to ultra-high enhanced (100,000 @ 1 Hz) using high energy collisional dissociation setting of 100. An enhanced product ion (EPI) spectrum was produced with a scan acquired using the LC system A, column A, mobile phase #1 and a triple quadrupole mass spectrometer (detector E) using the same flow conditions and mobile phase used for the accurate mass analysis. The products of *m*/*z* 180.1 were measured, scanning from 50-200 Da using 'high resolution' with the linear ion trap and a 20 ms trapping period.

2.3.4 Homoanatoxin-a storage and stability/homogeneity assessment

A stability study was conducted using homoanatoxin-a in ampoules stored at different temperatures (-20, 4, 23 and 40°C) and time points (3, 9, 27 and 180 days). Samples were analyzed by LC-UVD at an absorption wavelength of 230 nm using LC system A, column B, mobile phase #3 at a 1.0 mL min^{-1} flow rate, 8 µL injections, and a 40°C column temperature. While acquiring UV absorbance, the detector acquired wavelengths across a peak from 210 – 300 nm for the UV absorbance spectrum.

Unknown peaks from the stability study were investigated with an EPI scan acquired using LC system A, column A, mobile phase #1 and the triple quadrupole mass spectrometer (detector E) using the same flow conditions and mobile phase used for the

accurate mass analysis. The products of *m*/*z* 180.1 were measured, scanning from 50-200 Da using 'high resolution' with the linear ion trap and a 20 ms trapping period and a collision energy of 25 eV.

2.3.5 Dihydro and epoxy anatoxin-a and homoanatoxin-a synthesis

Syntheses of epoxy/dihydro anatoxin and homoanatoxin analogues on a microscale were carried out following the methods published by James et al. [58]. The reaction used a 300 μL aliquot of anatoxin-a (1.5 μg) and homoanatoxin-a (1.0 μg) mixed with acetic acid (100 μL) and Adam's catalyst (100 μg). The solution stirred for 1.5 hours under 80% CO_2, 10% N_2 and 10% H_2 before the reaction was stopped by evaporating the solution under nitrogen and redissolving in water. EPI scans were used to identify SRM transitions using the LC system A, column A, mobile phase #1 and the triple quadrupole MS (detector E). A gradient elution was used as follows: after a 12 min equilibration with an initial mobile phase (90% B, 10% A), the sample was injected and the percentage of solvent B was decreased linearly to 55% over 25 min, then to 25% over 2 min, and followed by a hold at 25% for 10 min before returning to initial conditions. A flow rate of 0.2 mL min^{-1} was used with a column temperature of 30°C and a 5 μL injection volume. The products of *m*/*z* 168 and 182 (dihydroanatoxin-a and dihydrohomoanatoxin-a, respectively) were measured, scanning from 50-200 Da.

For the epoxy analogues, 300 μL aliquot of anatoxin-a (1.5 μg) and homoanatoxin-a (1.0 μg) were freeze-dried down to near dryness and redissolved in acetone (200 μL) and sodium hydroxide (2 M, 20 μL). Hydrogen peroxide (30%, 200 μL) was added in portions to maintain a continuous bubbling of the solution for 35 min as

necessary while heated to a constant temperature of 45°C. The reaction mixture was then evaporated under nitrogen and redissolved in water before analysis. EPI scans were used to identify SRM transitions using the LC system A, column A, mobile phase #1 and detector E. A gradient elution was used as follows: after a 5 min equilibration with an initial mobile phase (80% B, 20% A), the sample was injected and the percentage of solvent B was decreased linearly to 75% over 9.5 min, then to 70% over 0.5 min, and followed by a hold at 70% for 4 min before returning to initial conditions. A flow rate of 0.2 mL min^{-1} was used with a column temperature of 30°C and a 5 µL injection volume. The products of *m*/*z* 182 and 196 (epoxyanatoxin-a and epoxyhomoanatoxin-a, respectively) were measured, scanning from 50-220 Da.

2.4 DNS-LC-MS/MS Method

2.4.1 Extraction of samples

All algal cultures were collected in pre-weighed VWR® SuperClearTM ultra-high performance polypropylene centrifuge tubes with flat caps (Ville Mont-Royal, QC, Canada), using either 50 mL or 15 mL volumes depending on the mass of wet algae. The algae were freeze-dried for over 24 hours, after which time the tubes were removed and the dry weight of the tube and algae were recorded. In all instances, the extraction volume was based on the dry mass of algae to minimize matrix effects; a ratio of approximately 100 mL per gram was maintained whenever possible. Extractions were performed using 0.1% AcOH in 50% MeCN. Tubes were shaken to suspend the lyophilized material and sonicated (5 min; 40 Hz) within a bath sonicator. After centrifugation (6300 *g*, 10 min), the supernatant was carefully transferred using a glass

pipette into a volumetric flask. The extraction was repeated twice. Prior to analysis, each sample was filtered through a Millipore Ultrafree centrifugal filter (0.45 μm; Billerica, MA, USA). Between analyses, all samples were stored in the dark at -20°C. Extractions were also carried out with different extraction solvents: 0.1% AcOH in MeOH and 75% MeOH were used for microcystin extraction.

2.4.2 Optimized method for derivatization and SPE cleanup

A mixture of standard (CRM or RM) or algal extract (100 μL), sodium borate buffer (100 μL, pH 9.4, 25 mM), 3-methylpiperidine solution (100 μL), pyrrolidine solution (100 μL), and DNS-Cl (30 μL, 1 mg mL^{-1} in MeCN) was shaken for approximately 10 min. The pyrrolidine (6 μg L^{-1}, 50% MeCN) and 3-methylpiperidine (84.5 μg L^{-1}, 50% MeCN) standard solutions were diluted to match the concentration of anatoxin-a in samples. The organic component of the reaction mixture was maintained at a minimum of 50% to ensure the solubility of DNS-Cl.

The reaction mixture was applied to a Phenomenex Strata X-AW 3-mL column; preconditioned with successive washes of acetonitrile (5 mL) and borate buffer (3 mL). The reaction vial was rinsed with 30% MeCN (3 x 1 mL); the washes were applied to the column and vacuum was used to move the mobile phase through the column. The column was eluted with 100% MeCN, which was then evaporated under nitrogen and reconstituted in 50% MeCN (150 μL).

2.4.3 DNS-LC-MS/MS Operational Method

The derivatization method described in section 2.4.2 was used for sample preparation, except pyrrolidine (65 μg L^{-1} in 50% MeCN) was used in place of 3-methylpiperidine as an internal standard.

An EPI scan acquired using LC system A, column C, mobile phase #4 and the triple quadrupole mass spectrometer (detector E) with a flow rate of 0.2 mL min^{-1} and a column temperature of 40°C. Sample injection (5 μL) was followed by a 3-s needle wash in 95% MeOH. Isocratic elution used mobile phase component B at 60% for 12 min followed by a flush at 90% B for 4 min. An EPI scan was acquired for dansyl phenylalanine, anatoxin-a, homoanatoxin-a, and all epoxidation and reduction analogues.

Collision energy (CE) and declustering potentials (DP) were optimized for dansyl-anatoxin-a by constructing a grid search with parameters to be optimized. This involved manually adjusting both CE and DP parameters and integrating peak areas.

LC-MS/MS separation of derivatized toxins were carried out on LC system A, column C, mobile phase #4 at a flow rate of 0.2 mL min^{-1} and a column temperature of 40°C. Sample injection (1-5 μL) was followed by a 3-s needle wash in 95% MeOH. Isocratic elution used mobile phase component B at 60% for 12 min followed by a flush at 90% B for 4 min. Both triple quadrupole mass spectrometers (detectors D and E) were used for HILIC-MS analysis and DNS-LC-MS/MS methods with the settings reported in Table 2.6.

Table 2.6: LC-MS/MS operating conditions for both HILIC-MS and DNS-LC-MS/MS methods.

Parameter	HILIC-MS/MS	DNS-LC-MS/MS
Q1 resolution	Unit	Unit
Q3 resolution	Low	Low
Dead time (ms)	5.007	5.007
Collision activated dissociation (eV)	6	9
Curtain gas (N_2, psig)	20	20
Nebulizer gas (psig)	50	50
Auxiliary gas (psig)	50	50
Ion spray voltage (V)	5500	5500
Source temperature (°C)	275	475
Exit potential (V)	10.5	10.5
Collision exit potential (V)	15	9

The transitions used for analysis of dansylated anatoxins (Table 2.7) involved the use of both quantitative and qualitative transitions whenever possible for quantitation and identification of analytes.

Table 2.7: LC-MS/MS SRM transitions with DP = 70 and CE = 35 for analysis of DNS-ATXs.

			Product Ion (*m*/*z*)	
Analyte	Retention Time (min)	Precursor *m*/*z*	Quantitative	Qualitative
DNS-anatoxin-a	3.8	399	170	335
DNS-homoanatoxin-a	5.6	413	170	349
DNS-dihydroanatoxin-a	4.5	401	170	337
DNS-dihydrohomoanatoxin-a	6.7	415	170	351
DNS-epoxyanatoxin-a	3.6	415	170	164
DNS-epoxyhomoanatoxin-a	5.0	429	170	178

2.4.4 DNS-LC-MS/MS relative molar response

A mixed calibration standard was prepared by mixing RM-hATX (655 µL) with CRM-ATX (500 µL). This solution was evaporated under nitrogen to remove methanol and to reduce the volume to 230 µL. A portion of the sample (25 µL) was derivatized in four separate reactions following the method described in section 2.4.2, but with slight

changes to accommodate the different volume of sample used: 25 µL of a 0.7 µg mL^{-1} solution of 3-methylpiperidine in an aqueous 50% MeCN, 100 µL of borate buffer, 70 µL of acetonitrile and 30 µL of a 1 mg mL^{-1} solution of DNS-Cl. Pyrrolidine was not used as an internal standard for this experiment, as the sample would be analyzed by FLD as well.

Four replicate reactions were performed for LC-MS/MS relative molar response experiments. The samples were run in quadruplet according to the operational methods listed in section 2.4.3, using 0.5 µL injections.

2.4.5 Quantitation

Cultured algal and field samples were quantified with DNS-LC-MS/MS after preparation using the method in section 2.4.2. The cultivated algal samples included *Aphanizomenon issatschenkoi* (CAWBG02) and *Oscillatoria formosa* (PCC6407); field samples included *Phormidium* sp. (collected in 2005), *Phormidium* sp. (collected in 2012), an algal sample collected from Ashley River (2005, New Zealand) and a sample collected from Hutt River (2005, New Zealand). Each sample was extracted using 50% MeCN according to the method described in section 2.4.1. All samples were quantified against standards of dansylated CRM-ATX diluted using a Hamilton MicroLab® 500 Series dilution apparatus (Reno, NV, USA) and analyzed using the DNS-LC-MS/MS operational method. Samples were bracketed with calibration standards constructed from diluted DNS-anatoxin-a standard solution and a solvent blank. Each sample was injected a minimum of three times with a minimum of four calibration points.

Quantified dansylated samples were compared with nonderivatized samples quantified with HILIC-MS/MS.

2.5 DNS-LC-FLD Method

2.5.1 DNS-LC-FLD Operational method

Derivatization reactions were carried out as described in section 2.4.2. Analysis was carried out using LC system A, column B, FLD (detector A), mobile phase #1 at a flow rate of 1.0 mL min^{-1} and a column temperature of 40°C. A 20-µL sample was injected, followed by a 3-s needle wash using 95% MeOH. Isocratic elution was used as follows: after a 10 min equilibration with an initial mobile phase (70% B, 30% A), the sample was injected and solvent B was maintained at 70% over 10 min, then increased to 90% B over 0.5 min and held for 3 min before returning to initial conditions. The FLD was set at an excitation wavelength of 350 nm, an emission wavelength 525 nm and a gain setting of 18. The instrument recorded emission wavelengths across peaks from 450 - 600 nm.

2.5.2 DNS-LC-FLD Relative Molar Response

The dansylated sample prepared in section 2.4.4 was also used for DNS-LC-FLD relative molar response evaluations. Four samples were run in quadruplicate according to the operational methods previously listed in section 2.5.1, except a 10 µL injection volume was used.

2.5.3 DNS-LC-FLD Quantitation

Samples quantified with the DNS-LC-FLD method included: *Aphanizomenon issatschenkoi* (CAWBG02), *Oscillatoria formosa* (PCC6407) and *Phormidium* sp. (2005). Derivatized samples and standards were prepared using the method described in

section 2.4.2, with the exception that pyrrolidine was not used as an internal standard. CRM-ATX was used for calibration. The dansylated standard was used to create a calibration curve with serial dilution using the MicroLab. Samples were run between calibration standards. Calibration curves included a minimum of four points and a solvent blank, with each point representing a minimum of three injections. Analysis of samples followed the method outlined in section 2.5.1.

2.6 Microcystin analysis methods

In screening for microcystins, a specialized method was used. The method used LC system A, column D, triple quadrupole mass spectrometer (detector E), mobile phase #1 at a flow rate of 0.25 mL min^{-1} and a column temperature of 30°C. Sample injection (1-5 µL) was followed by a 3-s needle wash using 95% MeOH. Gradient elution was used as follows: after a 15 min equilibration with an initial mobile phase (25% B, 75% A), the sample was injected and solvent B was increased linearly to 75% over 25 min, then to 100% over 0.5 min and followed by a hold for 5 min before returning to initial conditions. For characterization of the samples, information dependent acquisition (IDA) methods based on selected reaction monitoring (SRM) were used to examine the characteristic fragmentation pathways (Table 2.8). The SRM signals triggered the collection of enhanced resolution (ER) scans and enhanced product ion (EPI) scans. The EPI scans were used to deduce fragmentation and structure, while the ER scan helped separate analytes from interferences based on characteristic isotopic patterns and confirmed charge states. Important fragment ions selected from the EPI scans and were used to quantify the toxins. The samples examined for use in the algal reference material

included four different strains of *Microcystis aeruginosa* (LL-4-4, CPCC 300, UTCC 464 and CYA 548).

Table 2.8: LC-MS/MS SRM transitions, used for analysis including DP and CE parameters, for each microcystin analyte in the reference material and nutritional supplements.

		Product Ion (*m*/*z*)			
Analyte	Precursor *m*/*z*	Quantifier	Qualifier	CE	DP
Microcystin-RR	519	135	127	65	65
[Asp3]-Microcystin-LR	981	135	127	80	80
Microcystin-LR	995	135	375	85	85
Microcystin-LA	910	135	213	70	70
[Leu1]-Microcystin-LR	1037	135	375	70	70
[Leu1]-Microcystin-LY	1044	135	213	70	70
Microcystin-YR	1045	135	213	70	70
Microcystin-H4yR	1049	135	375	70	70

A microcystin method for LC-UVD was established. The method used LC system B, column D, mobile phase #4 and UVD (detector B). A flow rate of 0.25 mL min^{-1} was used with a column temperature set to 30°C. Gradient elution was used as follows: after a 15 min equilibration with an initial mobile phase (25% B, 75% A), the sample was injected and the percentage was increased linearly to 75% B over 25 min, then to 100% over 0.5 min, and followed by a hold for five min before returning to initial conditions. UVD absorbance was set at 238 nm, with the detector acquiring full spectra across each peak.

2.6.1 Nutritional Supplements

Several nutritional supplements were purchased and analyzed for anatoxin-a and microcystin contamination. Five samples labelled as *Aphanizomenon flos. aquae* and one sample labelled as *Spirulina* were extracted and analyzed using a method to concentrate

potentially low level toxins. Crushed or powdered nutritional supplement (approximately 0.1 g) was extracted using 0.1% AcOH in MeOH (10 mL) according to the method outlined in section 2.4.1. Half of the extract (5 mL) was diluted in 100 mL of H_2O and was passed through an Oasis® HLB 3 cc (60 mg) flangeless cartridge preconditioned with MeOH (3 mL). The column was washed with 5% MeOH (3 mL) and eluted with MeOH (3 mL). The sample eluent was evaporated under nitrogen gas and was reconstituted in 80% MeCN (300 μL). The samples were analyzed with the same MRM transitions described in section 2.6, and EPI scans were used to confirm the identity of transitions. The other half of the extract was analyzed by HILIC-MS/MS using the method described in section 2.3.1.

2.7 RM-BGA production

2.7.1 Anatoxin and microcystin cultures

When screening for anatoxin-a, six algal samples were analyzed to determine those with a high anatoxin-a concentration using HILIC-MS/MS, DNS-LC-MS/MS and DNS-LC-FLD methods. The methods were the same as those listed in section 2.3.1, 2.4.3 and 2.5.1. Microcystin cultures were analyzed with LC-MS/MS, according the method in section 2.6.

2.7.2 Operational method

Great care was taken to prevent the inhalation of toxic algae by the operator. Whenever possible, a glove bag (model 55-1) from Instruments for Research and Industry (Cheltenham, PA, USA) was used to contain the algae. Alternatively, a mask and full protective clothing were worn. Prior to use, all glassware and equipment were

washed multiple times with water and methanol and allowed to dry in an oven at 100°C. The glassware and stainless steel equipment were removed from the oven and allowed to cool to room temperature within a desiccator.

The algae were freeze-dried for 24 hours in a large VirTis general purpose freeze drier (SP Scientific; Warminster, PA, USA) equipped with a 25XL condenser and a Wizard 2.0 data center. Samples were placed on a shelf maintained at room temperature under a vacuum of 15 mTorr. Within an argon filled glove bag, the algal samples were weighed on a top loading balance to a specific mass and combined in a 500-mL stainless steel grinding jar purchased from Retsch (Newtown, PA, USA). The freeze-dried algae were partially ground with a glass pestle. The sample was mixed with a spatula and approximately 0.5 g was removed for analysis using a moisture balance from Ohaus (Parsippany, NJ, USA). Twenty-five stainless steel 20-mm balls (Retsch) were added to the grinding jar, after which it was sealed and placed within a planetary ball mill PM100 (Retsch) and operated at 400 rpm for 5 min. The powdered algae were carefully transferred to a 500-mL glass amber jar though a large stainless steel funnel lined with a wire mesh that was assembled from parts bought at a local hardware store. The funnel was placed on top of the open grinding jar with the 500 mL amber glass jar over the nozzle of the funnel. The entire setup was inverted, allowing the powder to flow through the funnel into the amber jar while trapping the stainless steel balls in the wire trap of the funnel. The amber jar was capped and the powder was homogenized at 32 rpm for 45 min using a Turbula mixer from WAB (Switzerland). Another 0.5 g was taken from the sample after homogenization and analyzed using the moisture analyzer. The

homogenized algae were further freeze-dried overnight and homogenized for 45 min at 32 rpm in the Turbula mixer. Moisture analysis was again conducted on an approximately 0.5 g algal sample.

The homogenized algae were bottled inside a glove bag filled with argon. Algae were taken from the jar using stainless steel measuring spoons (purchased from a local supermarket) that dispensed approximately 400 mg into 10-mL amber bottles, glass type 1 from Wheaton (Millville, New Jersey, USA). The vials were plugged with Wheaton 20 mm, 3 leg ultra-pure stoppers while within the glove bag and crimped with Wheaton 20 mm aluminum seals upon removal. Bottles were numbered and stored in a -80°C freezer. Characterization of the physical features of the RM-BGA with scanning electron microscopy was carried out at the NRC in Halifax courtesy of David O'Neil. Particle size analysis was performed at the NRC in Ottawa courtesy of Floyd Toll.

2.7.3 RM-BGA storage and stability/homogeneity assessment

The short term stability of RM-BGA was assessed through a reverse isochronous study where bottles of the RM were stored at different temperatures (-20, 4, 23 and 40°C) for select periods of time (3, 7, 14 and 27 days). Twenty-seven days after the start of the study, the 3, 7 and 14 day samples were analyzed; all stored samples were collected from each temperature and time point for triplicate analysis along with four -80°C reference materials. The extraction procedure was similar to the procedure outlined earlier (section 2.4.1), using approximately 0.1 g in 10 mL of extraction solvent (0.1% MeOH). Due to the large scale of extractions, a Thermo Sorvall Legend RT+ centrifuge

(Waltham, MA, USA) outfitted with four swinging buckets accommodating up to 48 15-mL conical tubes was used (10 min, 4140 *g*).

The homogeneity of microcystins was assessed using a LC-UVD analysis of 60 extracts in random fashion. The method used LC system B, column D, mobile phase #4 and UVD (detector B). A flow rate of 0.25 mL min^{-1} was used with a column temperature set to 30°C. Gradient elution was used as follows: after a 15 min equilibration with an initial mobile phase (25% B, 75% A), the sample was injected and the percentage was increased linearly to 75% B over 25 min, then to 100% over 0.5 min, and followed by a hold for 5 min before returning to initial conditions. The UVD wavelength was set at 238 nm. A standard mixture containing microcystin-dmLR and microcystin-LR was run for retention time identification. Homogeneity was calculated from the -80°C and -20°C samples, twenty-four in total, each with a 5 µL injection. See Table 2.8 for mass spectrometer conditions.

The stability of the microcystins was assessed through LC-MS/MS using LC system A and a quadrupole mass spectrometer (detector E). The mobile phases and column were the same as the homogeneity study, but 1 µL was injected instead of 5 µL to prevent saturation of the detector. Each of the 60 extractions was analyzed by integration of the microcystin peak areas, using transitions described in section 2.6.

The homogeneity of ATXs present in the RM-BGA was assessed using LC-MS/MS. Samples were diluted twenty-fold using the MicroLab and were run using the HILIC-MS/MS method with a 5-µL injection volume. Stability of anatoxin-a and homoanatoxin-a were also assessed using the LC-MS/MS HILIC-MS/MS method.

2.7.4 Quantitation of anatoxin and homoanatoxin in RM-BGA

Both anatoxin-a and homoanatoxin-a were quantified using three distinct methods: HILIC-MS/MS, DNS-LC-MS/MS and DNS-LC-FLD. Quantitation by HILIC-MS/MS used four samples that had been previously extracted for homogeneity and stability studies and used as -80°C control samples. These four samples were subjected to a 1/10 dilution using the MicroLab with 1-µL HILIC-MS/MS injection volumes. The samples were injected in random order and bracketed by a seven point calibration curve that included a solvent blank. The calibration curve was developed by mixing CRM-ATX with RM-hATX and a three-fold serial dilution. Due to the sensitivity of the instrument, concentrations of 0.131 to 31.2 ng mL^{-1} for anatoxin-a and 0.0939 to 22.3 ng mL^{-1} for homoanatoxin-a were injected in 5-µL volumes. In total, each sample was run six times bracketed within four calibration standards.

Analysis of samples by DNS-LC-MS/MS and DNS-LC-FLD required extraction with a different solvent to avoid formation of dansyl-methanol side products. Four samples were extracted using 50% MeCN instead of MeOH with 0.1% AcOH. A portion of each extract (25 µL) was reacted with DNS-Cl (100 µL of 1 mg mL^{-1} of MeCN) in a mixture of 3-methylpiperidine (0.73 µg mL^{-1}, 25 µL), borate buffer (100 µL), H_2O (25 µL) and MeCN (25 µL). Due to the complex nature of the reference material, a larger volume of DNS-Cl was used to ensure complete reaction with both anatoxin-a and homoanatoxin-a.

The four derivatized samples were run using the same chromatographic conditions developed for DNS-LC-MS/MS (section 2.4.3). A 2-µL injection was used

and each sample was bracketed by calibration standards. Calibration curves were constructed by derivatizing samples containing known amounts of anatoxin-a and homoanatoxin-a, and then performing serial dilution to give responses within the linear range of the instrument for 5-μL injections. The calibration curve consisted of a blank and six points, ranging in concentration of 15.7 ng mL^{-1} to 0.0672 ng mL^{-1} for DNS-anatoxin-a and 11.2 ng mL^{-1} to 0.0480 ng mL^{-1} for DNS-homoanatoxin-a. Each sample was run six times bracketed within four calibration standards that included solvent blanks. The DNS-3-methylpiperidine was used to assess and correct for drift within the samples or standards.

Samples were analyzed using LC-FLD. The standards used for the LC-FLD calibration curve were made from five separate derivatization reactions. A mixture of anatoxin-a (2.48 μg mL^{-1}) and homoanatoxin-a (1.77 μg mL^{-1}) was diluted 3-, 9-, 27- and 81-fold using serial dilution. These four dilutions, along with the stock solution, were derivatized as described above and run as a five-point calibration curve with a blank. The four derivatized samples were run randomly, bracketed by the calibration standards. In total each sample was injected three times using a 20 μL injection, bracketed by four calibration standards. The samples were run using the LC-FLD conditions described in section 2.5.1. A calibration curve was constructed by dividing the peak area of the analyte by that of the internal standard and plotting this ratio against the concentration of the analyte.

2.7.5 Quantitation of microcystins

Microcystins were quantified using LC-MS/MS and LC-UVD. Samples for quantification by both methods were extracted using 75% MeOH. The six samples were diluted five-fold, and injected in 2 µL volumes. A standard mixture of microcystin-RR, microcystin-LR and dmLR was diluted to accommodate the linear range of the instrument with 5 µL injections. Each sample was run randomly within a sequence, bracketed between four calibration standards. All samples were run according to the settings described in section 2.6.

Microcystins quantified by LC-UVD were analyzed using a 1-µL injection volume for samples and a 5 µL injection volume for calibration curve standards. The same standards used for the LC-MS quantitation of microcystins were used for the LC-UVD quantitation. Similar chromatography was used; however, the mobile phase was changed to mobile phase #6.

CHAPTER 3 RESULTS AND DISCUSSION

3.1 Preparation of homoanatoxin-a and other reference standards

The preparation of a homoanatoxin-a reference material was essential for accurate quantitation of samples and for the quantitation of homoanatoxin-a within the freeze-dried reference material. Epoxy and dihydro analogues of anatoxin-a and homoanatoxin-a were also prepared to serve as reference standards for the identification and quantification of ATXs in samples.

3.1.1 Isolation of homoanatoxin-a

The extractions of lyophilized *Oscillatoria formosa* were conducted on two batches, each in four stages. Homoanatoxin-a was efficiently extracted within the first two volumes of 100 and 50 mL (Figure 3.1). To maximize recovery of toxin in the reference material, all four extracts from each batch (Batch A and Batch B) were combined.

The pooled freeze-dried extracts (15 mL for each Batch A and B) were first purified using C18 silica column chromatography; no breakthrough was detected in the loading or washing steps. The majority of the homoanatoxin-a eluted with aqueous 20% MeOH (0.1% TFA) solution (91.8-96.6%), while a small percentage (3.4 - 8.1%) was eluted using an aqueous 50% MeOH (0.1% TFA) (Figure 3.2).

The liquid eluted in Elution 2 was colourless and was retained for future work. The liquid eluted in Elution 3 was slightly yellow in colour and was therefore discarded. Purity scans using mass spectrometry and LC-UVD found Elution 2 to contain several

minor impurities. These were resolved using preparative LC purification on a large (10 mm i.d.) C18-silica column.

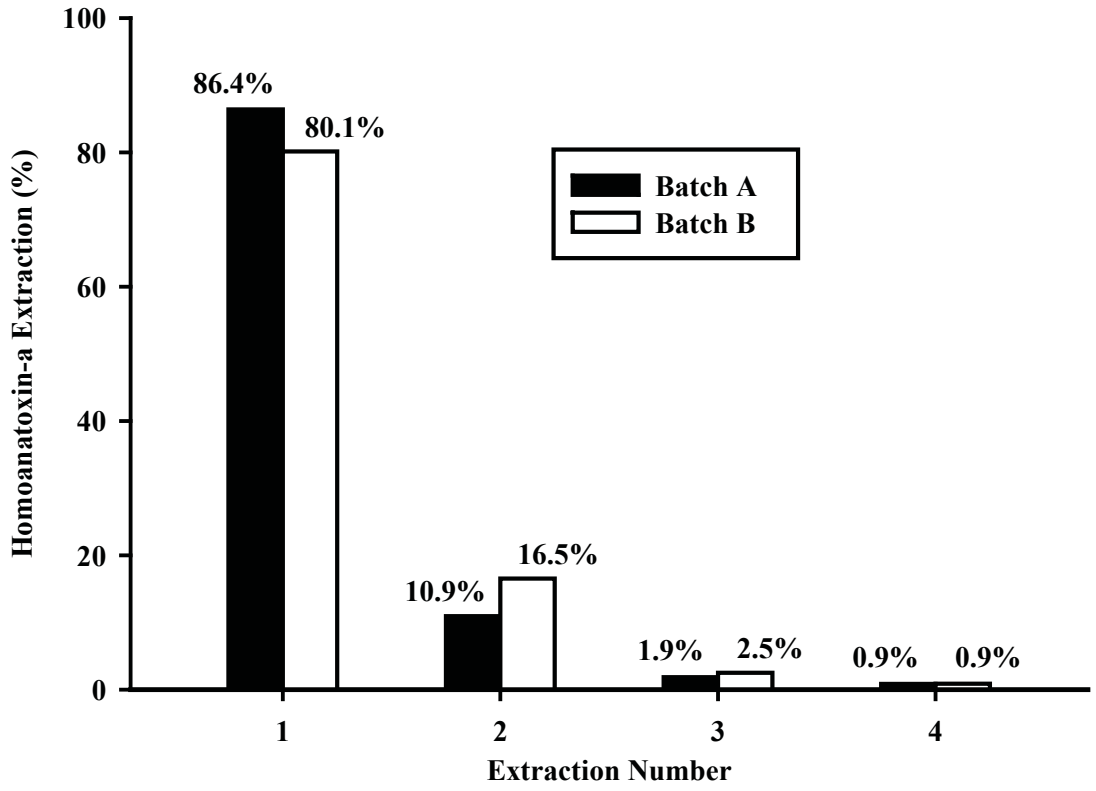

Figure 3.1**:** Percentage of homoanatoxin-a recovered per extraction step. The two extractions (Batch A and B), in aqueous 80% MeOH with 0.1% FA in volumes of 100, 50, 25 and 10 mL corresponded to the extraction numbers 1, 2, 3 and 4, respectively. With correction for volume, homoanatoxin-a recovery was calculated from sample peak areas obtained by HILIC-MS/MS analysis.

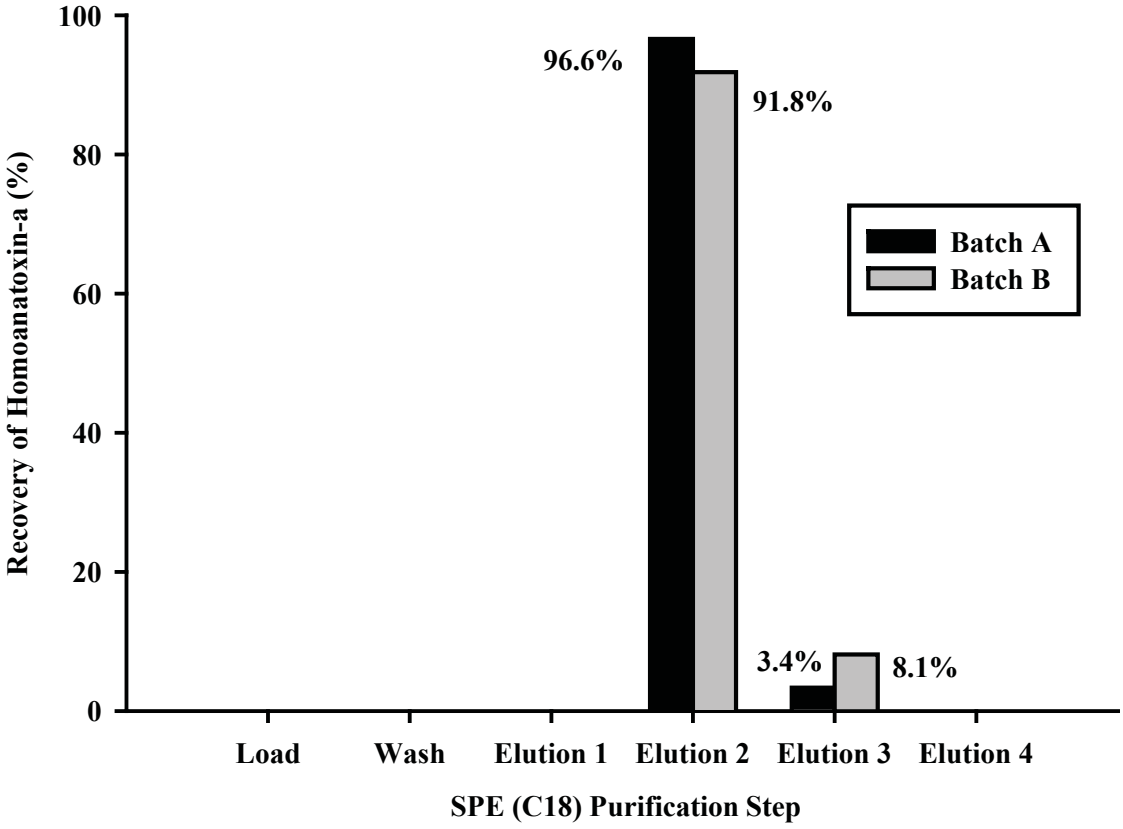

Figure 3.2*:* Recovery of homoanatoxin-a in different C18 purification steps. Solid phase extraction steps correspond to: Load (H_2O), Wash (H_2O + 0.1% TFA), Elution 1 (5% MeOH + 0.1% TFA), Elution 2 (20% MeOH + 0.1% TFA), Elution 3 (50% MeOH + 0.1% TFA) and Elution 4 (80% MeOH +0.1% TFA). Recovery was calculated from peak areas of samples run by HILIC-MS/MS.

3.1.2 Characterization of homoanatoxin-a

The compound isolated by preparative LC-UVD was characterized by several different methods. The UV absorbance spectrum of the material had a λ_{max} of 230 nm, which was characteristic of homoanatoxin-a [90] (Figure 3.3). The λ_{max} of homoanatoxin-a is the same as that of anatoxin-a.

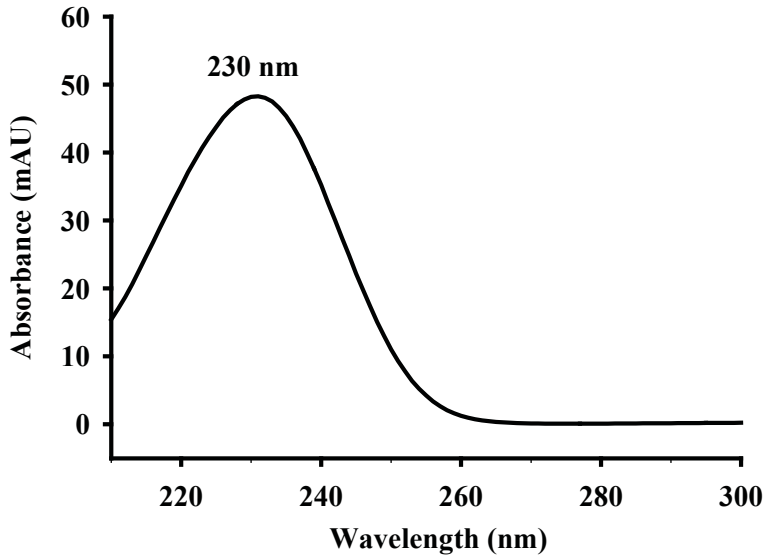

Figure 3.3**:** LC-UV absorbance spectrum of homoanatoxin-a in an isocratic mobile phase of 12.5% methanol with 0.05% TFA. The λmax is 230 nm.

A full scan mass spectrum acquired over *m/z* 50 - 400 showed a base peak at *m/z* 180, consistent with protonated homoanatoxin-a and no significant impurities. The product ion spectrum of this $[M+H]^+$ ion (Figure 3.4) matched the literature spectrum of homoanatoxin-a [91]. Accurate mass determination of the $[M+H]^+$ ion was *m/z* 180.13828 with an error of 0.06 ppm from the calculated m/z of 180.13829 for $C_{11}H_{17}NO$. The accurate masses of all major fragments had errors below 4 ppm (Figure 3.5).

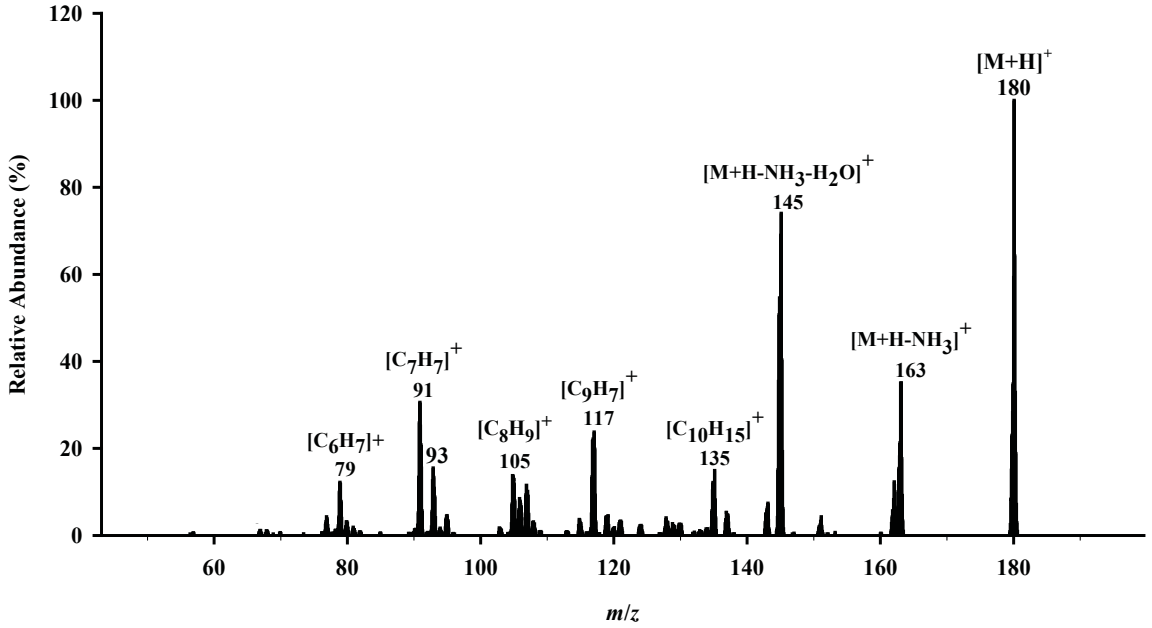

Figure 3.4: Product ion spectrum of the isolated homoanatoxin-a and the assignment of formulas each major fragment ion. A collision energy of 25 eV was used.

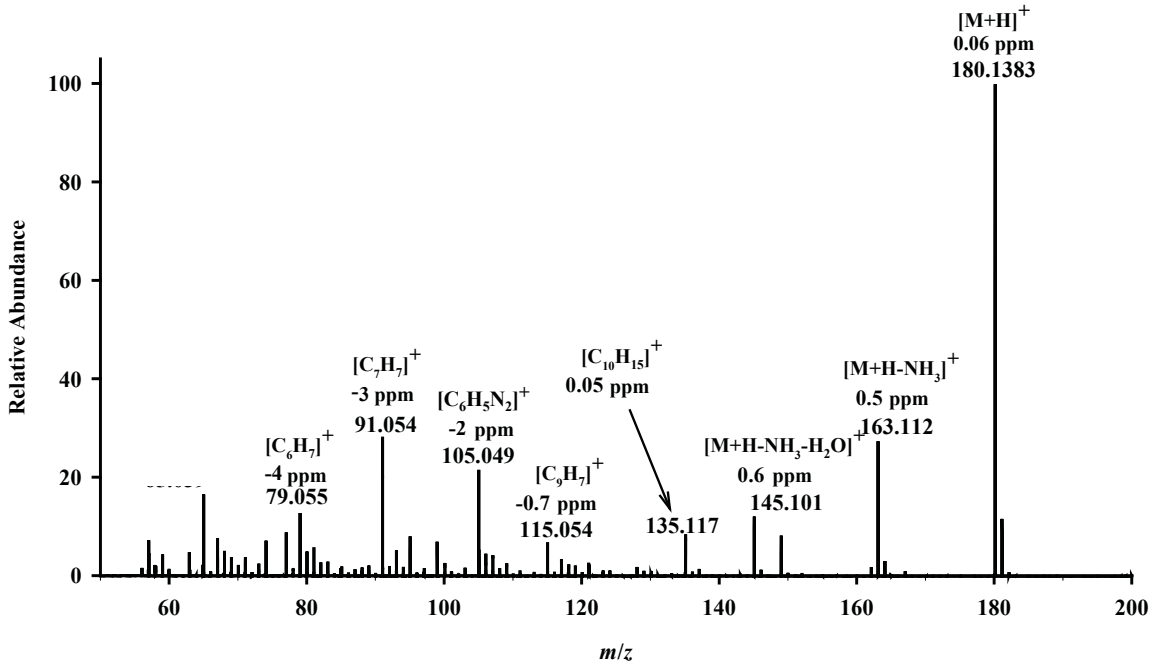

Figure 3.5: Accurate masses of homoanatoxin-a and its fragment ions. Masses are reported with errors in ppm.

Finally, ^{1}H NMR was used to confirm the structure of homoanatoxin-a. The ^{1}H NMR spectrum of the purified material collected at 700 MHz matched the spectrum of homoanatoxin-a published by Skulberg *et al* [92]. Although an exact purity value cannot be assigned to the isolated material, no other anatoxin related compounds were detected by NMR. Small amounts of unidentified impurities were observed by NMR and CLND, but these did not interfere with quantitation of the analyte. Therefore the isolated homoanatoxin-a was considered appropriate for use in preparation of the calibration solution RM.

3.1.3 Stability of homoanatoxin-a

Successful preparation of the homoanatoxin-a RM produced 83 ampoules each with approximately 300 μL of 9% MeOH and 0.01% AcOH (Figure 3.6). Information on the stability of homoanatoxin-a in solution was required as part of a feasibility study for the proposed preparation of a full CRM. This information is important for consumers and suppliers since data on the stability of homoanatoxin-a at various times and temperatures is imperative for both shipping and long term storage specifications and limitations. A previous stability study of the CRM for anatoxin-a found it to be stable at -20°C for up to one year but it was shown to degrade when stored at room temperature and 40°C (unpublished - K. Thomas *et al.*, NRC).

Figure 3.6: Photo of homoanatoxin-a reference material

The results of the homoanatoxin-a stability study spanning 6 months are shown in Table 3.1 and Figure 3.7. Partial decomposition of homoanatoxin-a was observed after 27 days when solutions were stored at 40°C and significantly greater decomposition was obtained after 180 days. After 180 days, partial decomposition was also observed when homoanatoxin-a was stored at 23, 4 and -20°C. Based on structural similarities and the results of a previous anatoxin-a stability study, decomposition of homoanatoxin-a at 23 and 4°C was not unexpected, but the decomposition of homoanatoxin-a at -20°C was not anticipated. Anatoxin-a was stable when stored at -20°C for up to one year, and similar

results were expected for homoanatoxin-a. Further investigation revealed that the homoanatoxin-a samples had been inappropriately moved from one freezer to another that had possible freeze thaw cycles shortly after the start of the experiment. In a similar study by Kozikowski et al [93], homoanatoxin-a stored in an unregulated freezer was shown to decompose faster than homoanatoxin-a stored at room temperature. Alternatively, homoanatoxin-a may be less stable than anatoxin-a. Further tests need to be conducted, but for now the RM-hATX is stored at -80°C as a precaution.

Table 3.1: Homoanatoxin-a stability study. Samples stored at -20, 4, 23, 40 and -80°C for 3, 9, 27 and 180 days in 9% MeOH and 0.01% AcOH. Samples were run with a Luna C18(2), 3 µm, 100A, 150 mm x 4.6 mm column, using 12.5% MeOH and 0.05% TFA in H_2O, 1.0 mL min^{-1}, column temperature of 40°C and 8 µL injection volume. The values reflect triplicate injection of a sample ± the standard deviation of the sample, normalized to the -80°C reference (n=3).

	Time			
Temperature	3 Day	9 Day	27 Day	180 Day
-80°C Reference	1.00 ± 0.01	1.00 ± 0.01	1.00 ± 0.01	1.00 ± 0.01
-20°C	0.996 ± 0.006	1.008 ± 0.006	1.003 ± 0.009	0.964 ± 0.007
4°C	0.99 ± 0.01	0.986 ± 0.007	1.016 ± 0.009	0.985 ± 0.003
23°C	1.011 ± 0.007	1.001 ± 0.006	1.001 ± 0.009	0.968 ± 0.004
40°C	1.015 ± 0.009	0.985 ± 0.006	0.960 ± 0.009	0.810 ± 0.005

Two decomposition products observed in solutions stored at 40°C eluted before homoanatoxin-a at 4.36 and 5.98 min in the LC-UVD chromatogram (Figure 3.8), possibly indicating that the two compounds are more polar than homoanatoxin-a. Absorbance spectra and product ion spectra of each decomposition product provided some information relating to structure (Figure 3.9). The first decomposition product (A) eluting at 4.36 min had a λ_{max} of 230 nm and a $[M+H]^+$ ion at *m*/*z* 196, 16 mass units higher than homoanatoxin-a. This suggested that

oxygen was incorporated into the structure, while still maintaining the conjugated α,β-unsaturated ketone in the parent structure.

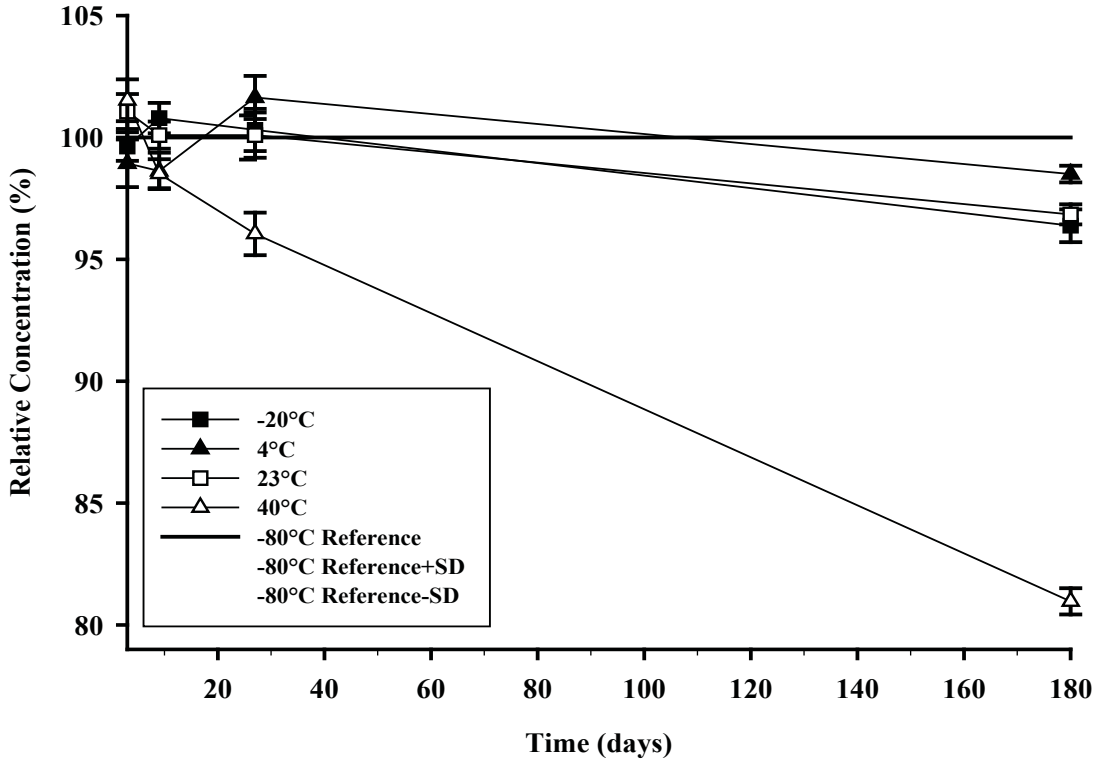

Figure 3.7: Stability of homoanatoxin-a at 3, 9, 27 and 180 days stored at temperatures of -20, 4, 23, 40 and -80°C as assessed through LC-UVD peak areas. Plot of data presented in Table 3.1.

The second decomposition product (B) eluted at 5.98 min and had a λ_{max} of 242 nm with an $[M+H]^+$ at *m*/*z* 194. This chromophore suggested a more highly conjugated structure such as a diene as well as incorporation of oxygen. The structure of (B) may be related to that of (A) although the loss of H_2 in solution chemistry is unlikely.

Other studies have revealed decomposition products of anatoxin-a corresponding to an increase in *m*/*z* of 16 and 14, but the structures were not identified [57, 90].

The molar response of homoanatoxin-a relative to that of anatoxin-a was also tested using LC-UVD. As with LC-MS/MS, the response factors for homoanatoxin-a and anatoxin-a were found to be different. LC-UVD analyses revealed the response of homoanatoxin-a as 88% of the anatoxin-a response. Although both compounds had the same $\lambda_{max,}$, the difference in response is best explained by the different effects of the ethyl versus methyl groups on the conjugated ketone molar extinction coefficient.

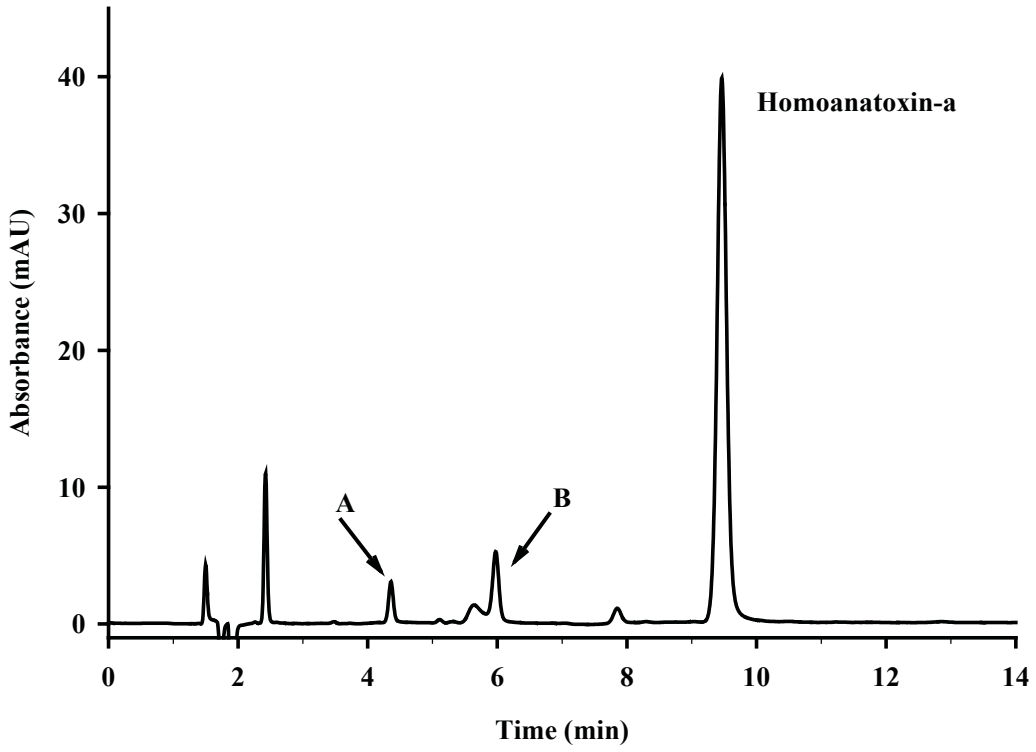

Figure 3.8: LC-UVD chromatogram RM-hATX standard stored at 40°C for 6 months. Decomposition products are observed at 4.36 min ad 5.98 min. The sample was run with a Luna C18(2), 3 µm, 100A, 150 mm x 4.6 mm column, using 12.5% MeOH and 0.05% TFA in H_2O, 1.0 mL min^{-1}, column temperature of 40°C and 8 µL injection volume.

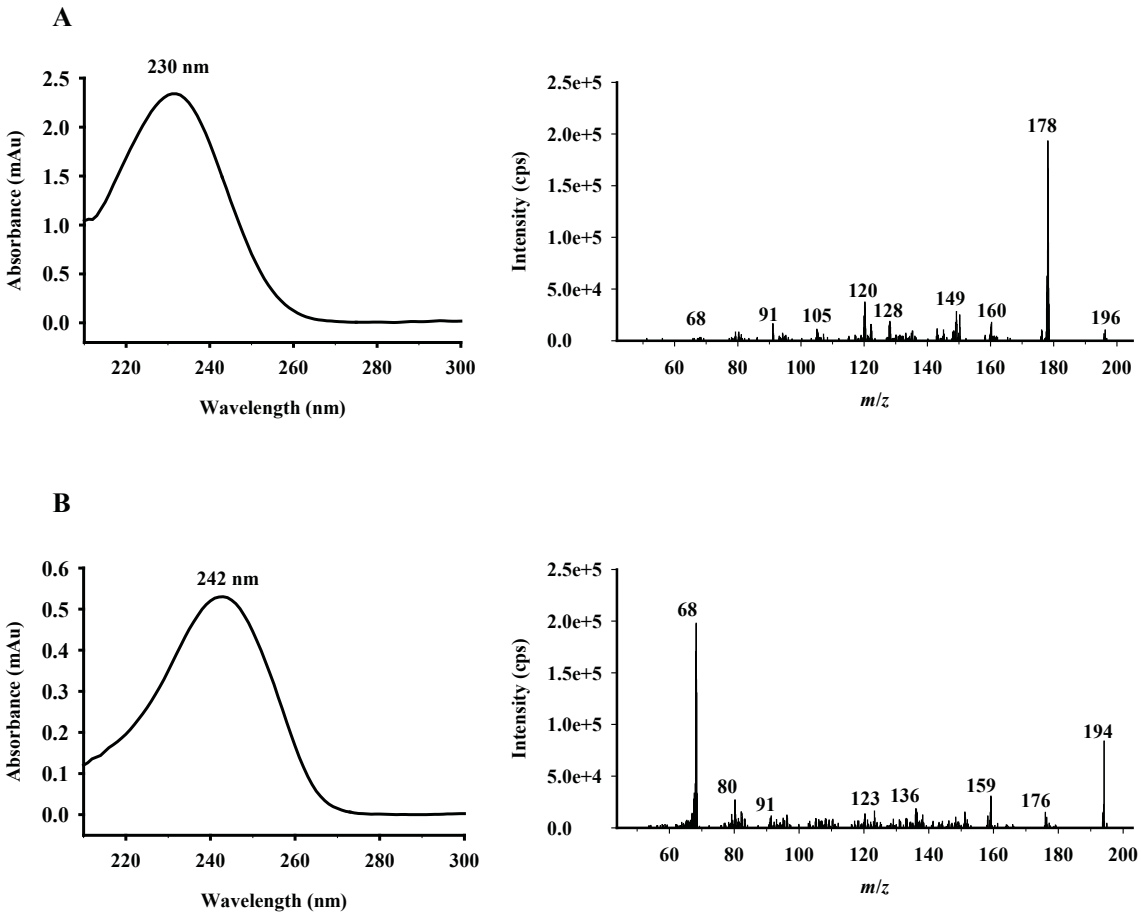

Figure 3.9: (A) LC-UVD absorbance spectrum (left) of product A in 12.5% methanol in 0.05% TFA and (right) product ion spectrum of product A with an $[M+H]^+$ of *m/z* 196. (B) LC-UVD absorbance spectrum (left) of product B in 12.5% methanol in 0.05% TFA and (right) product ion spectrum of product A with an $[M+H]^+$ of *m/z* 194. Samples were run with a Luna C18(2), 3 µm, 100A, 150 mm x 4.6 mm column, using 12.5% MeOH and 0.05% TFA in H_2O, 1.0 mL min^{-1}, column temperature of 40°C and 8 µL injection volume.

3.1.4 Preparation and Quantitation of Homoanatoxin-a RM

Quantitation of the homoanatoxin-a RM was performed using two different methods: (a) qNMR using caffeine as an external standard, and (b) CLND using CRM-ATX as an external standard. Both methods gave evidence of small impurities within the homoanatoxin-a solution and, while they did not interfere with quantitation,

they were noted for better cleanup in future projects. The result from each quantitation indicated the concentration of homoanatoxin-a to be 20.2 ± 0.7 μM (Table 3.2) with the uncertainty calculated according to Equation 3.1 in the Appendix [94].

Table 3.2: Quantitation of homoanatoxin-a in RM-hATX based on qNMR using an external caffeine standard and CLND using anatoxin as an internal standard.

Method	Calibrant	Average μM	Standard Deviation
qNMR	Caffeine	20.0	0.2
CLND	CRM-ATX	20.3	0.3
Average		*20.2*	
Uncertainty		*0.7*	

3.1.5 Synthesis of dihydro and epoxy anatoxin-a and homoanatoxin-a

Dihydro and epoxy products were synthesised for use as qualitative marker compounds to determine retention times and provide product ion spectra for the identification of compounds in samples. By using the hydrogenation method of James *et al*. [58], dihydroanatoxin and dihydrohomoanatoxin were successfully prepared from anatoxin-a and homoanatoxin-a, respectively, and characterized by HILIC-MS/MS (Figure 3.10).

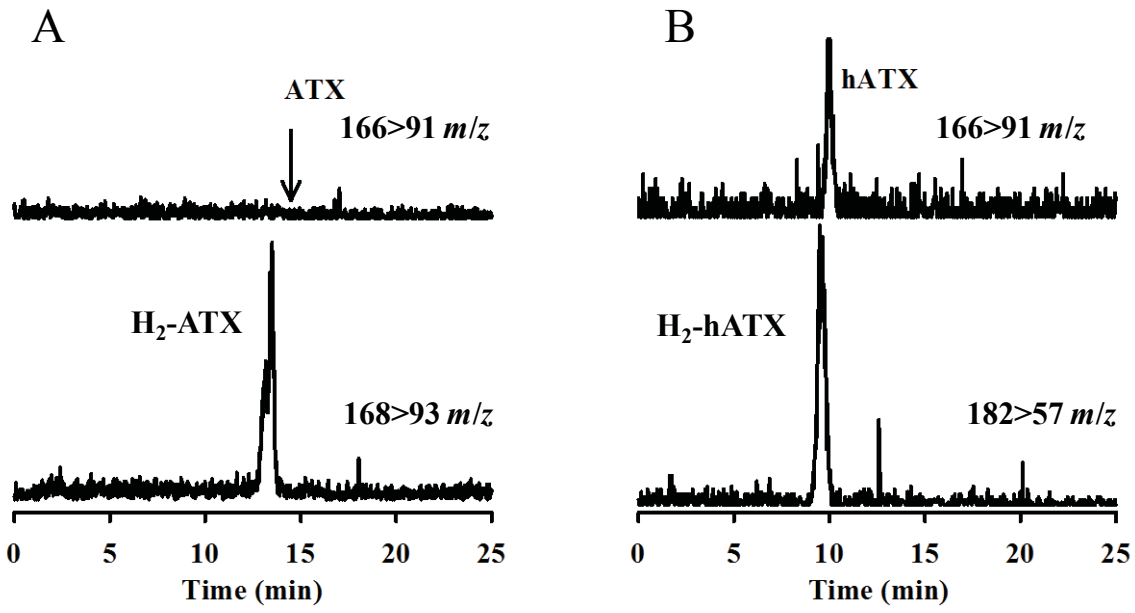

Figure 3.10: HILIC-MS/MS chromatograms of the reactions producing: (A) dihydroanatoxin-a (H_2ATX) from anatoxin-a (ATX); and (B) dihydrohomoanatoxin-a (H_2hATX) from homoanatoxin (hATX).

The epoxide derivatives of anatoxin-a and homoanatoxin-a were prepared using hydrogen peroxide as described by James et al. [58]. The reaction products, epoxy-anatoxin and epoxy-homoanatoxin, were determined by HILIC-MS/MS (Figure 3.11).

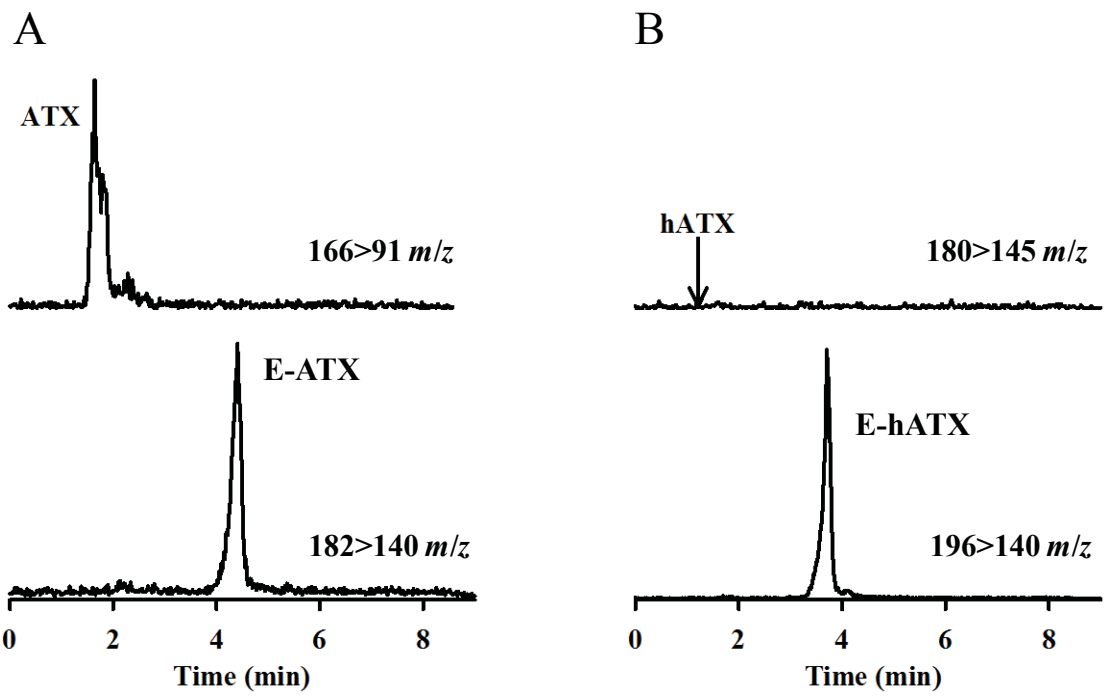

Figure 3.11: HILIC-MS/MS chromatograms of the reactions producing: (A) epoxy-anatoxin-a (E-ATX) from anatoxin-a (ATX); and (B) epoxy-homoanatoxin-a (E-hATX) from homoanatoxin (hATX).

3.2 Dansyl Chloride Derivatization and Cleanup

Dansyl chloride has been used successfully to derivatize amino acids. There are some significant advantages to using dansyl chloride over other reagents. Its reaction with both primary and secondary amines is fast and efficient and it is less expensive ($77 per gram) than many other commercially available reagents. It is highly fluorescent with an excitation wavelength of 350 nm and a large Stokes shift ($\lambda_{emission}$ = 525 nm), which can reduce noise from scatter of the excitation light. The excitation wavelength is also suitable for HeCd laser-induced fluorescence, which is being studied by Dr. M. Quilliam and associates at the NRC. Finally, the dimethylamino functional group ensures good ionization efficiency in electrospray mass spectrometry.

3.2.1 Reaction optimization

Methanol was carefully avoided throughout reaction and sample cleanup steps because it was observed that dansyl chloride slowly reacts with MeOH and the product co-elutes with DNS-anatoxin-a causing a very strong interference in HPLC-FLD. Therefore methanol was replaced by acetonitrile.

Optimization of the procedure for derivatization of anatoxin-a (Figure 3.12) established a reagent concentration of 0.1 mg mL^{-1} in the reaction mixture. This allowed for reaction with analytes and other components of sample while minimizing the production of side products, which were particularly troublesome for LC-FLD analysis. The reaction was allowed to proceed at a pH of 9.4, which is optimal for dansylation reactions [95]. It was determined experimentally that the reaction was robust over the pH ranges of 8.9–9.6. The reaction was performed in an amber glass vial, which shielded the reagent from light, as some studies have indicated the occurrence of side products when exposed to light [96].

One consideration in optimizing the reaction was the amount of organic co-solvent required in the reaction mixture. In early experiments, it was observed that dansyl chloride was not sufficiently soluble when the organic component was less than 40%. It was determined that 50% acetonitrile must be maintained in the reaction mixture to prevent precipitation.

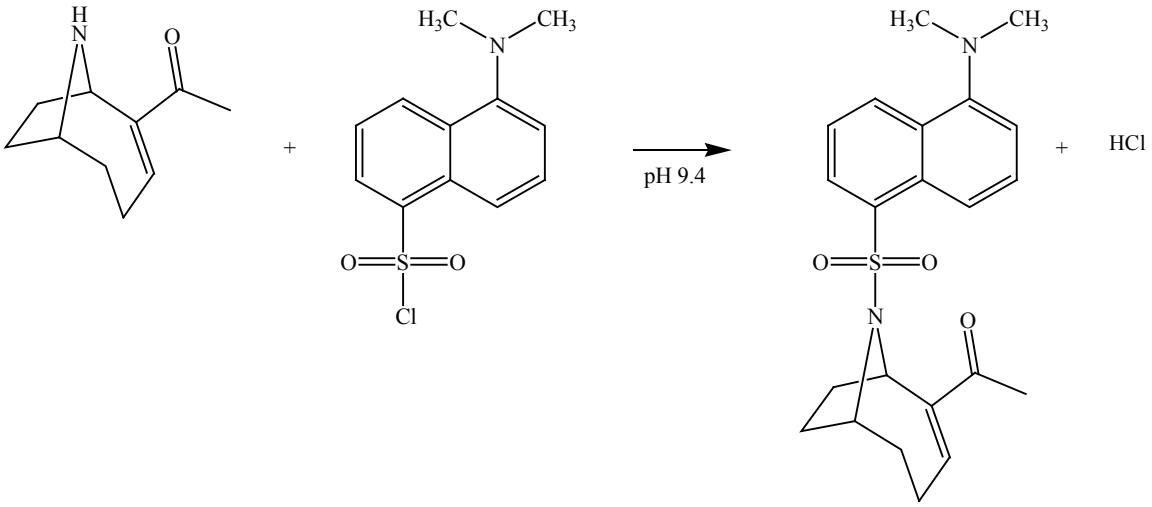

Figure 3.12: Reaction of anatoxin-a and dansyl chloride in borate buffer (pH = 9.4) producing the derivatized product, DNS-anatoxin-a.

3.2.2 Reaction Cleanup

The traditional liquid-liquid extraction (LLE) cleanup used for amino acids, in which hexane is used to extract excess reagent, is not appropriate for cleanup of dansyl anatoxins. The dansyl derivatives of anatoxins are non-polar and, as a result, both the derivative and the excess derivatization reagent will partition into the organic phase. Another issue with the LLE is that it is labor intensive. Several alternative methods were explored for removal of excess derivatization reagents from the reaction. Initial attempts to quench excess DNS-Cl by the addition of aqueous ammonia or amines gave intense and broad chromatographic peaks that tailed extensively and masked all analytes within the sample. Column deterioration can also occur when using basic samples (> pH of 8). Additionally, when working with high concentrations of salts and reagents in LC-MS, there was concern about contamination of the ion source, which can cause decreases in sensitivity and significant drift throughout a sample set. An additional goal of removing salts was established in the method development.

A method previously explored by another student, M. L. Tremblay, was revisited. This involved using a quenching reaction in which excess DNS-Cl was reacted with aminopropyl-silica packed in a centrifuge filter. After reaction, the reagent remained covalently bound when dansylated analytes were eluted from the centrifuge filter. Unfortunately, the dansylated analytes could not be separated from salts with this method. Therefore, in a second step the dansylated analytes were retained on a column packed with hydrophobic Oasis-HLB, allowing salts to pass through. Overall, the spin filter/Oasis-HLB method was effective at removing the derivatization agent and reducing salt levels. Unfortunately higher costs and errors associated with sample loss with this two-step procedure were not ideal.

Another approach was then examined in which DNS-Cl quenching and salt separations could be accomplished in one step using a Phenomenex Strata X-AW column. The excess DNS-Cl reacted with the primary and secondary amines in this packing material and was permanently immobilized, while the dansyl derivatives were adsorbed on the hydrophobic polymeric stationary phase, allowing salts to be washed away (Figure 3.13). More than 98% of the dansylated analyte could then be eluted from the cartridge using 3 mL of MeCN (Figure 3.14). The organic elution allowed for evaporative pre-concentration under nitrogen and solvent exchange prior to analysis. Analysis after the reaction and cleanup with this method showed no detectable levels of reagent or unreacted anatoxin-a, indicating complete reaction of anatoxin-a, effective removal of the reagent, and quantitative recovery as the dansyl derivative.

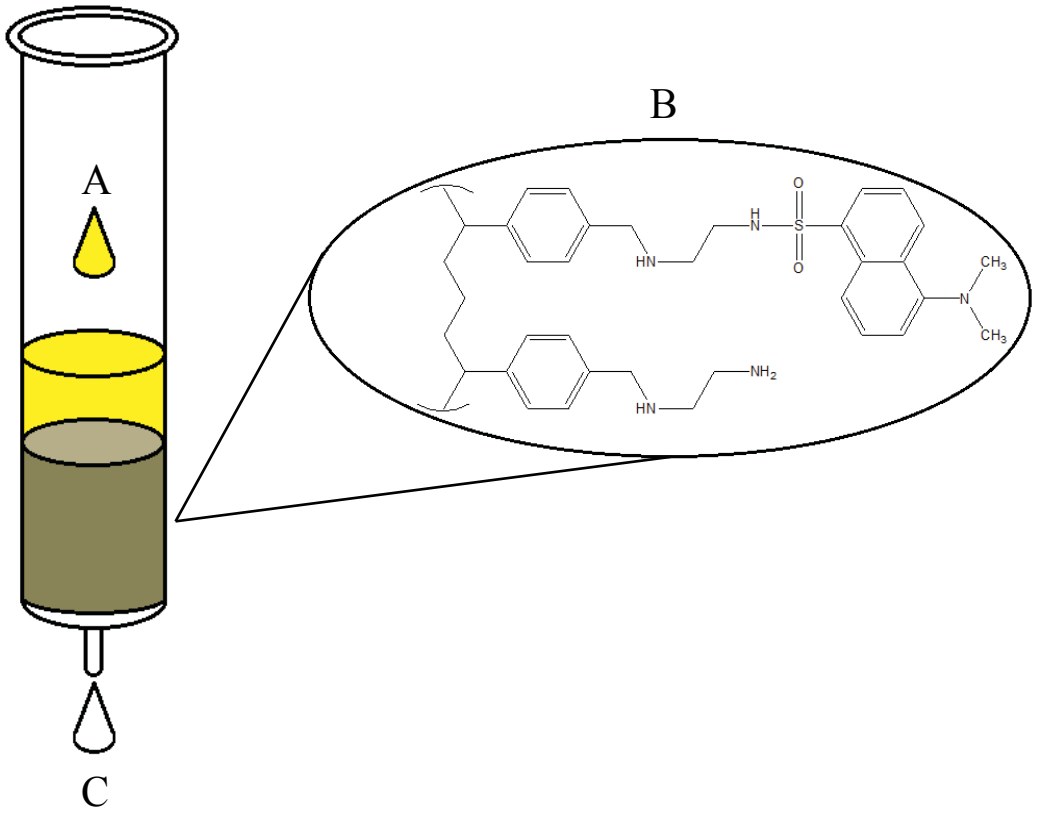

Figure 3.13: Optimized DNS-Cl quenching method with the Strata X-AW column: A) Reaction mixture was loaded onto the column. The reaction mixture was a yellow colour prior to quenching excess derivatization reagent; B) Excess dansyl chloride in the mixture reacts with the primary and secondary amines of the stationary phase, while derivatized analytes were retained through hydrophobic interactions; C) The liquid eluted was free from excess derivatization reagent because of stationary phase quenching and derivatized analyte due to retention on stationary phase.

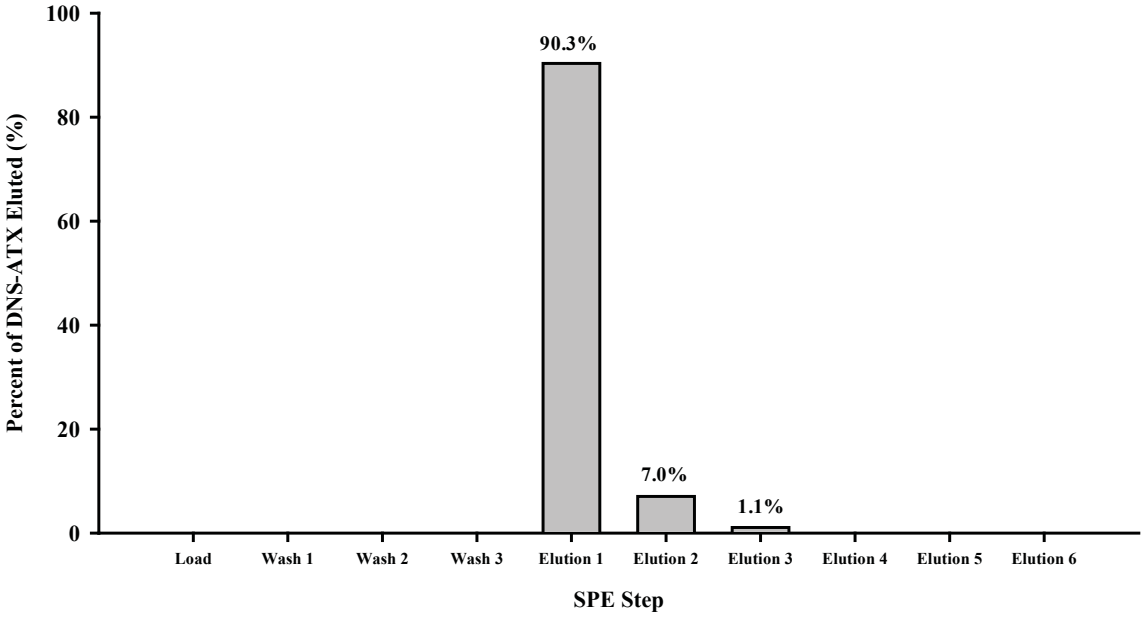

Figure 3.14: Percentage of DNS-anatoxin-a eluted at each step through the optimized Strata X-AW SPE method. The column was preconditioned with 5 mL of MeCN followed by 3 mL of borate buffer (pH = 9.4). The reaction mixture (0.5 mL, 50% MeCN) was loaded and slowly passed though the column. A 3 mL wash of 30% MeCN in water was used to wash out the reaction vial and then passed through the column. After being sucked dry to remove water from the column, MeCN was then passed through the column to elute the analyte, which eluted quantitatively within 3 mL.

3.3 DNS-LC-MS/MS Method

3.3.1 Mass Spectrometer Optimization

Dansyl derivatives of anatoxin-a and homoanatoxin-a gave strong $[M+H]^+$ ions at *m*/*z* 399 and 413, respectively. Product ion spectra of the derivatives (Figure 3.15) and had several common ions due to the similar structures. The spectrum of the dansyl derivative of phenylalanine, a potential isobaric interference for anatoxin-a (Figure 3.15), showed the formation of several different ions. Notably the base peak of *m*/*z* 157 observed in DNS-phenylalanine was not observed in the product ion spectrum of DNS-anatoxin-a and provided an improved means of distinguishing these compounds.

Selection of the ions to be used in selected reaction monitoring (SRM) experiments was based on ion abundance and uniqueness. The transitions selected for quantitative purposes were *m*/*z* 399→170 and *m*/*z* 413→170 for DNS-anatoxin-a and DNS-homoanatoxin-a, respectively. The following transitions were deemed suitable for qualitative confirmatory purposes: *m*/*z* 399→301 and 399→261 for anatoxin-a, and *m*/*z* 413→301 and 413→261 for homoanatoxin-a. The anatoxin-a response in the SRM mode was optimized in the mass spectrometer by varying declustering potential (DP) and collision energy (CE) voltages through a grid search experiment. SRM response at each setting was recorded and a contour plot was constructed for DNS-anatoxin-a (Figure 3.16). Since the two anatoxin analogues have very similar degrees of fragmentation and a common fragment ion at *m*/*z* 170 in their product ion spectra and because we were limited to the anatoxin-a standard in the early stages, the same DP and CE settings were selected for homoanatoxin-a, as well as the other analogues. As indicated in Figure 3.16, higher peak areas were observed at a CE setting of 35 eV, however the highest peak area occurred with DP settings of 30 V and 65 V. A DP setting of 65 V was selected because higher signal to noise ratios were observed at the higher DP setting.

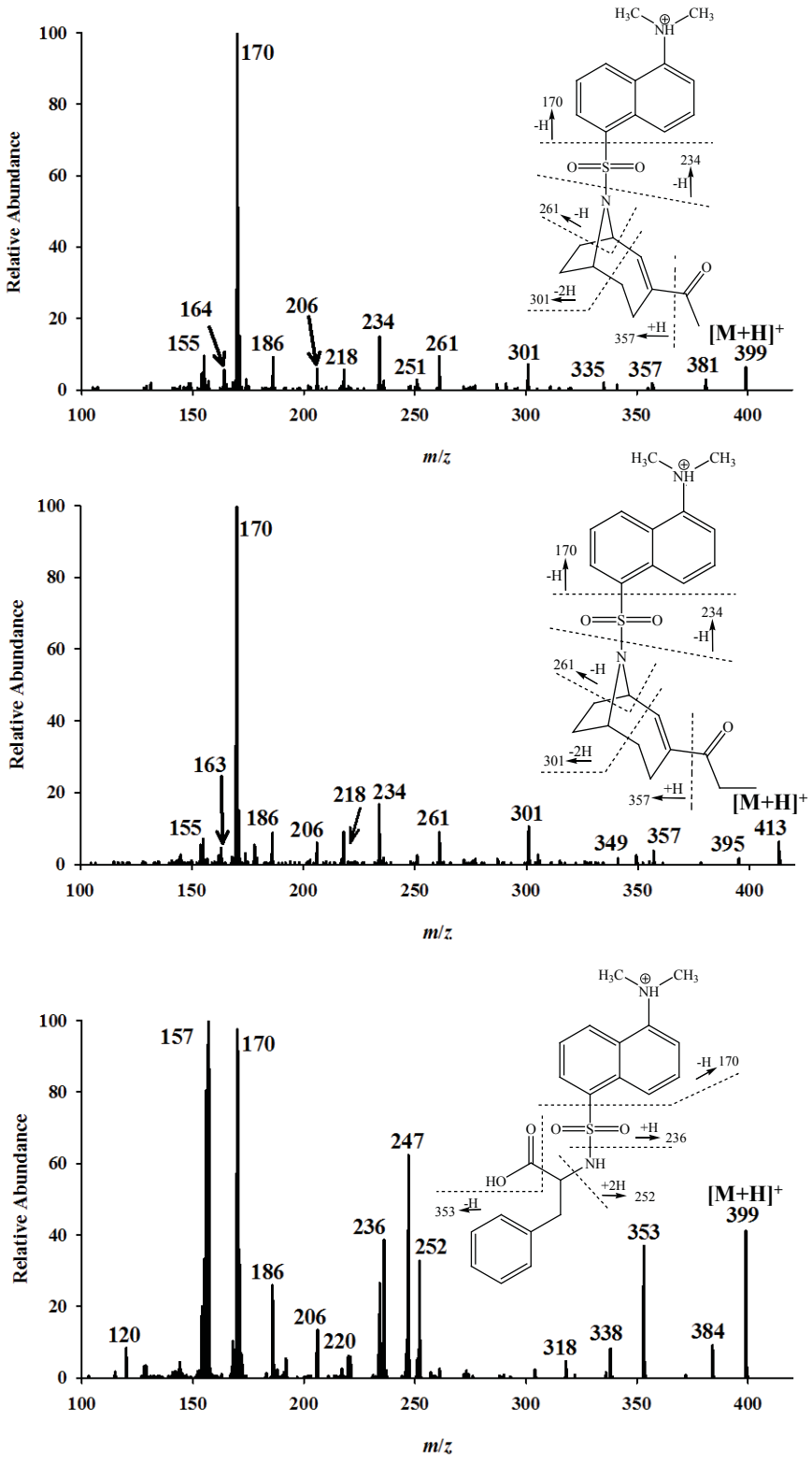

Figure 3.15: Product ion spectra of the $[M+H]^+$ ions of DNS derivatives of anatoxin-a (top), homoanatoxin-a (middle) and phenylalanine (bottom).

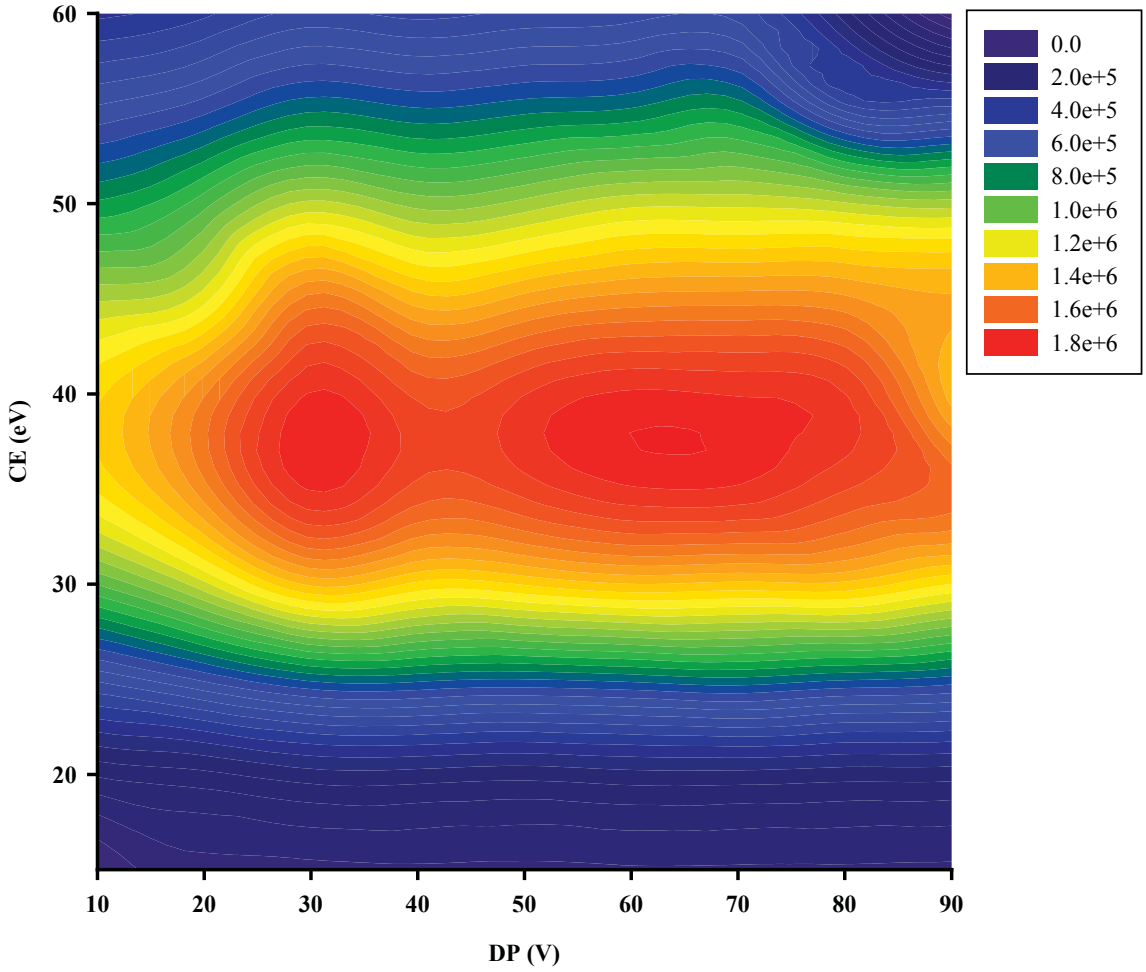

Figure 3.16: Contour plot constructed by altering the DP (V) and CE (eV) voltages while recording the response for *m/z* 399→170. Contours represent the SRM response of dansylated anatoxin-a.

3.3.2 LC-MS/MS Method

The Luna C18 silica column selected for LC-MS/MS provided good peak shapes; a 50 mm x 2.0 mm i.d. column size gave fast analysis at a low flow rate (0.2 mL min^{-1}). Selection of an appropriate mobile phase was important for successful LC separation of all analytes in addition to optimal mass spectrometry detection. An acidic (pH = 2.3) mobile phase was used for analysis based on favorable peak separation, as well as efficient ionization of the analytes. The mobile phase concentration of 60% organic was

selected because this allowed for sufficient retention and elution of analytes in a reasonable time.

Synthesized dihydro and epoxy anatoxin-a and homoanatoxin-a analogues were dansylated to determine retention times. Derivatization reactions were successful for the dihydro analogues (Figure 3.17), but the epoxy analogues were not successfully derivatized. The unsuccessful derivatization of the epoxy analogues may be due to a problem with the synthetic procedure used or it may be that the procedure caused a decomposition of the standards. It is curious however that later work on algal samples (see section 3.3.4) revealed the presence of possible epoxy analogues by HILIC-MS/MS and dansylation of these samples yielded peaks that gave retention time and spectra that supported their assignment as epoxy analogues. More effort must be made to prepare authentic epoxy analogue standards and show their reactivity with dansyl chloride.

The sample of dihydroanatoxin-a prepared by catalytic hydrogenation gave two peaks upon chromatography (Figure 3.17). The two peaks were observed a ratio of 62:38 (first isomer : second isomer). The presence of dihydro isomers was noted in literature by James et al. [58], as detected by LC-FLD detection after derivatization. These diastereomers (Figure 3.18) are formed by the creation of a third chiral center in the hydrogenation of the double bond in anatoxin-a and homoanatoxin-a. The two diastereomers will have different physical and chemical properties and can therefore be separated by liquid chromatography.

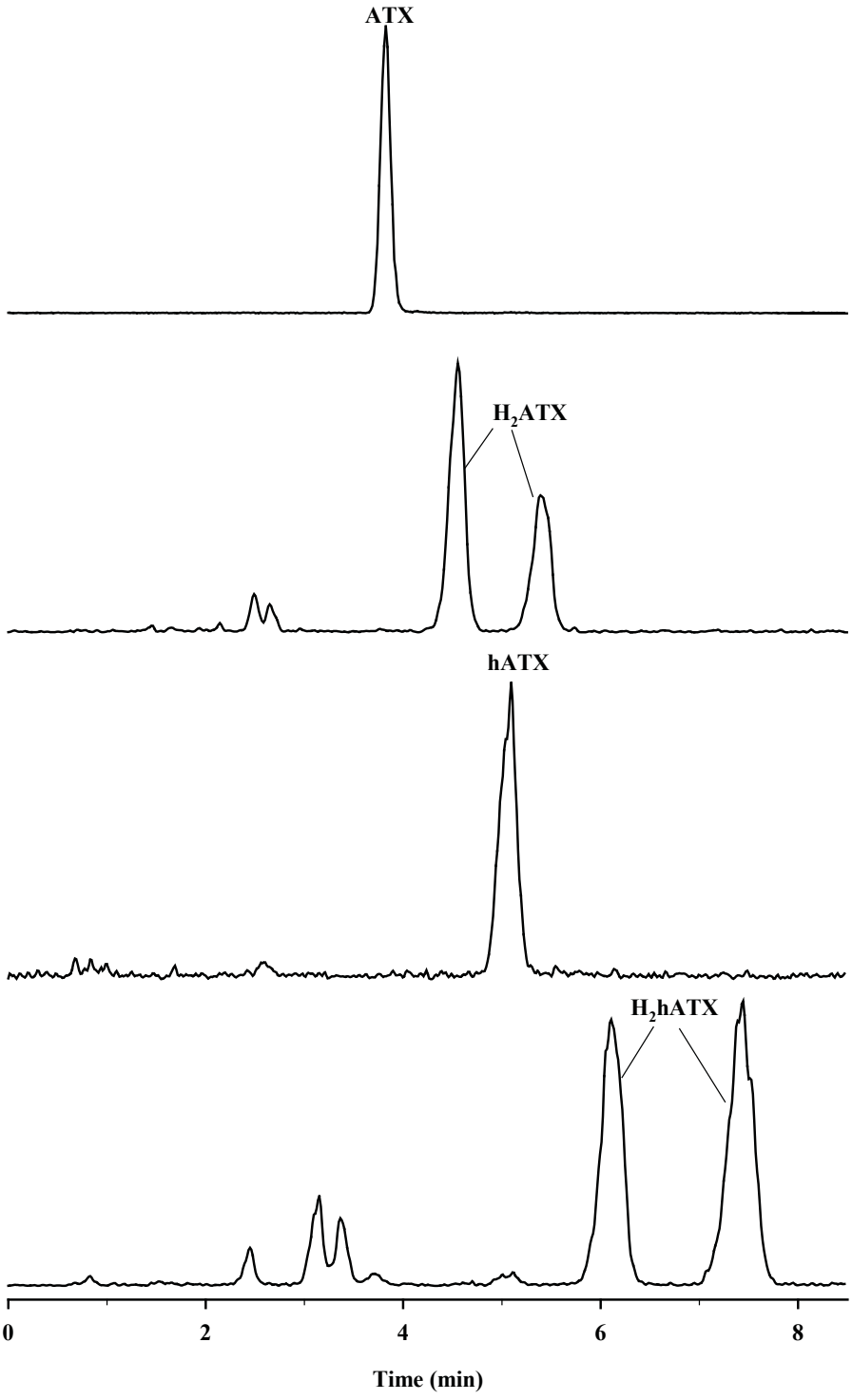

Figure 3.17: LC-MS/MS SRM chromatograms of dansylated standards from top to bottom: anatoxin-a (ATX), dihydroanatoxin-a (H_2ATX), homoanatoxin-a (hATX) and dihydrohomoanatoxin-a (H_2hATX).

R = CH_3 or CH_2CH_3

Figure 3.18: Structures of the diastereomers of dihydroanatoxin-a (R = CH_3) and dihydrohomoanatoxin-a (R = CH_2CH_3).

The relative molar responses of the dansyl derivatives of anatoxin-a and homoanatoxin-a were measured using LC-MS/MS analyses of accurately mixed standards. The DNS-homoanatoxin-a had 89.1 ± 2.5 % of the response of the DNS-anatoxin-a signal using SRM (Figure 3.19). The difference in response was possibly due to differences in structure that could affect the ionization efficiency or the degree of fragmentation following collision induced dissociation.

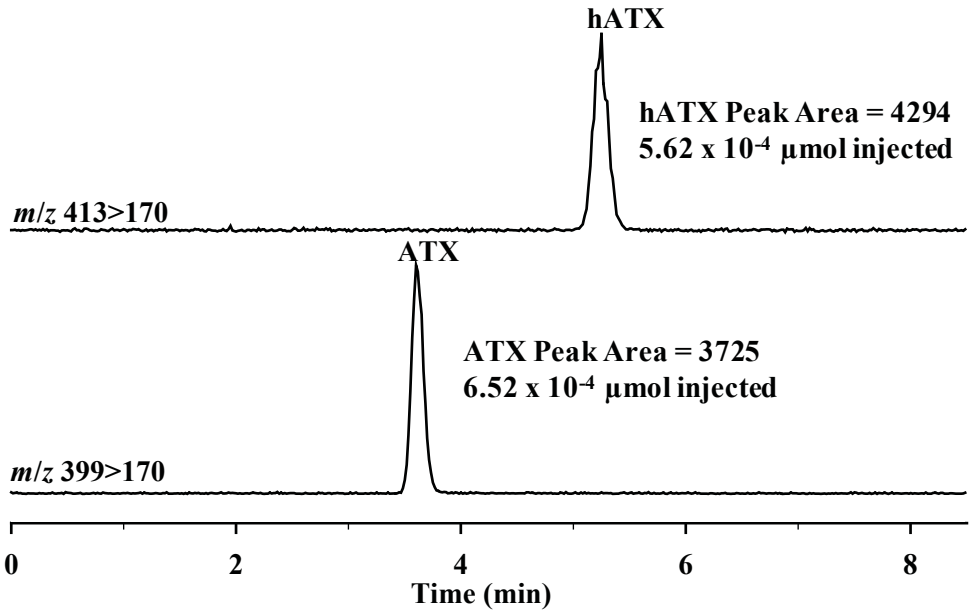

Figure 3.19**:** Mass chromatograms for the LC-MS analysis of a mixture of homoanatoxin-a (hATX) to anatoxin-a (ATX) standards as DNS derivatives. These data were used to determine relative molar response.

3.3.3 Internal Standards

For quantitative analysis with LC-MS/MS, internal standards can be used to deal with matrix effects that are commonly observed with electrospray ionization. Pyrrolidine, piperidine and 3-methylpiperidine were tested as possible internal standards for anatoxin-a and homoanatoxin-a. As shown in Figure 3.20, the similar retention of pyrrolidine to that of anatoxin and the matching retention time of piperidine with that of homoanatoxin-a and piperidine could allow for the correction of matrix effects for these two toxins. 3-Methylpiperidine can also be used as an additional internal standard for retention time correction, injection volume correction and assessment of the derivatization reaction.

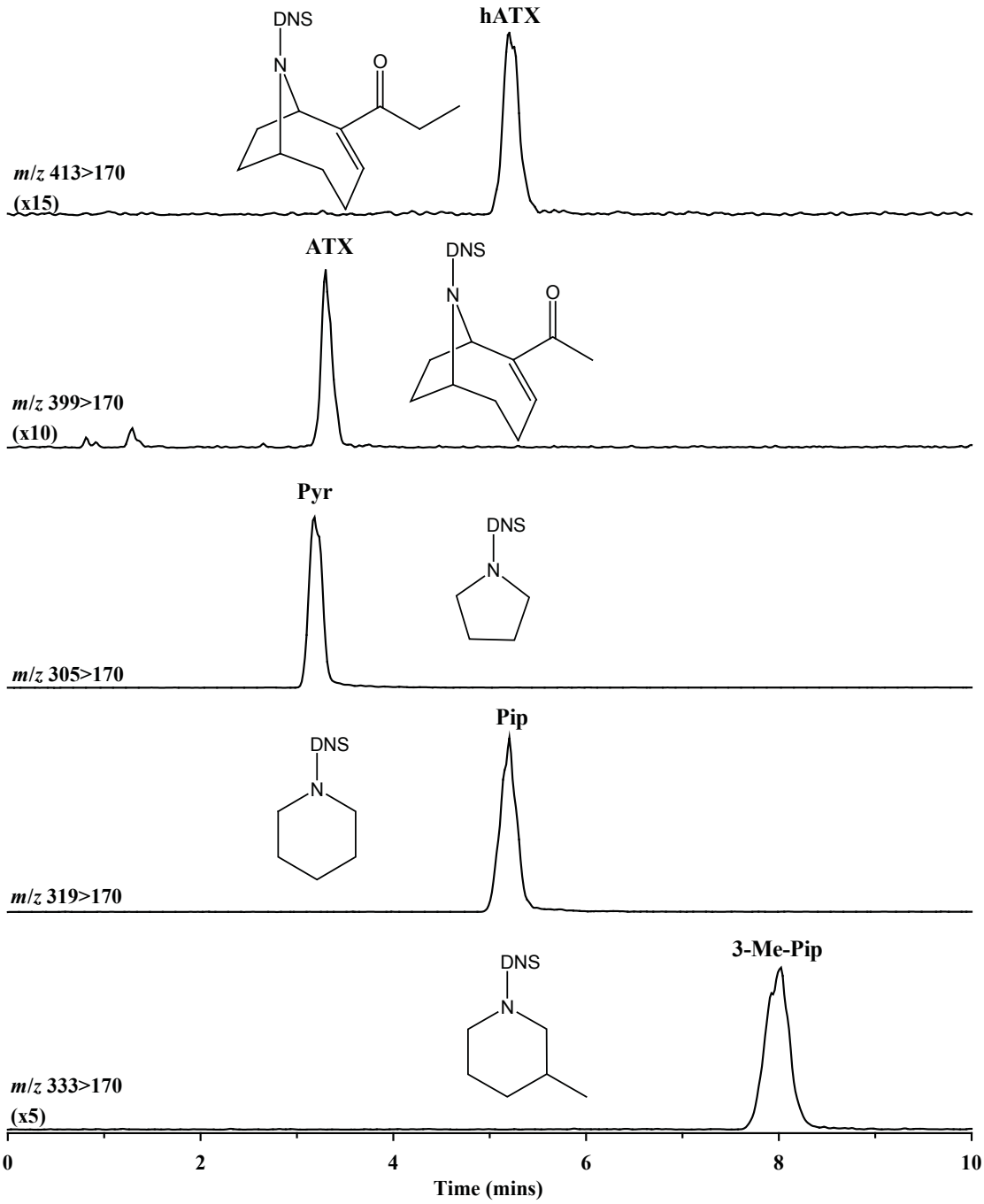

Figure 3.20: LC-MS/MS chromatogram of dansylated (DNS) samples and standards (from top to bottom): homoanatoxin-a (hATX), anatoxin-a (ATX), pyrrolidine (Pyr), piperidine (Pip), 3-methylpiperidine (3-Me-Pip). The overlap in retention time of dansylated Pyr and Pip with the anatoxins allows for matrix effect correction in extremely complex samples.

3.3.4 Quantitative Performance

Method assessment of the LC-MS/MS method provided crucial information to assess the linearity, accuracy, limits of detection and quantitation of the method. Linearity experiments found analysis of the DNS-anatoxin-a analogue to be highly linear over the range of 9.7 pg mL^{-1} to 42 ng mL^{-1} with an R^2 value of 0.999994. Examining spikes (6.6 - 1598 ng g^{-1}) of anatoxin-a in extractions of freeze-dried algae found the accuracy of the method to be very good (94-102%).

To evaluate the suitability of the method for the analysis of trace amounts of toxins in water, the MAC of anatoxin-a within drinking water was first considered. With a MAC of 6 μg L^{-1} [97] established in New Zealand by the Ministry of Health, a successful new method should provide a strong signal at this concentration such that lower levels can be detected as a warning in screening programs. Analysis of a simulated water sample with an anatoxin-a spike of 6 μg L^{-1} gave a recovery of 102% and a signal to noise ratio (S/N) of 478 (Figure 3.21). It should be noted that DNS-phenylalanine was detected in the *Microcystis* sample but eluted much earlier than DNS-anatoxin-a.

The limit of detection (LOD, which was defined as the concentration of analyte required to give a signal 3 times the noise in the baseline) and limit of quantitation (LOQ, which was defined as 3 x LOD) for the underivatized samples using HILIC-MS/MS were 250 ng L^{-1} and 750 ng L^{-1}, respectively, while the LOD and LOQ for the derivatized samples were 20 ng L^{-1} and 60 ng L^{-1}, respectively. It should be noted that both methods were able to detect and quantify well below the MAC of anatoxin-a (6 μg L^{-1}). The lower values for the derivatized sample can be attributed to less ESI noise experienced by the

derivatized analytes due to the higher molecular weight of the compounds and increased ionization efficiency provided by the dansyl group. There is significance in having LOQ values well beneath the MAC, as detecting increasing levels of anatoxin-a within water bodies known to produce anatoxin-a allows scientists to suggest proactive avoidance of these contaminated water bodies to people and livestock.

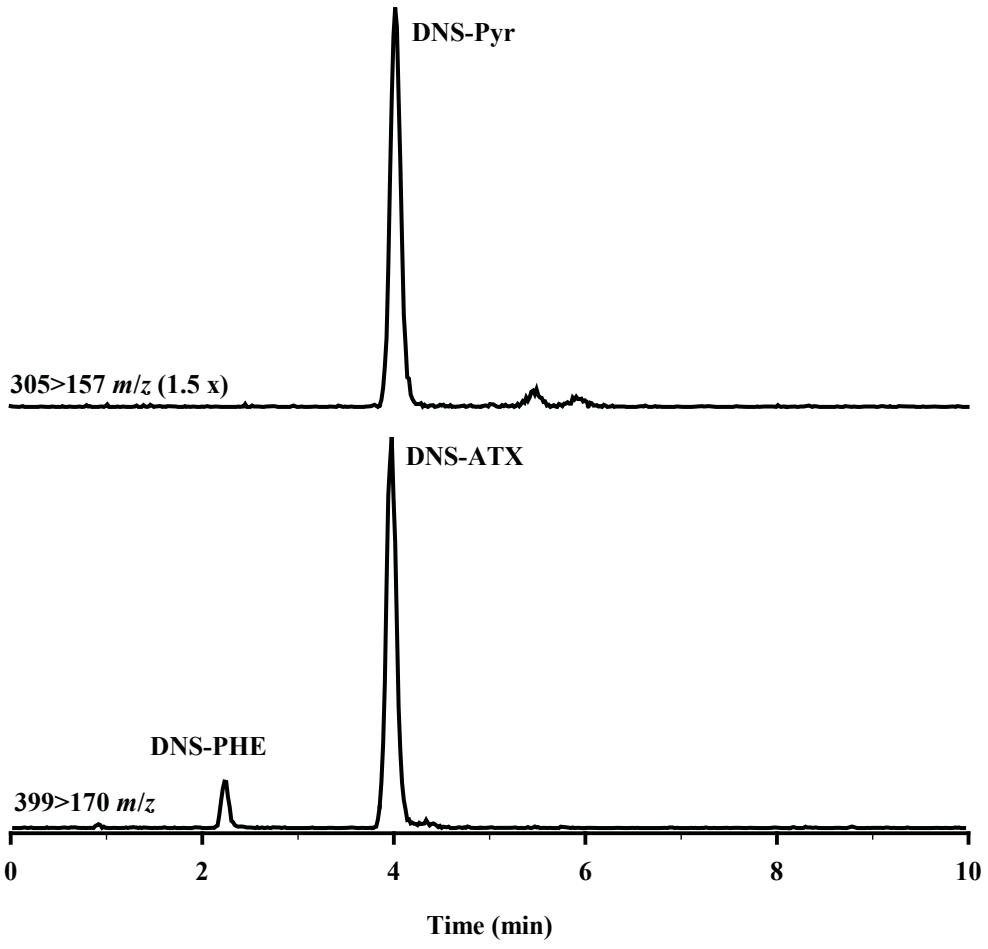

Figure 3.21: LC-MS chromatogram of a dansylated sample prepared by dissolving 180 mg of freeze-dried Microcystis in 10 mL of H_2O and spiking with anatoxin-a (DNS-ATX; 6 µg mL^{-1}, $9.1x10^{-12}$ mol) and IS (DNS-Pyr) ($7.0x10^{-12}$ mol). Phenylalanine (DNS-PHE) was also detected.

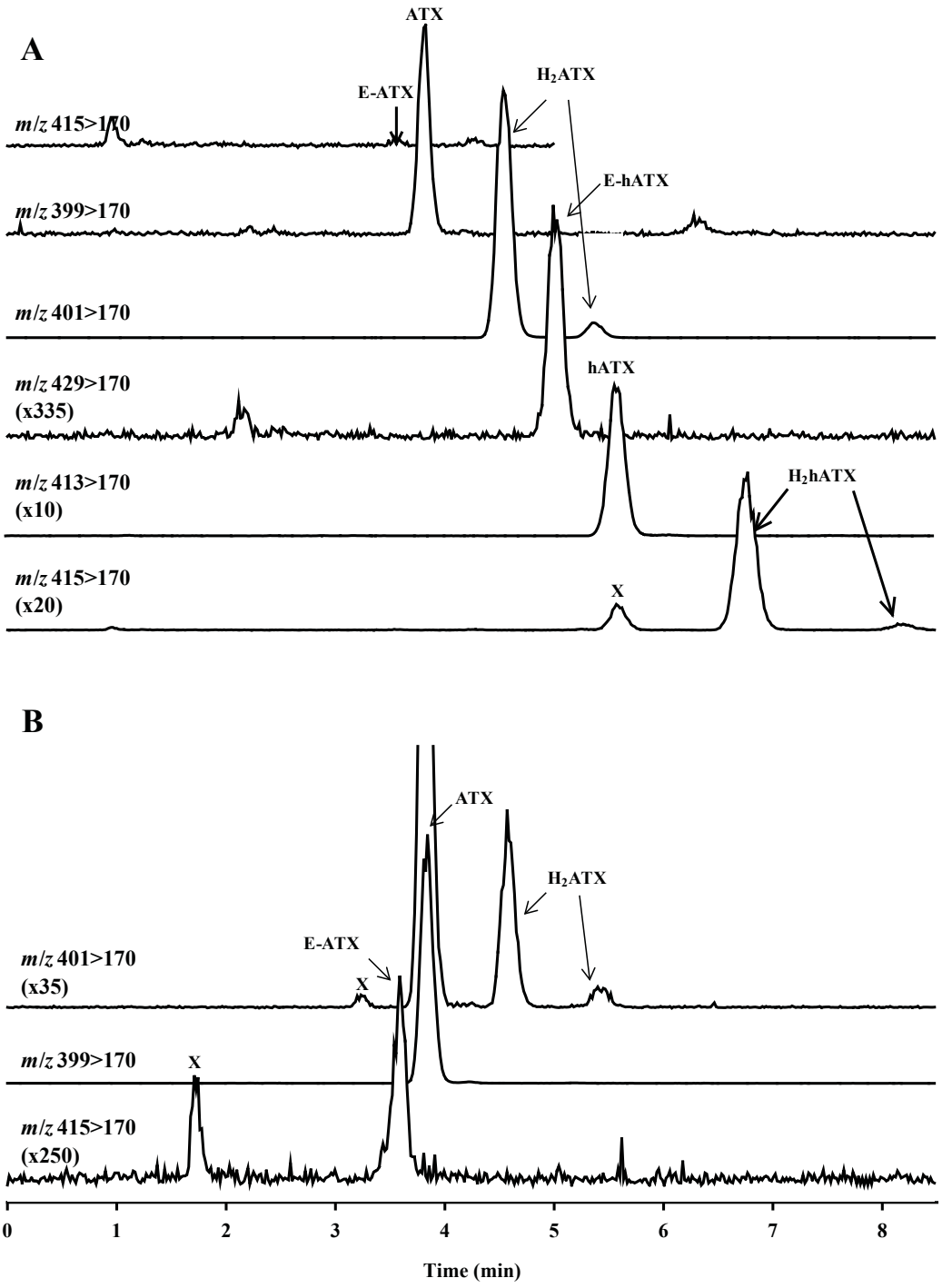

Figure 3.22: LC-MS/MS (SRM) of anatoxins present in a dansylated field sample from (A) Ashley River in New Zealand. (B) *Phormidium* collected in 2005. Internal standard not used in this experiment. From top to bottom: epoxy-anatoxin-a (E-ATX) transition, anatoxin-a (ATX), dihydroanatoxin-a (H_2ATX), epoxy-homoanatoxin-a (E-hATX), homoanatoxin (hATX) and dihydrohomoanatoxin-a (H_2hATX), dihydroanatoxin-a (H_2ATX), anatoxin-a (ATX) and epoxy-anatoxin-a (E-ATX). 'X' represents interferences in the chromatogram.

Application of the DNS-LC-MS/MS method to two samples of algae is shown in Figure 3.22. An 8.5 minute analysis allowed the resolution and selective detection of each analyte and was fast enough to allow screening of multiple samples within an hour. Analysis of a field sample taken from the Ashley River in New Zealand revealed five of the six anatoxin analogues. Epoxy-anatoxin-a was not found in the Ashley River sample, but it was found in a sample of *Phormidium* (collected 2005) in New Zealand. The retention pattern, in order of elution was: epoxy-anatoxin-a, anatoxin-a, dihydroanatoxin-a, epoxy-homoanatoxin-a, homoanatoxin-a and dihydrohomoanatoxin-a. This same retention pattern was also observed by James et al. [58] while using the NBD-F derivatization reagent.

Dihydroanatoxin-a field samples had a ratio of 96:4, with the first eluted diastereomers as the major isomer in the case of field samples (Figure 3.22). The detection of primarily one dihydroanatoxin-a diastereomer in field samples suggests that addition of hydrogen to anatoxin-a occurs in a specific orientation, which is consistent with enzymatic catalysis. Similarly, two diastereomers with a ratio of 97:3 were separated upon chromatography for dihydrohomoanatoxin-a (Figure 3.22).

The quantitation results from the underivatized and derivatized analyses (Table 3.3) were similar for both methods. Anatoxin-a analogues were found in the survey of six algal samples. The genera of algae collected along the Ashley River and Hutt River (New Zealand) are unknown, although it was likely that there was more than one present within the samples due to the various analogues observed within the samples. Several slight discrepancies were observed between quantitation of analogues by the different methods,

however this could likely be explained by different response factors exhibited by different analytes. It was initially assumed that each analyte would have similar responses; however, discrepancies suggest that the response for each analogue was different than anatoxin-a. Unfortunately, quantitative calibration standards were not available for all the analogues.

The data illustrated that both methods produced similar results for anatoxin-a quantitation; however, the LOQ and LOD achieved with the derivatization method was superior. Differences in HILIC-MS/MS and DNS-LC-MS/MS methods for anatoxin-a analysis were not found to be statistically significant with a 95% confidence interval. Results for some of the anatoxins were not as well matched but this was probably due to the lack of individual standards for those compounds and anatoxin-a being used as the calibrant. The use of derivatized samples also allowed the use of reverse phase chromatography, allowing for more flexibility in column and mobile phase selection, providing more efficient ionization, and improving signal-to-noise ratio within chromatograms.

Table 3.3**:** Quantitation (µg/g) of anatoxin-a (ATX), dihydroanatoxin-a (H_2ATX), epoxy-anatoxin-a (E-ATX), homoanatoxin-a (hATX), dihydrohomoanatoxin-a (H_2hATX) and epoxy-homoanatoxin-a (E-ATX) toxins found in each respective sample. The underivatized analytes (HILIC-MS/MS) were compared to the analytes derivatized with the dansyl moiety (DNS-LC-MS/MS). Values are reported as averages ± standard deviation (n). Samples codes correspond to: A – *Aphanizomenon*, B – *Phormidium* 2005, C – Ashley River, D – *Oscillatoria*, E – *Phormidium* 2012, F – Hutt River.

		Sample					
Analyte	**Method**	**A**	**B**	**C**	**D**	**E**	**F**
ATX	HILIC-MS/MS	17.8 ± 1.7 (5)	3547 ± 452 (6)	1.9 ± 0.4 (3)	nd	nd	nd
	DNS-LC-MS/MS	14.8 ± 1.8 (3)	3404 ± 458 (5)	2.5 ± 0.4 (4)	nd	nd	nd
H_2ATX	HILIC-MS/MS	4.8 ± 0.2 (3)	130.3 ± 1.2 (3)	1040 ± 84 (5)	nd	335 ± 55 (3)	391 ± 27 (3)
	DNS-LC-MS/MS	4.4 ± 2.8 (3)	75 ± 10 (5)	720 ± 140 (4)	nd	289 ± 27 (3)	237 ± 19 (3)
E-ATX	HILIC-MS/MS	nd	4.3 ± 1.4 (4)	nd	nd	nd	nd
	DNS-LC-MS/MS	nd	9.8 ± 2.1 (3)	nd	nd	nd	nd
hATX	HILIC-MS/MS	nd	nd	117 ± 13 (6)	7.5 ± 2 (3)	1.5 ± 0.5 (3)	8.3 ± 1.5 (5)
	DNS-LC-MS/MS	nd	nd	64.1 ± 5.6 (5)	5.73, 4.43	1.17 ± 0.05 (3)	5.7 ± 0.9 (3)
H_2hATX	HILIC-MS/MS	nd	nd	52.7 ± 6.2 (6)	nd	6.0 ± 2.1 (4)	54.5 ± 4.3 (3)
	DNS-LC-MS/MS	nd	nd	43.8 ± 3.4 (5)	nd	6.52, 6.93	37.9 ± 3.4 (3)
E-hATX	HILIC-MS/MS	nd	nd	9.2 ± 1.3 (4)	nd	nd	nd
	DNS-LC-MS/MS	nd	nd	2.2 ± 0.7 (4)	nd	nd	nd

nd = not detected (LOD = 0.252 µg/L for HILIC-MS/MS and 0.0195 µg/L for DNS-LC-MS/MS).

3.4 DNS-LC-FLD Method

The dansyl derivatives are also fluorescent and should therefore be suitable for analysis by LC-FLD. As the European Commission has approved LC-FLD analysis of one of its two official methods for toxin screening, this technique is an obvious choice for laboratories without LC-MS/MS equipment. LC-FLD also provides a complementary method for characterization of CRMs. Additionally, the use of fluorescent derivatization reagents may be useful in instances where accurate calibrants are not available for every structural analogue. It might be possible for calibration to be conducted accurately with just one standard, provided the FLD molar response is equal among the analogues [98].

3.4.1 Fluorescence Spectra

Dansyl derivatives of the anatoxins were highly fluorescent with excitation and emission wavelength maxima at 350 nm and 525 nm, respectively. Initially, only neutral pH mobile phases were considered for analysis of the dansyl derivatives, as it has been reported that fluorescence is quenched under acidic conditions [99, 100] due to protonation of the dimethyl amino group. However, separation issues (section 3.4.2) prompted the testing of low pH mobile phases to see if fluorescence could still be achieved even to some extent. It was a surprise to find that the compounds were still very fluorescent in a mobile phase under acidic conditions (aqueous phase = pH 2.3) despite pKa of 3.6 for the dimethylamine functional group of dansyl chloride [100]. Figure 3.23 shows the fluorescence spectra measured when a neutral and acidic aqueous mobile phase was mixed with either MeOH or MeCN as the organic modifier. The strongest emission

signals were observed in MeCN based mobile phase and were almost equal under acidic or neutral conditions.

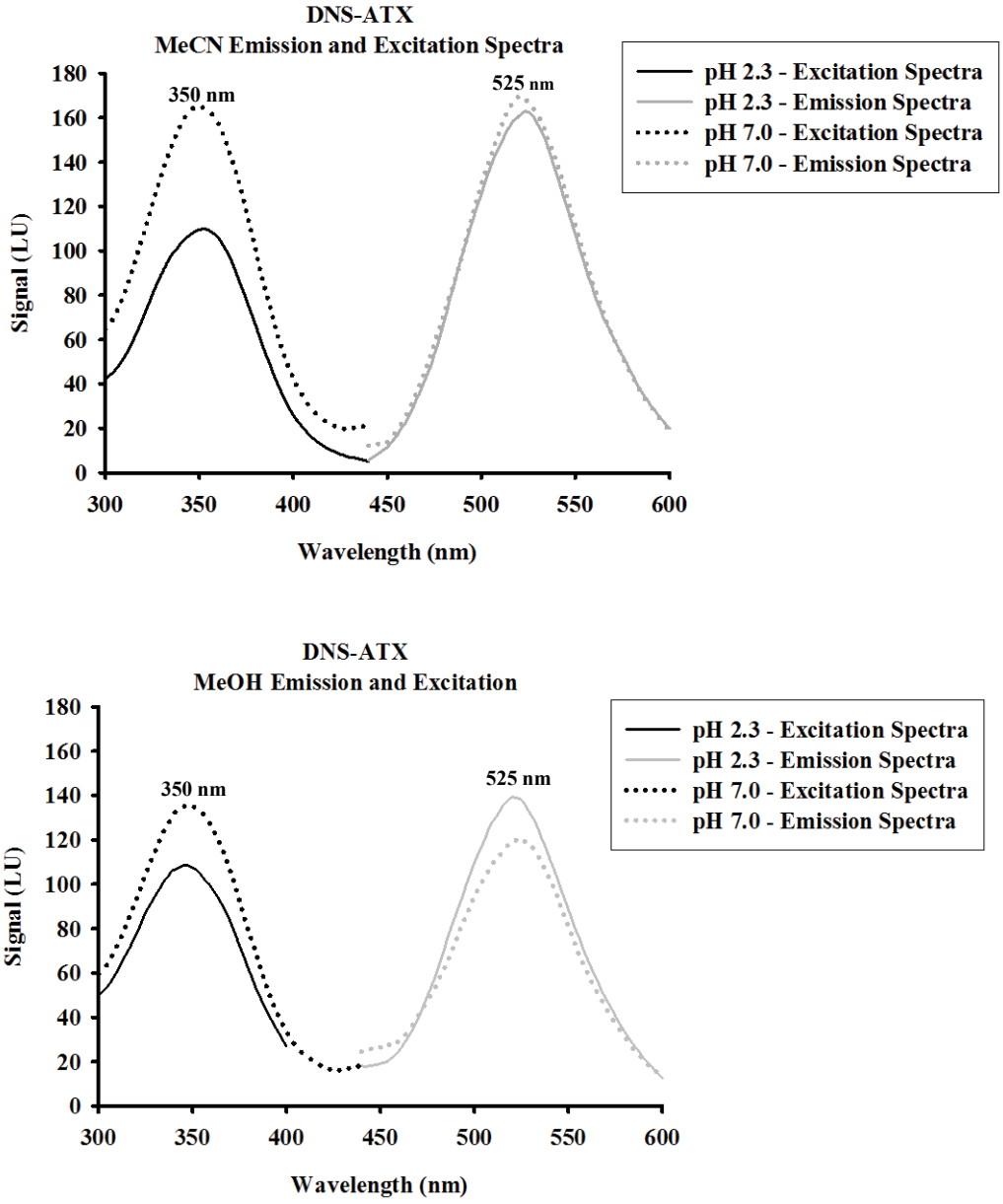

Figure 3.23: Excitation and emission fluorescence spectra of dansyl anatoxin-a in mobile phases produced from: (A) MeCN, and (B) MeOH. A solid line indicates an acidic mobile phase pH, while a dotted line indicates a neutral pH (pHs were measured in aqueous solution without organic). The sample was run on a LC-FLD with Luna C18(2) column (150 mm x 4.6 mm i.d.) and 60% organic.

The composition of mobile phase used for the analysis in Figure 3.23 consisted of a 60% MeCN solution, containing formic acid and ammonium formate as modifiers. The general assumption that the pH of the mixed mobile phase is the same as that of the aqueous buffer is a common and problematic error [101]. In one experiment with acetonitrile-water mixtures using tartaric acid, the pKa increased from 3.03 to 5.17 in 70% acetonitrile solutions [101]. Increases in pKa were also noted for all other buffer systems tested, including citric acid, boric acid, phthalic acid and acetic acid [102]. The pKa of formic acid is 3.75, which could conceivably experience an increase in pKa to 5 or 6 in a 60% acetonitrile mobile phase as seen in solutions with similar pKas [102]. Alternatively, the shift in pKa in the other direction due to inefficient ionization within a high organic solution should be seen with the dimethylamine of dansyl chloride, thus resulting in a decrease in pKa from 3.6 to a lower value. The decrease in pKa of the amine combined with an effective increase in pH of the solvent would result in fluorescence of the compound due to the absence of ionization. Certainly, this information highlights the need for scientists to carefully consider the changes in pH that will occur in aqueous acetonitrile mixes for analytical purposes, but also explains the findings for no observable loss in fluorescence in this study.

3.4.2 LC Optimization

The complexity of algal field samples led to the formation of many derivatized compounds that potentially interfere with the analysis of dansyl anatoxins by LC-FLD. Thus the separation of derivatized samples constituents was more important than with LC-MS/MS methods. Several stationary phases, such as Phenomenex Luna C18(2), XB-C18 and Max-RP were investigated. The Luna C18(2) provided the best separation

and peak shape. However, the shorter, narrow bore columns (50 mm x 2.0 mm) used in the LC-MS methods provided inadequate resolution. Eventually, a longer Phenomenex Luna C18(2) (150 mm x 4.6 mm) column was selected and the wider bore allowed a flow rate (1.0 mL min^{-1}) most compatible with the FLD flow cell. The neutral mobile phase was tested initially, but phenylalanine and anatoxin-a were not resolved. Acidic mobile phases gave superior separation and fortunately it was found that fluorescence could still be achieved (section 3.4.1). Conditions were then optimized using an acidic mobile phase with an isocratic elution of 60% MeCN at a column temperature of 40°C. Excellent separation of analytes, other derivatives and reagent components were achieved (Figure 3.24). The analytes anatoxin-a and homoanatoxin-a were separated from other peaks in the complex dansylated *Microcystis* sample, which serves as negative control because it does not produce anatoxin-a or homoanatoxin-a. The use of 3-methylpiperidine as an internal standard was useful in correcting for variations in dilution volumes, injection volumes and, retention times, as well as to assess reaction completeness and to achieve correct quantitation.

The method was applied to a more complex Ashley River field sample. Figure 3.25 illustrates the chromatogram of the LC-FLD response from the derivatized Ashley River sample overlaid with LC-MS/MS SRM chromatograms acquired using the same column and conditions assist of peak identification in the LC-FLD chromatogram. As indicated in Figure 3.25, the low levels of compounds such as anatoxin-a and epoxy-homoanatoxin-a in the sample were not detected by the LC-FLD method. As previously mentioned,

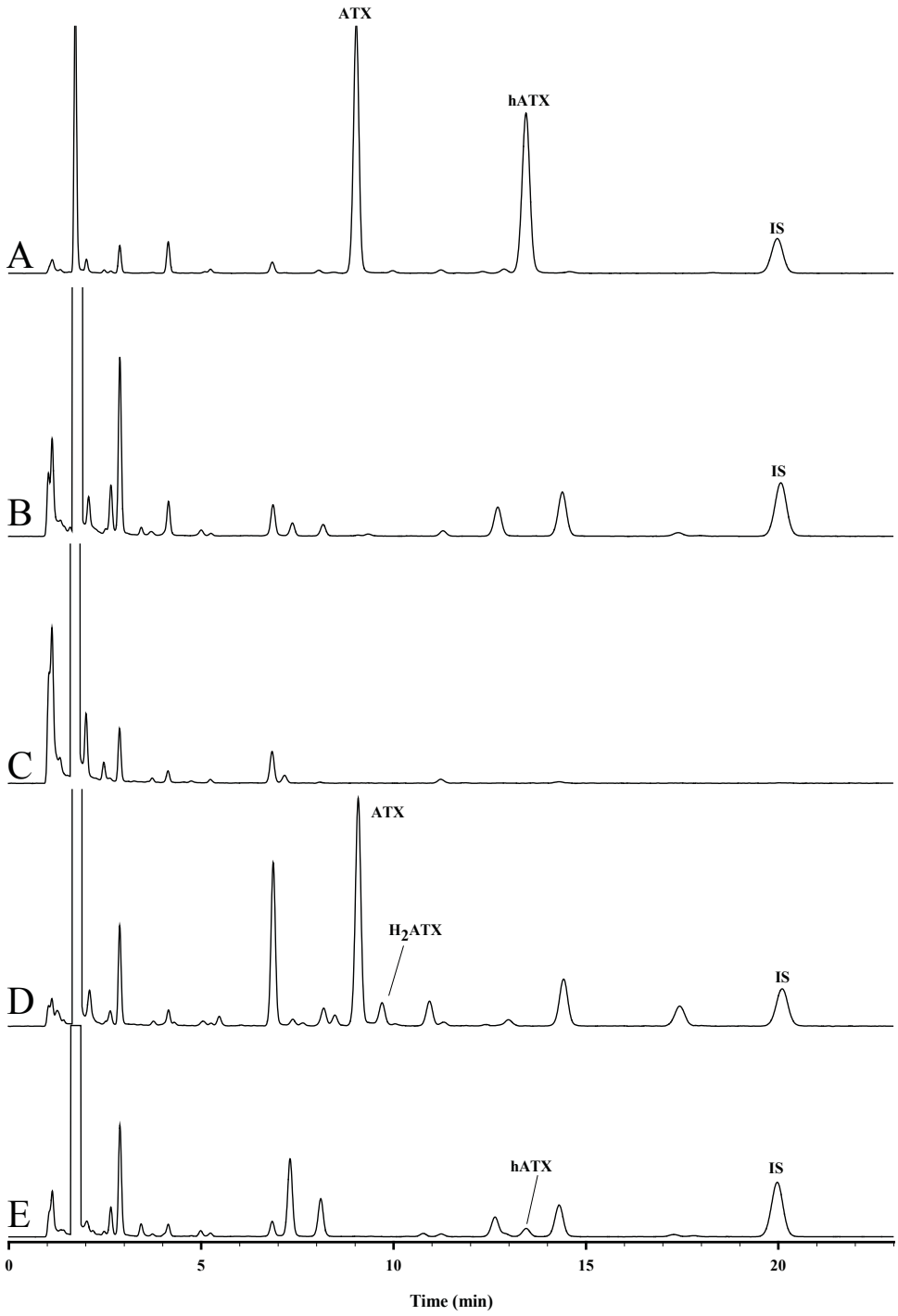

Figure 3.24: LC-FLD chromatograms illustrating method resolution in separating dansylated anatoxin (ATX), homoanatoxin-a (hATX) and the internal standard (IS) in several different samples: (A) ATX, hATX and IS standards; (B) *Microcystis* with IS; (C) Reagent Blank; (D) *Phormidium* 2005 with IS; and (E) *Oscillatoria formosa* with IS. All samples were run on a Luna C18(2) column (150 mm x 4.6 mm i.d.) using 60% MeCN mobile phase (50 mM HCOOH and 2 mM $HCOONH_4$, pH 2.3).

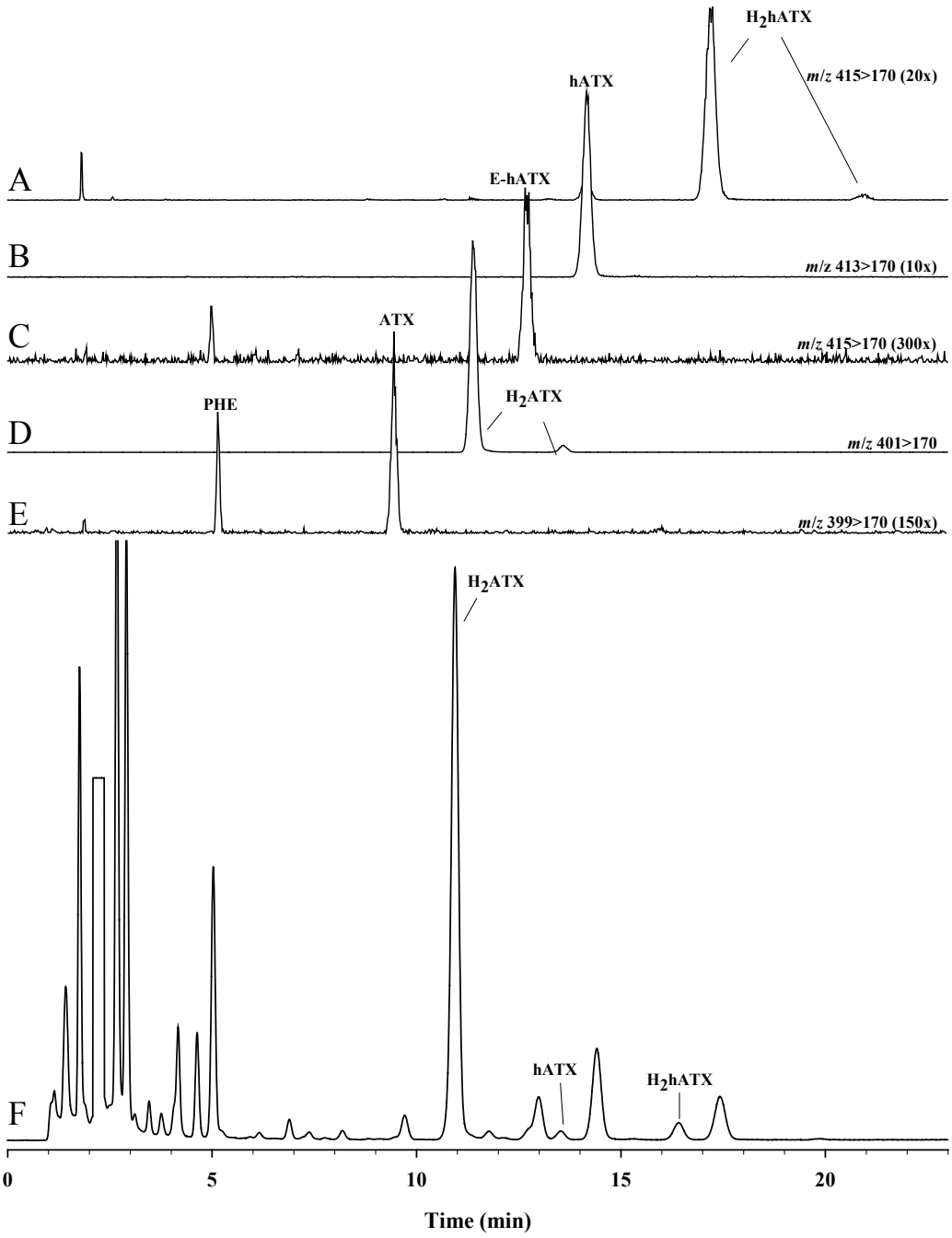

Figure 3.25: LC-MS/MS SRM chromatograms (A-E) and LC-FLD chromatogram (F) of dansylated sample from Ashley River, New Zealand: Transitions (A) for dihydrohomoanatoxin-a (H_2hATX); (B) homoanatoxin-a (hATX); (C) Epoxy-homoanatoxin-a (E-hATX); (D) dihydroanatoxin-a (H_2ATX); (E) phenylalanine (PHE) and anatoxin-a (ATX); and (F) an LC-FLD spectrum of the Ashley River sample. Samples were run on a Luna C18(2) column (150 mm x 4.6 mm i.d.) using 60% MeCN mobile phase (50 mM HCOOH and 2 mM $HCOONH_4$, pH 2.3) with a flow rate of 1.00 mL min^{-1}.

the separation of phenylalanine from the anatoxins using the acidic mobile phase was very important as dansylated phenylalanine can co-elute with dansylated anatoxin-a in a neutral mobile phase. As shown in Figure 3.25, phenylalanine is clearly resolved from anatoxin-a.

3.4.3 DNS-LC-FLD Method Validation

Validation experiments of the LC-FLD method determined the linear range to be 1.6 ng mL^{-1} to 1.1 mg mL^{-1} with a limit of detection of 31 pg injected and a 94 pg limit of quantitation for standard solutions of anatoxin-a. In spiking experiments using 6 μg L^{-1} levels of anatoxin-a within a solvent spike (simulated to represent a freshwater sample at the MAC), was detectable and quantifiable with an RSD of 2.7%. This information revealed that the LC-FLD derivatization method is sensitive enough to use on freshwater for routine screening as meaningful results can be obtained without direct algal analysis. Due to the extremely complex nature of most algal samples, co-eluting peaks may interfere with some of the anatoxin-a and homoanatoxin-a analogues. For this purpose, the fluorescence method presented in this paper may be used to monitor anatoxin-a and homoanatoxin-a of complex algal samples. LC-MS/MS provides a better tool for monitoring all of the ATX analogues.

The DNS-LC-FLD method had reproducible retention times for the analytes (0.02% RSD, n = 4), as well as reproducible fluorescence responses (0.87% RSD, n = 4). Drift was observed through routine operation using the LC-FLD, which is believed to be due to small amounts of evaporation from the concentrated samples (150 μL). The internal standard calibration method was used to correct for the observed drift, however

other options, such as using a larger sample volume (~ 1 mL) where the effects of evaporation would not be as evident, may also be used. A concentrated sample volume of 150 μL was used because it allowed for analysis at a low level of toxins, but the reaction could easily be scaled up to a larger volume, which would allow a larger volume of concentrated sample for analysis if users were not interested in using the internal standard calibration method.

The relative molar response for DNS-homoanatoxin-a and DNS-anatoxin-a differed from that measured in LC-UVD and LC-MS. The relative fluorescence response of DNS-homoanatoxin-a was 134.0 ± 0.7 % of the DNS-anatoxin-a response (after correcting the peak area for concentration differences: 6.52×10^{-10} mol anatoxin-a and 5.62×10^{-10} mol homoanatoxin-a (Figure 3.26 and Table 3.4). Both compounds possessed the same excitation and emission wavelengths, and the difference in response must be related to the structural differences.

The observation of differing fluorescent response has been reported for other fluorescent compounds, including the intramolecular quenching of tryptophan fluorescence with carbonyl functional groups in peptide bonds [103]. The quenching is believed to occur through excited state electron transfer from the excited fluorophore (donor) to the carbonyl group (acceptor) [103]. The carbonyl groups in anatoxin-a and homoanatoxin-a are likely in close proximity to the dansyl functional group, resulting in some intramolecular quenching and a lower relative molar response than that of the internal standard, which does not possess a carbonyl group. It was observed that dansyl-homoanatoxin-a had a higher relative molar response than dansyl-anatoxin-a. The

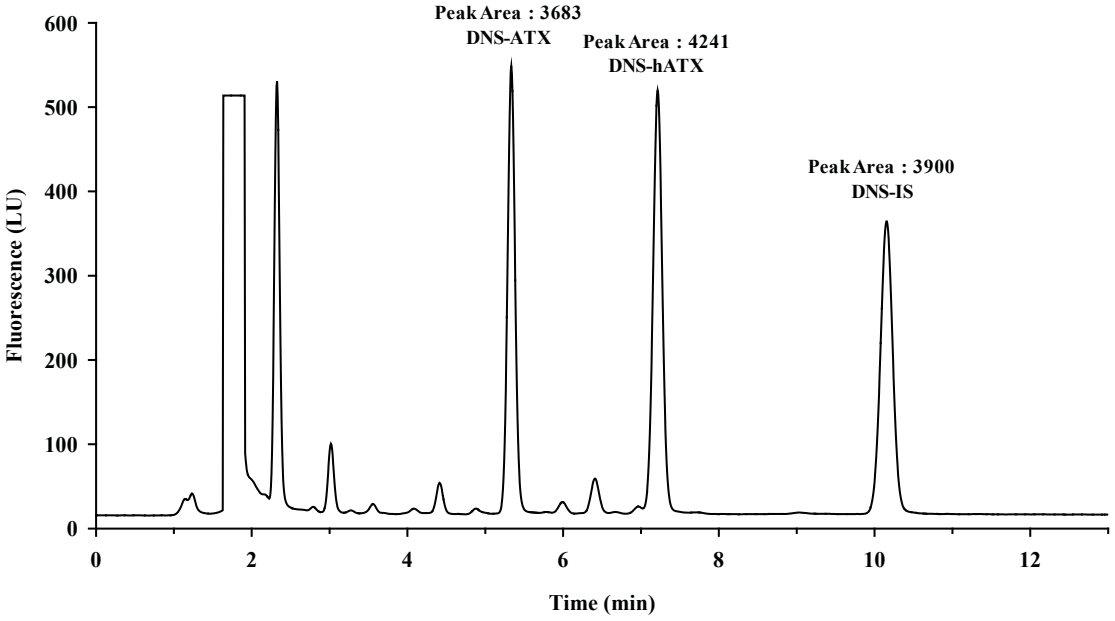

Figure 3.26: LC-FLD chromatogram of dansylated anatoxin-a ($6.52x10^{-10}$ mol), homoanatoxin-a ($5.62x10^{-10}$ mol) and 3-methylpiperidine ($1.84x10^{-10}$ mol) investigating relative molar response. The sample was run on a Luna C18(2) column (150 mm x 4.6 mm i.d.) using 60% MeCN mobile phase (50 mM HCOOH and 2 mM $HCOONH_4$, pH 2.3).

observed difference may be due to different structural orientation of the carbonyl group in relation to the dansyl moiety, or perhaps the additional methylene group in homoanatoxin-a provides donation of electrons to the carbonyl group, which reduces the excited state electron transfer from dansyl to the carbonyl group.

With this evidence, it is clear that the concept of using one dansylated standard to quantify other anatoxin analogues is not practical due to different relative molar responses. This information does stress the need for proper calibrants when performing LC-FLD analysis. With the availability of homoanatoxin-a RM, LC-FLD becomes

another calibration method for quantifying toxins in field samples and algal reference materials.

Table 3.4: Relative molar response of ATX, hATX and IS to RM-hATX. Analyses using LC-UVD on underivatized compounds used the TSK Gel Amide 80 column (250 mm x 2.0 mm i.d.) using a mobile phase of 20% MeOH with 0.1% AcOH (λ_{abs} = 230 nm), while analyses with LC-FLD on the dansyl derivative used a Luna C18(2) (150 mm x 4.6 mm i.d.) and a mobile phase of 70% MeCN (50 mM HCOOH and 2 mM $HCOONH_4$, pH 2.3, λ_{ex} = 350 nm, λ_{em} = 525 nm). LC-UVD samples did not contain an IS.

	UVD (underivatized)			**FLD (dansyl derivative)**		
	ATX	hATX	IS	ATX	hATX	IS
RMR to ATX	1.00	0.88 ± 0.03	--	1.00	1.34 ± 0.02	2.8 ± 0.1

3.4.4 DNS-LC-FLD Quantitation

Three samples were selected for quantitation with LC-FLD to evaluate the performance of this method compared to that of HILIC-MS/MS. Quantitation of anatoxin-a and homoanatoxin-a as dansyl derivatives was performed on *Aphanizomenon, Oscillatoria* and *Phormidium* (collected 2005) samples. Although many of the analytes were at low concentrations, meaningful quantitative data was collected from the LC-FLD analogues (Table 3.5) and all values were found to have no statistical difference between those measured with HILIC-MS/MS at a 95% confidence interval.

The similarity of the results obtained by DNS-LC-FLD and HILIC-MS/MS is a strong indication that LC-FLD gave meaningful quantitative determinations of toxins. Thus, the LC-FLD method can be used as an additional method for quantitation of anatoxin-a and homoanatoxin-a in CRMs and for those labs without LC-MS.

Table 3.5**:** Quantitation of toxin found in algal samples by HILIC-MS/MS and DNS-LC-FLD. Values are reported as averages ± standard deviation (n). Samples codes correspond to: A – *Aphanizomenon*, B – *Phormidium* 2005, C –*Oscillatoria*.

		Sample (μg g^{-1}, dry weight)		
Analyte	**Method**	**A**	**B**	**C**
Anatoxin-a	HILIC-MS/MS	17.8 ± 1.7 (5)	3550 ± 450 (6)	nd
	DNS-LC-FLD	17.6 ± 2.6 (3)	3310 ± 450 (3)	nd
Homoanatoxin-a	HILIC-MS/MS	nd	nd	7.50 ± 2.0 (3)
	DNS-LC-FLD	nd	nd	6.24 ± 0.46 (3)

nd = not detected (LOD = 0.252 μg L^{-1} for HILIC-MS/MS and 1.53 μg L^{-1} for DNS-LC-FLD).

3.5 Microcystin Analysis Methods

In light of recent and ongoing concerns surrounding algal dietary supplements [24, 25], part of this study was aimed at assessing whether cyanobacterial toxins are present in algal dietary supplements available to Canadian consumers. The presence or absence of cyanobacterial toxins, such as anatoxin-a or microcystins in algal dietary supplements, would add an application for a freeze dried algal reference material used for environmental testing purposes. The following section presents the methodology implemented for microcystin detection and then applies these methods, plus the anatoxin method, to the analysis of six algal supplements available to consumers in Canada.

3.4.5 Microcystin Method Optimization

Analysis of microcystins was carried out by LC-MS/MS and LC-UVD with calibration using available standards. Despite the large number of known microcystins, there are only a few RMs or CRMs available for use as calibrants. Standards for microcystin-RR, microcystin-LR, dmLR and microcystin-LA were available. A related cyclic peptide, nodularin (NOD), which also possesses the ADDA adduct, was used as an

internal standard because it is usually associated with marine cyanobacteria and was not present in the types of samples examined in this project.

For microcystin analysis, methods developed by M. Quilliam and coworkers [72] were adapted. Recent work by a post-doctoral fellow in the group, Dr. Khalida Berki, initiated the use of a new class of column, Poroshell from Agilent, which is based on a microparticulate superficially-porous stationary phase. This column gave enhanced resolution and excellent peak shape for microcystins. The Poroshell column had the added benefit of stability over a wider range of mobile phase pHs (1.0-8.0) and was able to withstand temperatures up to 90°C. The LC-MS/MS method produced good peak shape for all analytes, with a 14 min analysis time. As shown in Figure 3.27, microcystin-LR eluted slightly ahead of the dmLR, although SRM detection allowed for selective measurement of each. However, this presented problems with the less selective technique of LC-UVD, where the microcystin-LR and dmLR co-eluted as a single peak (Figure 3.28). These two methods were used to screen for toxin concentration in various dietary supplements and algal cultures.

A brief validation of the LC-MS/MS method was carried out for microcystin-LR. The LOQ for the standard was 3.8 μg L^{-1}. This is higher than the MAC of 1 μg L^{-1} in drinking water but it is possible to utilize a 15-fold pre-concentration step using solid phase extraction with an OASIS-HLB, thus making the method well suited for the detection of microcystin in drinking water well below the MAC. The linear range of 3.8 to 2800 μg L^{-1} (R^2 = 0.9998) was established using a 5 μL injection volume. Concentrations higher than 2800 μg L^{-1} were avoided to prevent instrument

contamination and detection saturation. Higher concentrations can be handled with dilution.

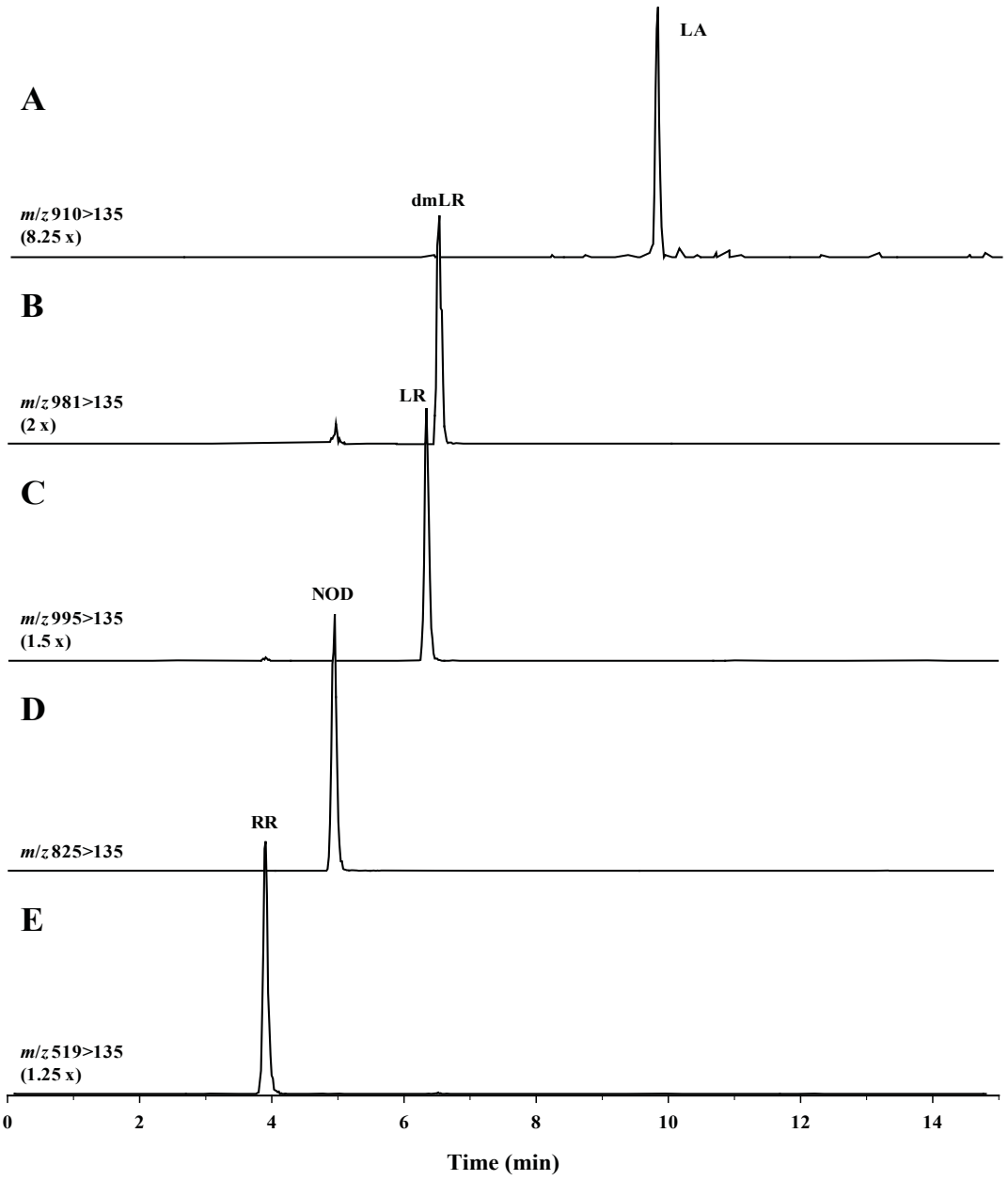

Figure 3.27: LC-MS/MS chromatogram of a calibration solution containing: (A) microcystin-RR, (B) nodularin (NOD), (C) microcystin-LR, (D) dmLR and (E) microcystin-LA. This method used a Poroshell 120 SB C18 150 mm x 2.1 mm column and a mobile phase gradient at a flow rate of 0.2 mL min^{-1}.

The method was reproducible with a relative standard deviation (RSD) of 4.6% for peak area and 0.13% for retention time of a 283 μg L^{-1} microcystin-LR standard (n = 4). A pre-concentration step using the Oasis HLB column gave 98% recovery of microcystin-LR, indicating that no significant level of toxin was lost during sample loading and elution steps.

Validation of LC-UVD systems provided a higher level of complexity with dmLR co-eluting with microcystin-LR (Figure 3.28). For this purpose, validation information was used from microcystin-RR. Microcystin-RR had an LOQ of 97 μg L^{-1}, which was much higher than the LOQ reported for LC-MS/MS analysis. The higher LOQ in LC-UVD did not come as a surprise, as LC-UVD detection is generally much less sensitive than LC-MS/MS detection [70]. The LC-UVD method for microcystin-RR was very reproducible giving an RSD of 0.3% for peak area along with an RSD of 0.2% for retention time when using a 2.55 μg mL^{-1} standard (n = 4).

Co-elution of dmLR and microcystin-LR required the calibration of these analytes be made together (i.e., the peak area was plotted against the sum of the concentration of both analytes in constructing a calibration curve). This was considered appropriate, as M. Quilliam and workers have determined that the two toxins have equal molar extinction coefficient at 238 nm (unpublished data). However, this may not be the case for other microcystins. Microcystin analogues generally differ by amino acids in the 2 and 4 positions (Figure 1.3) and the amino acids tyrosine and tryptophan strongly absorb UV radiation.

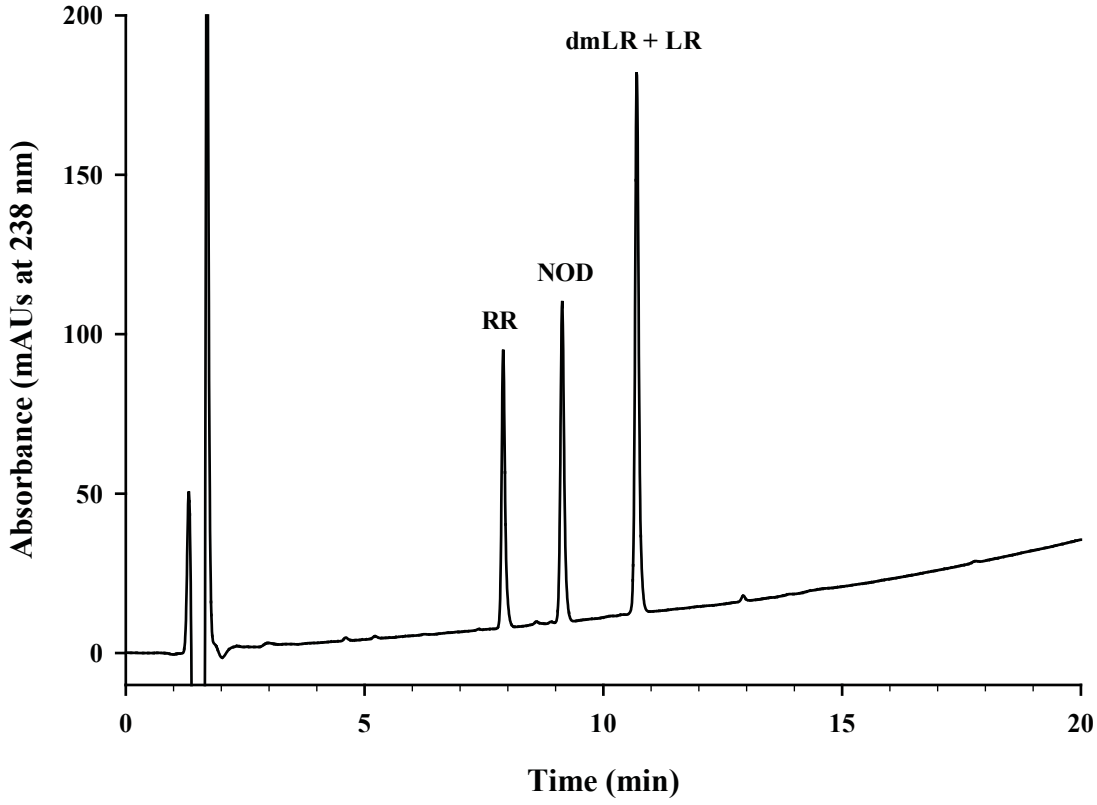

Figure 3.28: LC-UV chromatogram of calibration mix containing nodularin (NOD) and microcystins RR, dmLR and LR. The samples were run on the Poroshell 120 SB C18 150 mm x 2.1 mm column using a mobile phase gradient and a flow rate of 0.2 mL min^{-1}. Concentrations for NOD, microcystins RR, and dmLR and LR were 2.5, 2.6 and 4.9 µg mL^{1}, respectively

3.4.6 Quantitation of toxins in Algal Nutritional Supplements

Algal nutritional supplements were tested using both LC-UVD and LC-MS/MS methods to search for toxins present within the six samples. Unfortunately, the LC-UVD method was unable to detect the low levels of toxins in the samples, so only LC-MS/MS was used for quantitation of toxins in algal nutritional supplements. While no anatoxins were detected in any of the nutritional supplements, the presence of microcystins in all the *A. flos-aquae* samples tested within this work (Table 3.6 and Figure 3.29) is a cause

for concern. While quantitation was performed only on one extract per nutritional supplement, future work will involve repetition of extraction and quantitation so that an uncertainty can be assigned to each toxin concentration. The microcystins found in this study were microcystin-LA and microcystin-LR, which are two microcystins frequently found in nutritional supplements tested [24, 25]. Identities of these two toxins were confirmed by matching retention times and by acquiring product ion spectra (Figure 3.30), which matched those of standards. Even more troubling was that some samples were found to exceed regulatory levels that have been established to protect the health of consumers (OR = Oregon Regulations, SR = Switzerland Regulations). The results were also examined in terms of microcystin ingestion per kg of body weight to determine if the product recommended daily intake (RDI) resulted in levels above nominal tolerance of 0.04 μg kg^{-1} body weight (bw) for infants (5 kg), children (20 kg) and adults (60 kg) [104]. Four of the five samples examined exceeded the tolerance for infants, three of the five exceeded the tolerance for children and one of the five exceeded the tolerance for adults. It should be noted that some parents turn to algal supplements as an alternative method to treat symptoms of ADHD in children [47] who, due to their body weight, may end up consuming toxic levels of microcystins.

The results from this study, as well as those from other studies reviewed in this thesis, emphasize the need for regulation of algal dietary supplements. It is disturbing that all the *A flos-aquae* samples tested in this small study contained microcystins. Though anatoxins were not detected in any of the samples, certain *Aphanizomenon* species are

known to produce anatoxins (section 3.3.4) so it is conceivable that a toxic strain could end up in a dietary supplement if testing is not conducted.

Table 3.6: Microcystin dietary supplements (*Aph.* = *Aphanizomenon flos-aquae*, *Spir.* = *Spirulina*). Exposure is based on RDI as indicated on the label of each bottle. The total mass of microcystins consumed was compared with regulatory values according to Oregon Regulations (OR; < 1 μg g^{-1}) and Switzerland Regulations (SR; < 1 μg per day) as well as the Dietrich Provisional Tolerance (DPT; < 0.04 μg kg^{-1} bw). Microcystins were quantified using LC-MS/MS.

Sample	MC-LR (μg g^{-1})	MC-LA (μg g^{-1})	RDI (g)	Mass MC consumed (μg)	Exceed OR	Exceed SR	DPT Infant	DPT Child	DPT Adult
Aph-1[1]	0.1	nd	1.1	0.1	No	No	No	No	No
Aph-2[2]	0.4	0.6	3.8	4.0	Yes	Yes	Yes	Yes	Yes
Aph-3[3]	0.2	0.3	2.2	1.2	No	Yes	Yes	Yes	No
Aph-4[4]	0.3	0.2	1.6	0.8	No	No	Yes	Yes	No
Aph-5[5]	0.3	nd	1.6	0.5	No	No	Yes	No	No
Spir.[6]	nd	nd	3.0	NA	NA	NA	NA	NA	NA

nd = not detected, NA = not applicable.

1. Source Naturals (no batch number), purchased from TheVitaminShoppe.com
2. American Health Klamath Shores, Batch Number: 458330-01, purchased from TheVitaminShoppe.com
3. Sunny Green, Batch Number: 172201, purchased from TheVitaminShoppe.com
4. Omega Sun, Simplexity (formerly Cell Tech International)
5. Alpha Sun, Simplexity (formerly Cell Tech International), Batch Number: 49704
6. Earthrise Organic, Batch Number: 40997

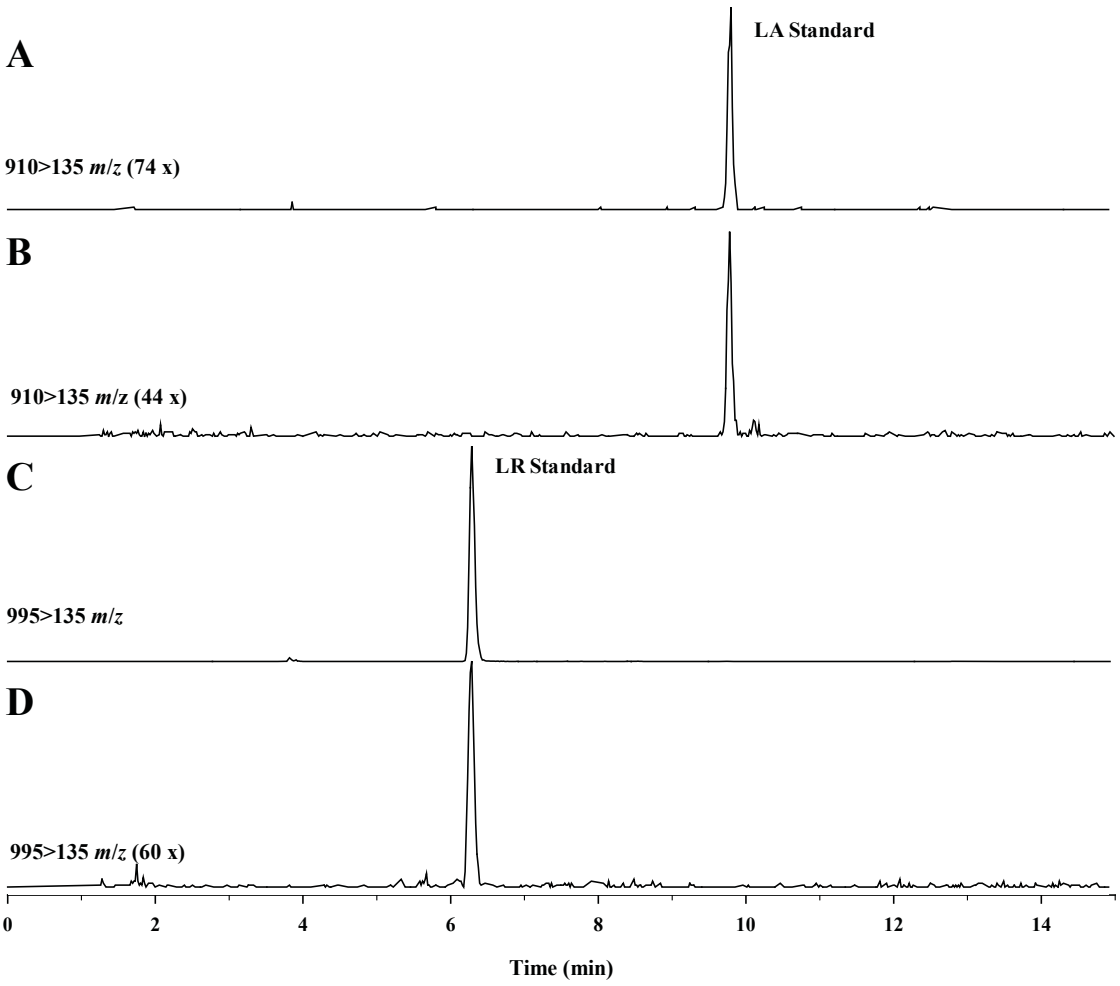

Figure 3.29: LC-MS/MS SRM chromatogram for (A) microcystin-LA standard; (B) *Aph*. 2 sample; (C) microcystin-LR standard, (D) *Aph*. 2 sample. All algal nutritional supplements were pre-concentrated from 10 mL to 0.3 mL using the Oasis HLB column cartridge and run on the Poroshell 120 SB C18 150 x 2.1 mm column using a mobile phase gradient at a flow rate of 0.2 mL min^{-1}.

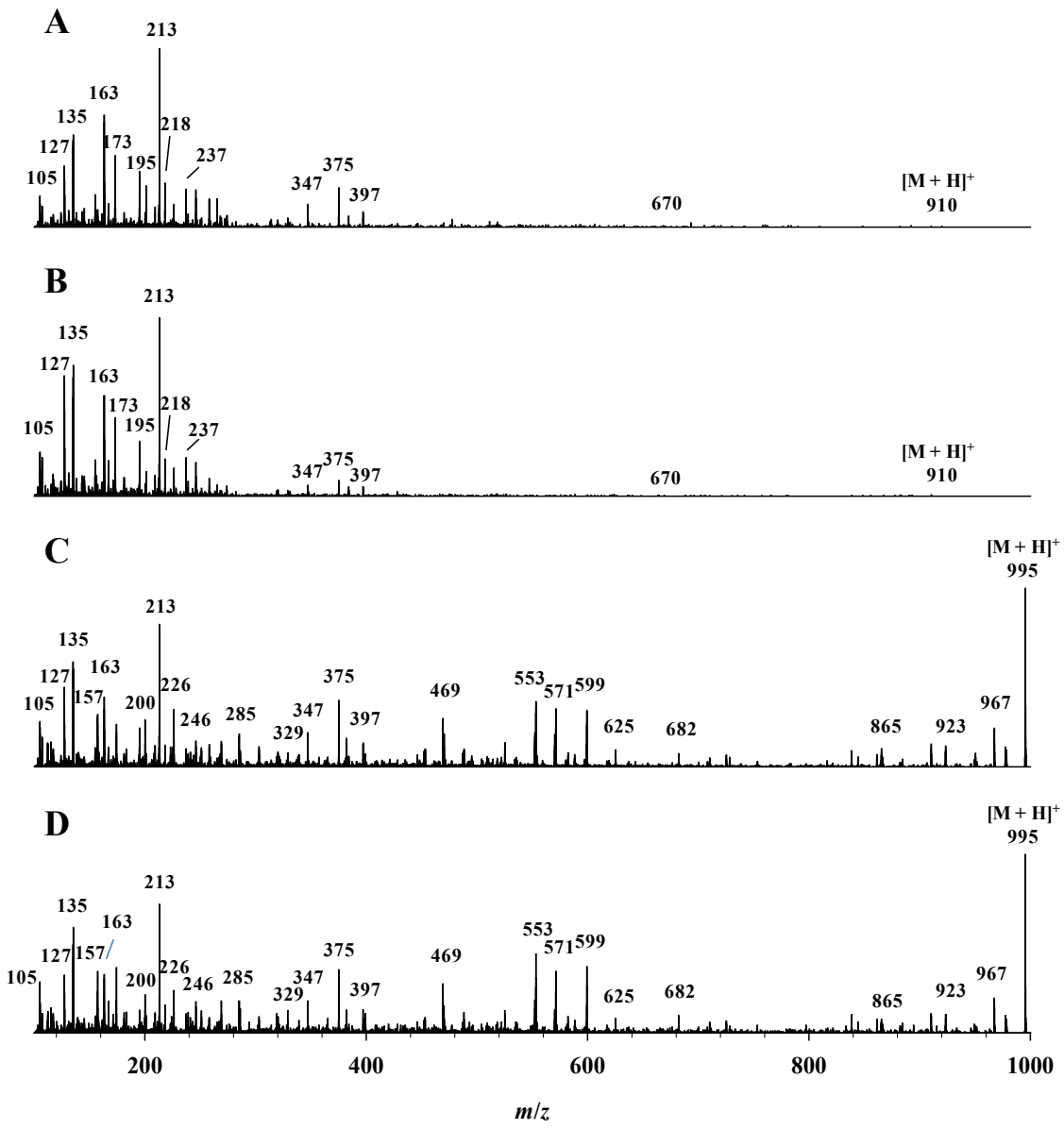

Figure 3.30: LC-MS/MS product ion spectra for (A) microcystin-LA standard using a collision energy of 60 eV; (B) *Aph*. 4 sample using a collision energy of 60 eV; (C) microcystin-LR standard using a collision energy of 70 eV, (D) *Aph*. 5 sample using a collision energy of 70 eV. All algal nutritional supplements were pre-concentrated from 10 mL to 0.3 mL using the Oasis HLB column cartridge and run on the Poroshell 120 SB C18 2.1 x 150 mm column using a mobile phase gradient at a flow rate of 0.2 mL min^{-1}.

3.5 Feasibility of an Algal Matrix RM

3.5.1 Selection of Materials

The first step in preparing an algal matrix RM for feasibility studies was to select algal material that could be blended. Due to the low concentration of microcystins in dietary supplements, algal cultures were the only viable source of microcystins for preparation of the RM. Ideally, a nutritional supplement free of cyanobacterial toxins would serve as an excellent negative control sample. Unfortunately, as discovered in section 3.4.6, no *A. flos-aquae* samples were free of microcystins. Further work in identifying a batch of nutritional supplements without cyanobacteria toxins, or culturing a biomass of toxin free algae will be necessary to serve as a negative control. Four cultures of *Microcystis aeruginosa* (strains LL-4-4, CPCC 300, UTCC 464 and CYA 548) were grown and harvested by Nancy Lewis at the NRC's field station in Ketch Harbour for microcystin determination (Table 3.7). All cultures were available in significant quantities, so emphasis was placed on the cultures that contained microcystins for which calibration solution CRMs were available to aid in analysis. Cultures LL-4-4 and CPCC 300 contained microcystin-LR and microcystin-RR, for which standards were available, while UTCC 464 had several other microcystins that were of interest such as microcystin-YR. Culture CYA 548 was not selected for use within the matrix RM. Although it contained many toxins, most were low in concentration with the exception of one microcystin, [Asp3]-microcystin-RY.

When selecting anatoxin-a and homoanatoxin-a materials for the matrix RM, several factors were important to consider. The concentration of the toxin had the largest

influence on materials selection (Table 3.8). The *Phormidium* sp. sample collected in 2005 had the largest amount of anatoxin-a (3.4 mg g^{-1}). This sample was not cultured so presence of other material, such as dirt or other vegetation was expected. Ideally, all samples used within an RM would be free from unknown contaminants, however the high concentration of anatoxin-a within the *Phormidium* made it an attractive choice as only a very small mass would be required.

Table 3.7: Amount of microcystins (µg g^{-1}) in each culture of *Microcystis aeruginosa* along with the amount available in wet weight. Microcystins were quantified using LC-MS/MS analysis.

	Culture			
	CPCC 300	**LL-4-4**	**UTCC 464**	**CYA 548**
Wet weight (g)	2240	951	850	313
Microcystin-LR	2709	419		
[Asp3]-Microcystin-LR	1848	97		
[Leu1]-Microcystin-LR			1176	
Microcystin-RR		1705		
Microcystin-(H4)YR		201		
Microcystin-YR		161		
Microcystin-LY				24
[Leu1]-Microcystin-LY			414	
[Asp3,Mser7]-Microcystin-LY				9
[Asp3,Dha7]-Microcystin-LY				8
[Asp3]-Microcystin-RY				2162
[Asp3,Mser7]-Microcystin-RY				11
[Asp3,Dha7]-Microcystin-RY				17
[Asp3, DMAdda5]-Microcystin-RY				9
[Asp3]-Microcystin-RF				6
[Asp3]-Microcystin-VY				5
[Asp3]-Microcystin-LF				10

When selecting the material for homoanatoxin-a, the Ashley River sample had the highest level of any available sample or culture; however, in order to have similar concentrations of homoanatoxin-a and anatoxin-a, a large amount of Ashley River algae would be required and only 5 g was available for use. The *Oscillatoria* culture had a large biomass and was a culture that did not have environmental contaminants, so despite the low (7 μg g^{-1}) concentration *Oscillatoria* was chosen along with the *Phormidium* 2005 sample for use in the matrix RM.

Table 3.8**:** Amount of anatoxin-a (ATX) and homoanatoxin-a (hATX) reported as μg g^{-1} in each culture or sample and the amount available for preparation of a matrix RM. Quantitation was made through LC-MS/MS.

Culture/sample	**Amount Available (g wet weight)**	**ATX (μg g^{-1})**	**hATX (μg g^{-1})**
Aphanizomenon	542	17	nd
Phormidium 2005	1	3400	nd
Ashley River	5	1	90
Oscillatoria	851	nd	7
Phormidium 2012	20	nd	1
Hutt River	1500	nd	7

The *Oscillatoria* culture and *Phormidium* 2005 sample, along with UTCC 464, CPCC 300 and LL-4-4 (section 3.5.1) were freeze dried as a preliminary step to RM production. Steps described in section 2.7 were followed for the preparation of the blue-green algae reference material, named as RM-BGA (Figure 3.31). Particular care was taken throughout weighing of the freeze dried algae, grinding, homogenization and moisture monitoring. The RM-BGA was bottled under argon and stored at -80°C until needed.

Figure 3.31: Photo of RM-BGA.

3.4.7 Characterization of RM-BGA

The moisture level was assessed throughout the experiment because of the relationship between moisture level and stability of a freeze dried sample [105]. Moisture analysis was performed after combining the freeze-dried algae in the ball mill prior to grinding. The moisture content of the algae was 6.6%, which was compared with a reading taken after grinding with the ball mill and homogenization with the Turbula mixer (7.4% moisture). It is unknown whether the observed increase in moisture was due to analysis taken before proper homogenization of the material, or if the material picked up additional moisture in handling. Excessive moisture prompted a final freeze drying and homogenization step that reduced the moisture level to 2.9%. This level is an ideal

level for the blue-green algae reference material, as the preferred moisture range of most lyophilized biological material is within 1-3% as these levels allow for the best long-term stability of the material [105].

Scanning electron microscopy (SEM) images (Figure 3.32) taken from the batch demonstrate that the mix was sufficiently homogenous for use as a reference material. The larger particles in the SEM images are likely due to the use of the *Phormidium* field sample. This field sample may have included various vegetation and particulate matter that could be a source of size distribution. A bimodal distribution was observed for particle size analysis of three samples of RM-BGA (Figure 3.33). The distribution may also be indicative of the algal profile used – 50% of the algae (by weight) was *Microcystis*, while 48% was *Oscillatoria* and 2% was *Phormidium*. The cell size of *Microcystis aeruginosa* is reportedly very small (between 2-8 μm in diameter) [106], while *Oscillatoria* and *Phormidium* algae are filamentous and form large sheets of cells that can have a wide range of sizes and are often reported as over 100 μm [107].

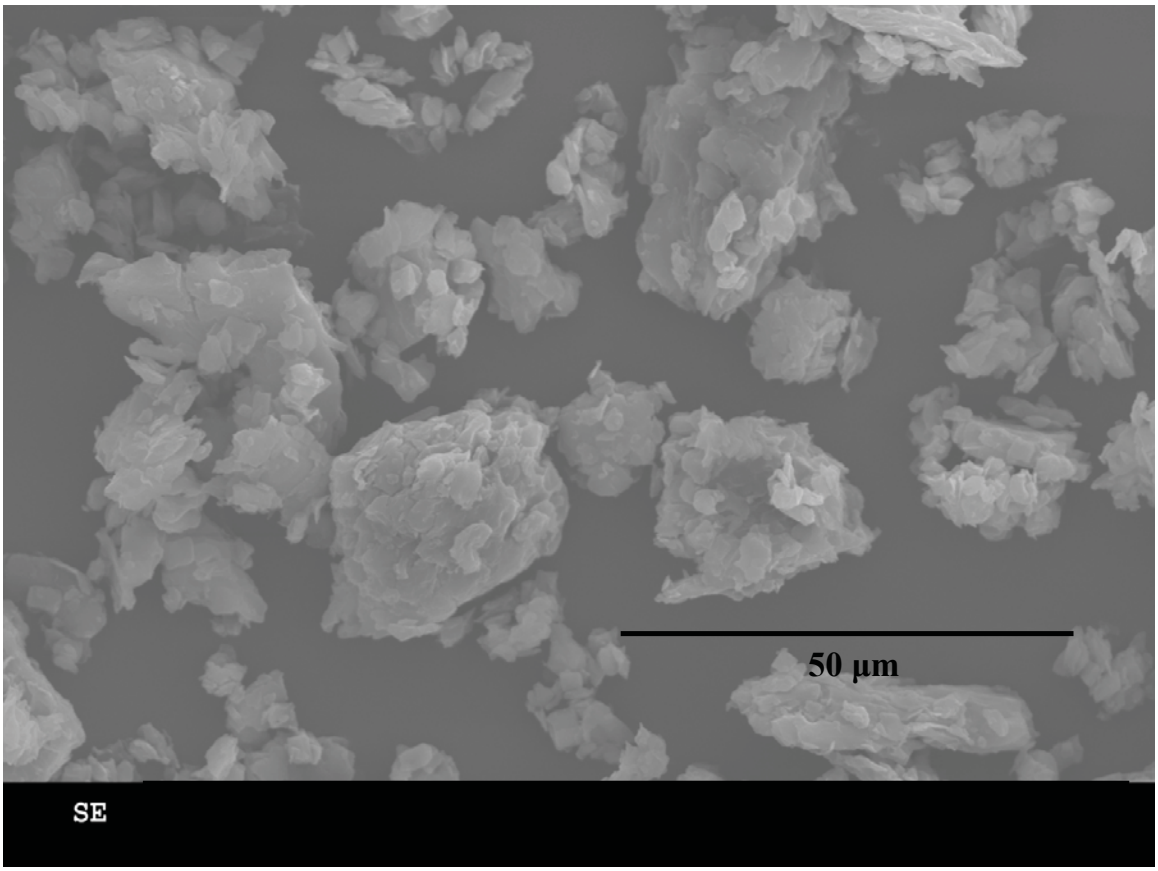

Figure 3.32: SEM image taken of RM-BGA courtesy of David O'Neil at NRC Halifax. The scale indicates 50 µm in length.

It is possible that this bimodal distribution of particle sizes is a reflection of the two cell sizes; small diameter *Microcystis* particles and 10-100 µm diameter particles of *Oscillatoria* and *Phormidium*. Despite the inhomogeneity in particle size, the RM-BGA was thoroughly homogenized prior to bottling and bottles were shown to be homogenous in terms of toxin content. A bimodal distribution would not be expected if using one algal culture, but it is also possible that using the ball mill for a longer period of time may have resulted in a narrower distribution as well.

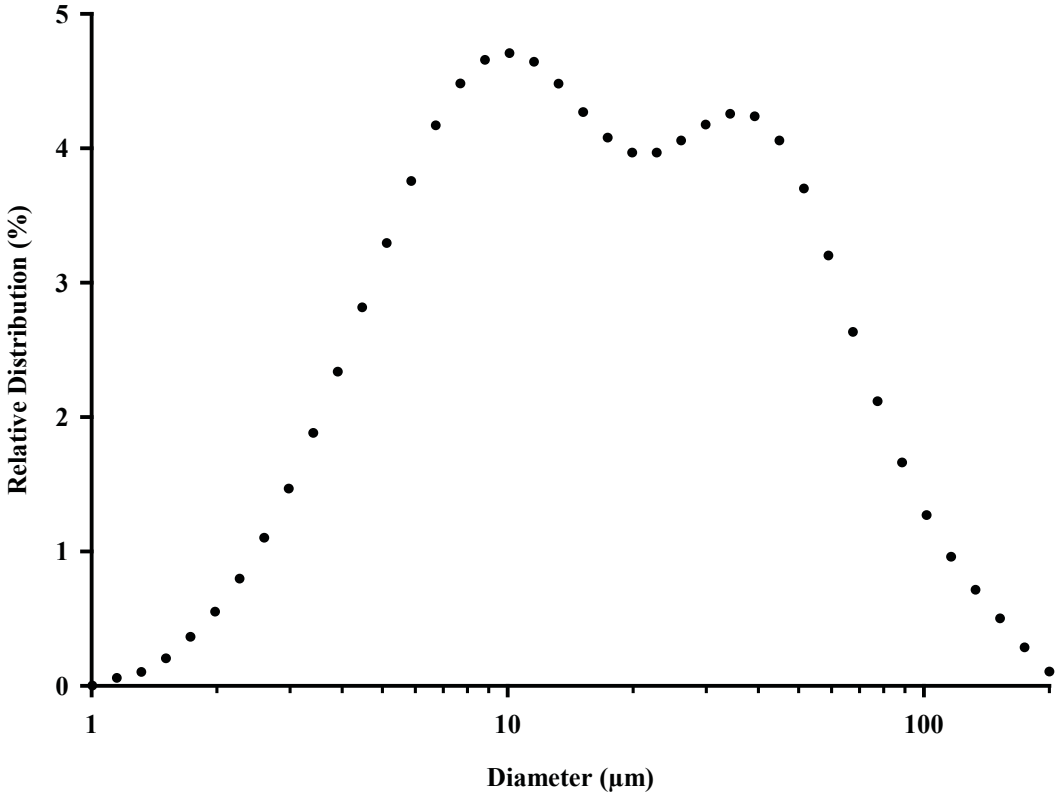

Figure 3.33: Particle size analysis of RM-BGA, illustrating a bimodal distribution of particle sizes present within the sample. Particle size analysis was carried out at the National Research Council (Ottawa) courtesy of Floyd Toll.

3.4.8 Homogeneity and Stability of RM-BGA

It was important to identify any inhomogeneity of toxin distribution within the samples as homogeneity is necessary for use as a reference material. Homogeneity of RM-BGA was assessed using LC-UVD determination of microcystin-RR, which was resolved from all other interferences in the sample. Injections of 22 different samples stored at -80°C and -20°C had a relative standard deviation of 6.7%. Based on the

number of steps required in extraction and sample preparation, this number was considered acceptable for homogeneity of a matrix reference material.

As was the case with the homoanatoxin-a standard, it was important to assess the stability of RM-BGA as part of a feasibility study for eventual preparation of a CRM. It was very important that the RM maintain stability over both short and long term. A reverse isochronous stability study was conducted for short term stability (7, 14 and 27 days) at different temperatures (-20, 4, 23 and 40°C) and compared to reference standards stored at -80°C (Table 3.9). LC-MS/MS was used as the analytical method and microcystin-LR was selected as the model microcystin for the stability study. Microcystin-LR was stable at all temperatures and all time points with the exception being 14 days at 4°C. The instability of the sample at 4°C at 14 days is peculiar, especially when time points at 7 and 27 days are within the standard deviation of the reference. The most likely cause of the discrepancy at the time and temperature point is error in sample extraction of the 14 day 4°C sample.

Table 3.9: A reverse isochronous stability study of microcystin-LR conducted at -80, -20, 4, 23 and 40°C over three time points of 7, 14 and 27 days. Stability was assessed using LC-MS/MS and the Poroshell column. Values are represented as concentration relative to the -80°C reference sample ± the standard deviation obtained through analysis of three extractions per sample stored at each time and temperature point with three replicate injections (n=3).

	Time		
	7 Day	**14 Day**	**27 Day**
-80°C Reference	1.00 ± 0.06	1.00 ± 0.06	1.00 ± 0.06
-20°C	1.01 ± 0.05	1.06 ± 0.08	1.0 ± 0.1
4°C	0.9 ± 0.1	0.87 ± 0.04	0.95 ± 0.08
23°C	1.0 ± 0.1	0.90 ± 0.09	0.96 ± 0.05
40°C	1.02 ± 0.06	1.0 ± 0.1	0.98 ± 0.03

Regardless of the discrepancy at the 4°C/14 day time point, the RM-BGA is considered to be stable for microcystins across all temperature (-20°C to 40°C) and short term time points.

Homogeneity of anatoxin-a in the RM was investigated using LC-MS/MS analysis. Measurement of anatoxin-a by HILIC-MS/MS over 24 samples found a relative standard deviation of 5.7%, which is considered to be a representation of a homogenous mixture.

Stability of anatoxin-a over 27 days was similar to that of microcystin-LR. Aside from one time points that suggested instability (23°C at 14 day), no instability in anatoxin-a was observed (Table 3.10). As with microcystin-LR, the time point indicating instability of anatoxin-a was bracketed by two time points (7 days and 27 days) that were found to be stable. It is believed that a small discrepancy in sample handing may be the cause for the discrepancy in stability for the single point. Strictly speaking, the 40°C at 27 day time point does not fall out of the standard deviation of the -80°C reference point, however some decomposition would be expected over longer periods of time. Long term stability studies will provide a more information about the instability of a freeze dried algal reference material.

Table 3.10: Stability of microcystin-LR as reported from a reverse isochronous stability study conducted at -80, -20, 4, 23 and 40°C over three time points of 7, 14 and 27 days. Results were obtained from analysis with LC-MS/MS using the Amide 80 column. Values are represented as concentration relative to the -80°C reference sample ± the standard deviation obtained through analysis of three extractions per sample stored at each time and temperature point with three replicate injections (n=3).

	Time		
	7 Day	**14 Day**	**27 Day**
-80°C Reference	1.00 ± 0.05	1.00 ± 0.05	1.00 ± 0.05
-20°C	1.04 ± 0.03	1.05 ± 0.05	1.06 ± 0.04
4°C	0.97 ± 0.05	1.01 ± 0.07	1.04 ± 0.03
23°C	0.98 ± 0.07	0.93 ± 0.01	0.99 ± 0.01
40°C	1.00 ± 0.02	1.06 ± 0.04	0.92 ± 0.04

3.4.9 Quantitation of Anatoxin-a in RM-BGA

Quantitation of anatoxin-a and homoanatoxin-a in RM-BGA was carried out using three separate methods: HILIC-MS/MS, DNS-LC-MS/MS and DNS-LC-FLD. Quantitation by HILIC-MS/MS was accomplished with calibration using the anatoxin-a CRM and the homoanatoxin-a RM. Calibration curves were constructed using a solvent blank and 6 points including a solvent blank ranging in concentration of 1.3×10^{-1} ng mL^{-1} to 31 ng mL^{-1} for anatoxin-a and 9.4×10^{-2} ng mL^{-1} to 22 ng mL^{-1} for homoanatoxin-a, using SRM transitions for each (Figure 3.34). A second-order curvature was observed, which required nonlinear calibration for the HILIC-MS/MS quantitation (Figure 3.35).

Quantitation of anatoxin-a in RM-BGA with HILIC-MS/MS was 54.4 ± 2.1 μg g^{-1} (n = 4) while the concentration of homoanatoxin-a was 18.5 ± 1.0 μg g^{-1} (n = 4). Four separate samples were injected four times each and run between four calibration curves

for the quantitation of analytes. Uncertainties were determined using the standard deviation of the quantified values.

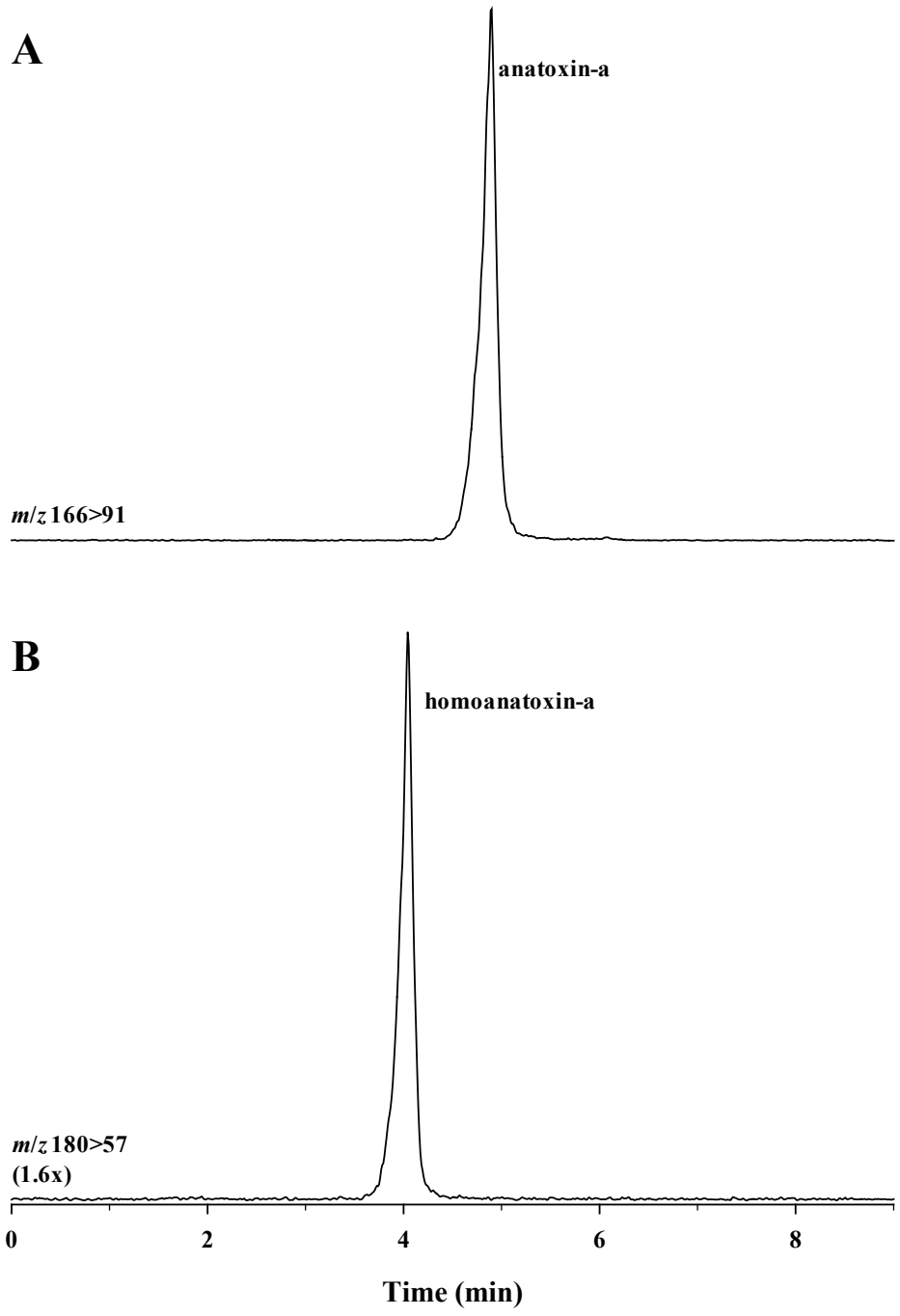

Figure 3.34: HILIC-MS/MS SRM transitions of (A) anatoxin-a and (B) homoanatoxin-a separation on an Amide 80 column using gradient elution at a flow rate of 0.20 mL min^{-1}.

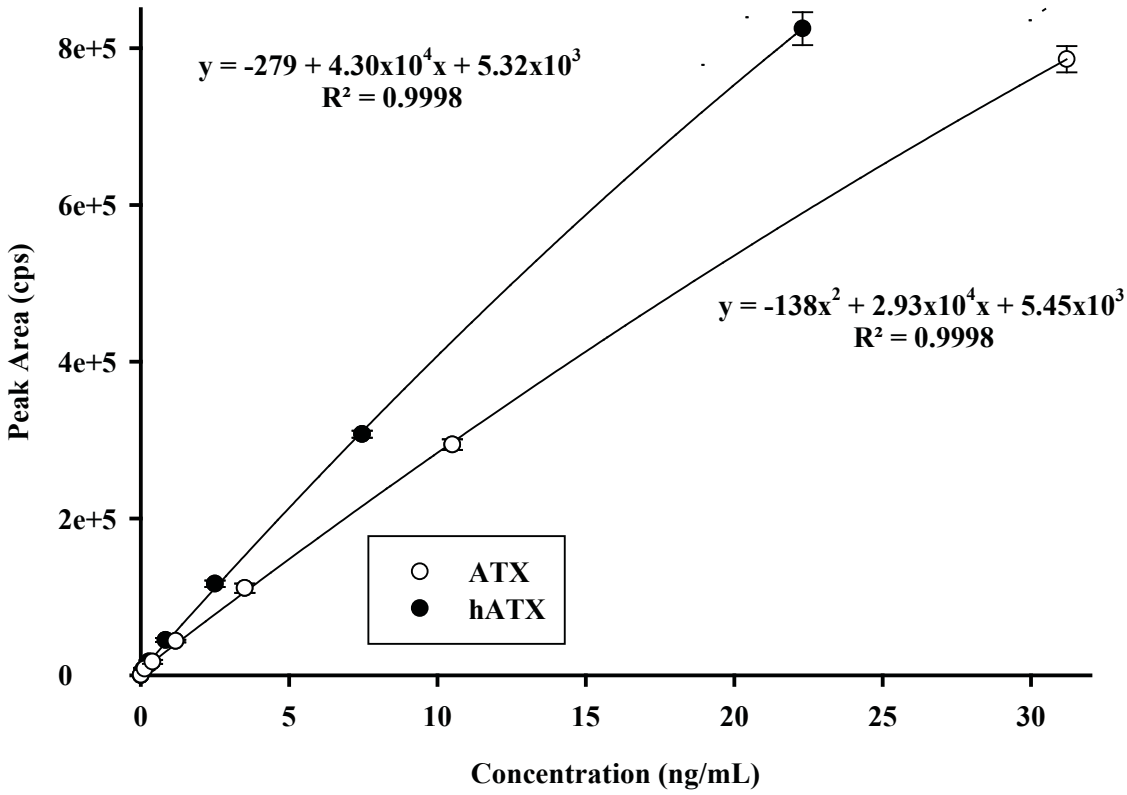

Figure 3.35: Calibration curves for anatoxin-a (ATX) and homoanatoxin-a (hATX) used for RM BGA quantitation using HILIC-MS/MS. Samples were run on an Amide 80 column with gradient elution at a flow rate of 0.20 mL min^{-1}. The solid lines are polynomial fits to all points, while the dashed lines represent a linear fit to the data excluding the highest values. The plotted points are averages of 4 replicates.

Dansylated samples were analyzed by LC-MS/MS. Due to the sensitivity of the LC-MS/MS method, dansylated samples were diluted 15-fold for SRM analysis (Figure 3.36). Each of the four samples was injected six times and run between calibration curve standards. A high degree of linearity was observed for both anatoxin-a and homoanatoxin-a dansyl derivatives in the calibration curve as shown in Figure 3.37. Quantitation of the RM-BGA with LC-MS/MS determined levels of 50.1 ± 4.0 μg g^{-1} (n = 4) for anatoxin-a, 15.5 ± 1.9 μg g^{-1} (n = 4) for homoanatoxin-a.

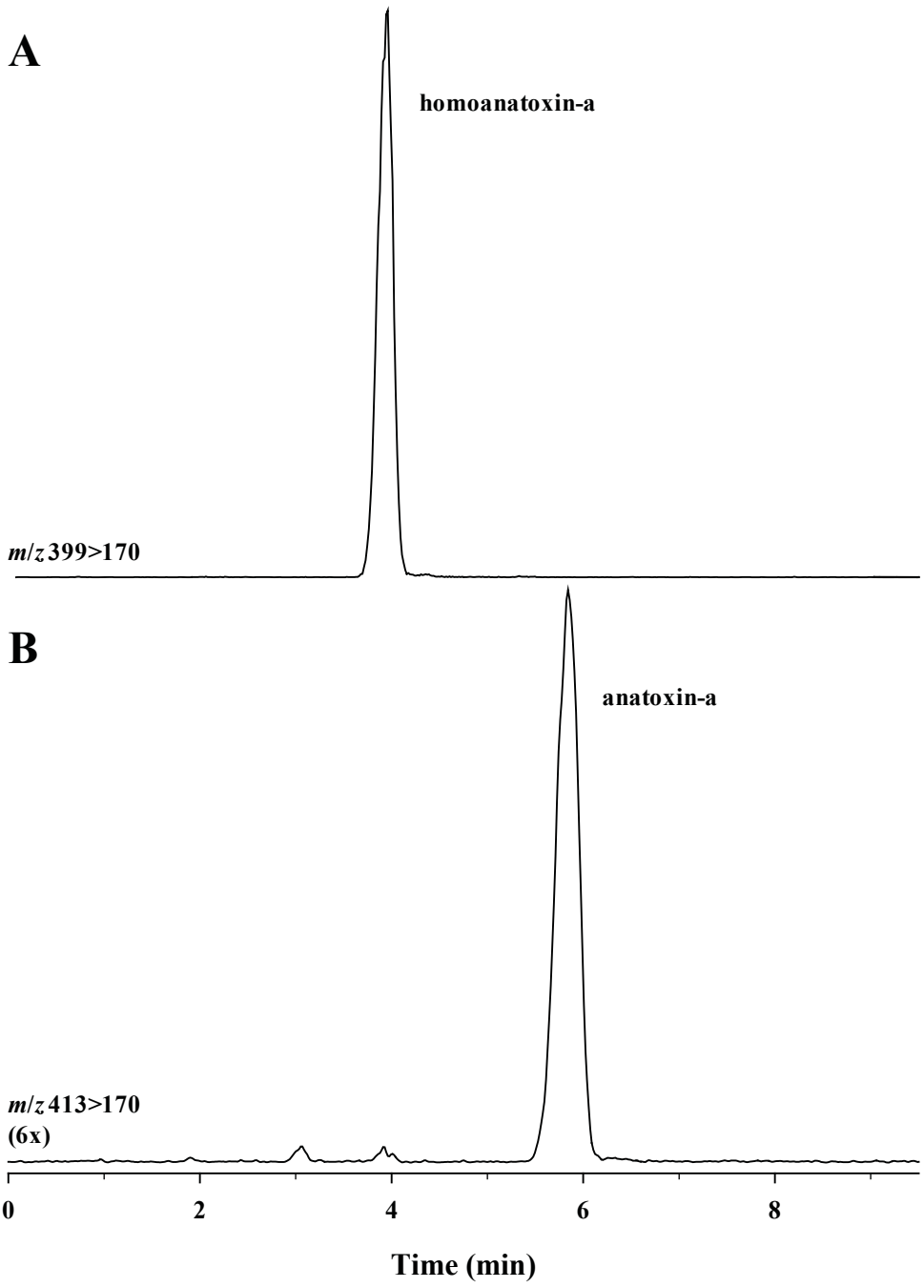

Figure 3.36**:** LC-MS/MS SRM chromatograms of dansylated RM-BGA containing (A) homoanatoxin-a and (B) anatoxin-a. The sample was separated with a Luna C18(2) (50 mm x 2.0 mm) column at a flow rate of 0.20 mL min^{-1}.

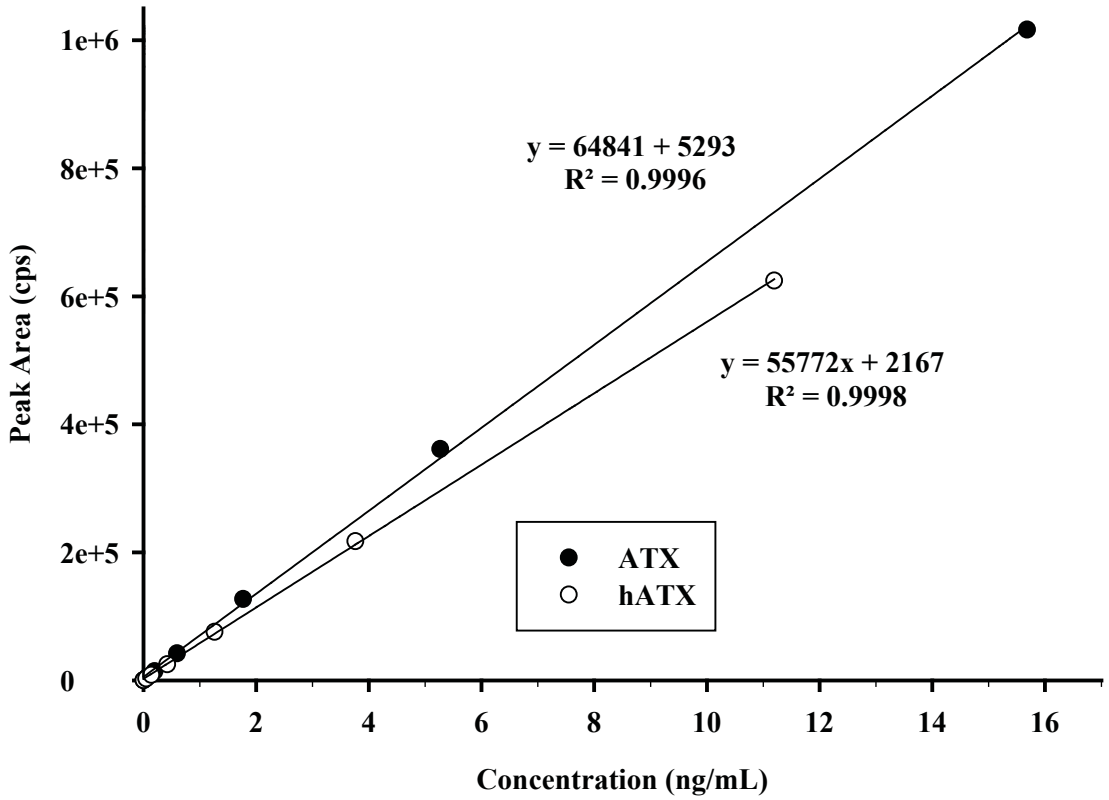

Figure 3.37: Calibration curve for dansylated anatoxin-a (ATX) and homoanatoxin-a (hATX) constructed from the peak area of each analyte. The sample was separated on a Luna C18(2) (50 mm x 2.0 mm) column at a flow rate of 0.20 mL min^{-1}. Each plotted point represents an average of 4 replicates.

Prior to analysis with DNS-LC-FLD, dansylation of anatoxin-a and homoanatoxin-a and was performed in the presence of 3-methylpiperidine as an internal standard (Figure 3.38). The use of the internal standard was valuable as drift due to evaporation of samples was observed when run on the LC-FLD. Calibration curves were constructed by using standards with increasing concentrations of anatoxin-a while maintaining constant concentrations of IS. In this internal standard method, the ratio of anatoxin-a or homoanatoxin-a FLD response to that of the internal standard plotted against the concentration of anatoxin-a or homoanatoxin-a (Figure 3.39). Each calibration

curve was constructed from 6 points including a blank. Each sample was run three times in between four calibration curve standards.

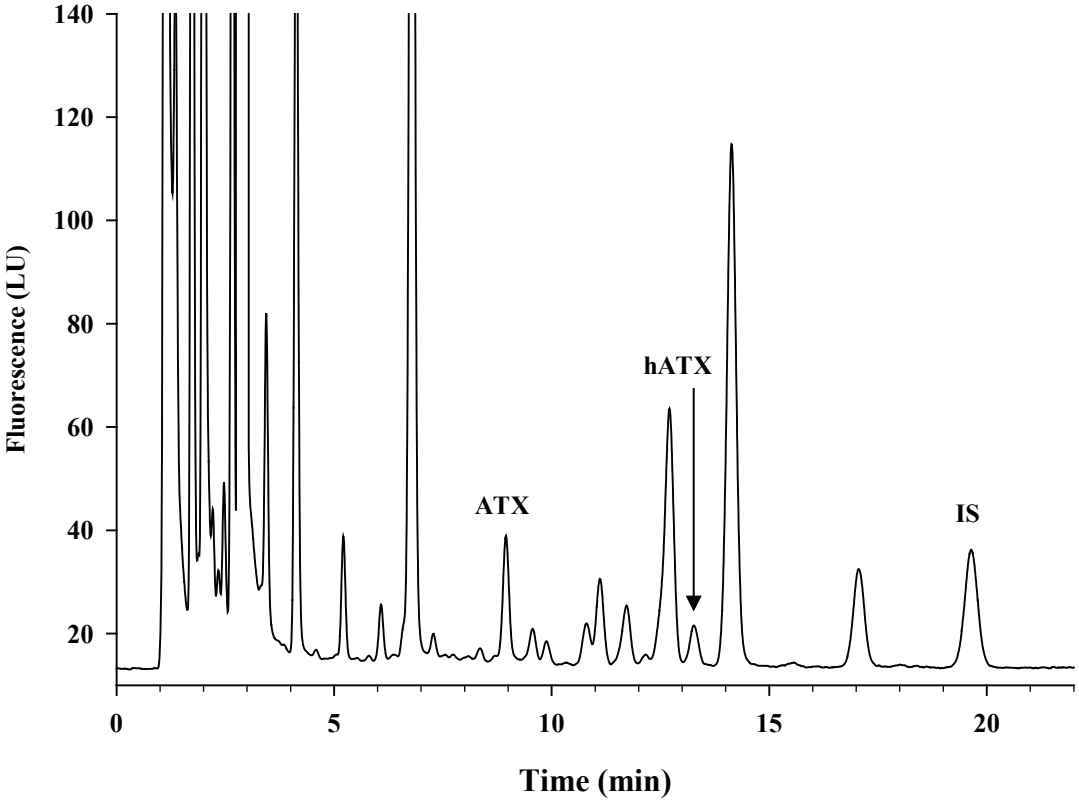

Figure 3.38**:** LC-FLD chromatogram of dansylated RM-BGA with 3-methylpiperidine (IS) spikes. Anatoxin-a (ATX), homoanatoxin-a (hATX) and the internal standard are clearly resolved in this LC-FLD chromatogram. The LC-FLD analysis used the Luna C18(2) (150 mm x 4.6 mm) column at a flow rate of 1.00 mL min^{-1}.

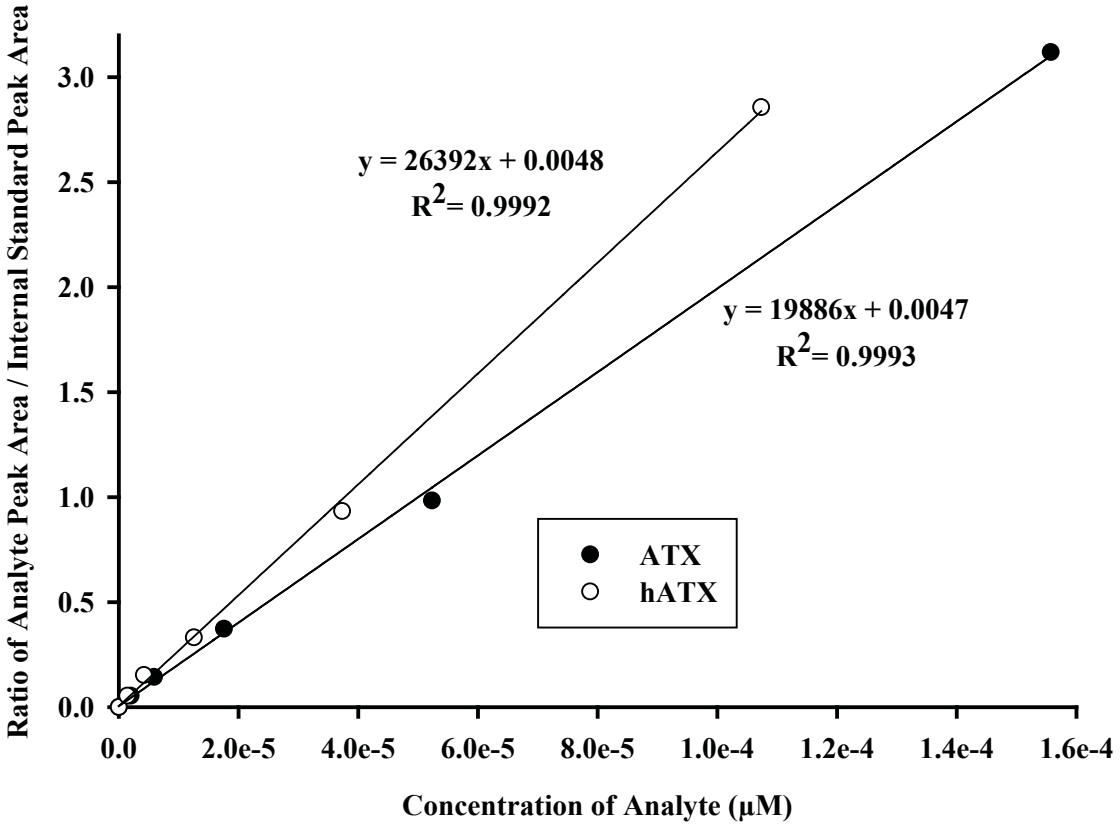

Figure 3.39**:** Calibration curves for dansylated anatoxin-a and homoanatoxin-a (ATX and hATX, respectively) constructed by using the ratio of analyte to internal standard peak areas for each point plotted against increasing analyte concentration. The LC-FLD analysis used the Luna C18(2) (150 mm x 4.6 mm) column at a flow rate of 1.00 mL min^{-1}. Each plotted point represents the average of 4 replicates.

Quantitation of anatoxin-a and homoanatoxin-a as dansyl derivatives was surprisingly successful despite the large potential for error due to the amount of handling and reliance on pipettes with small volumes. After the internal standard correction for evaporation, the RM-BGA contained anatoxin-a at 48.5 ± 4.5 µg g^{-1} (n = 4) and homoanatoxin-a at 15.9 ± 2.2 µg g^{-1} (n = 4). Together, a comparison of all three methods illustrates a strong agreement between anatoxin-a quantitation using HILIC-MS/MS, DNS-LC-MS/MS and DNS-FLD (Table 3.11).

Table 3.11: Quantitation results from anatoxin-a and homoanatoxin-a using HILIC-MS/MS, DNS-LC-MS/MS and DNS-FLD quantitation when n = 4. Quantitaion is illustrated as the average ± the standard deviation in µg g^{-1}.

	Anatoxin-a (µg g^{-1})	**Homoanatoxin-a (µg g^{-1})**
HILIC-MS/MS	51.2 ± 2.3	17.4 ± 1.0
DNS-LC-MS/MS	50.1 ± 4.6	15.5 ± 2.2
DNS-FLD	48.5 ± 6.2	15.9 ± 2.5

While the anatoxin-a and homoanatoxin-a values are all in agreement using the three different methods, the standard deviation for the HILIC-MS/MS method is smaller than the dansyl methods. This is believed to be due to the additional steps involved with the dansylation process.

3.4.10 Quantitation of Microcystins in RM-BGA

Quantitation of microcystins was performed using two methods, LC-UVD and LC-MS/MS. Using LC-MS/MS as the first analysis method for microcystins, microcystin-LR and dmLR were resolved with use of SRM (Figure 3.40). This allowed for the construction of a calibration curve with standards for microcystin-RR, microcystin-LR and dmLR. Calibration curves were constructed from dilutions of the three standards with good linear agreement (Figure 3.41). Seven point calibration curves were used, including a solvent blank, and samples were injected four times over the experiment in between the calibration curves. Through LC-MS/MS measurement of the RM-BGA, the following concentrations were determined: 508 ± 21 for microcystin-RR, 579 ± 16 for microcystin-LR, 305 ± 16 for dmLR, 15 ± 1 for microcystin-(H4y)R, 64 ± 2 for microcystin-YR, 419 ± 14 for [Leu1]-microcystin-LR and 275 ± 14 for [Leu1]-microcystin-LY.

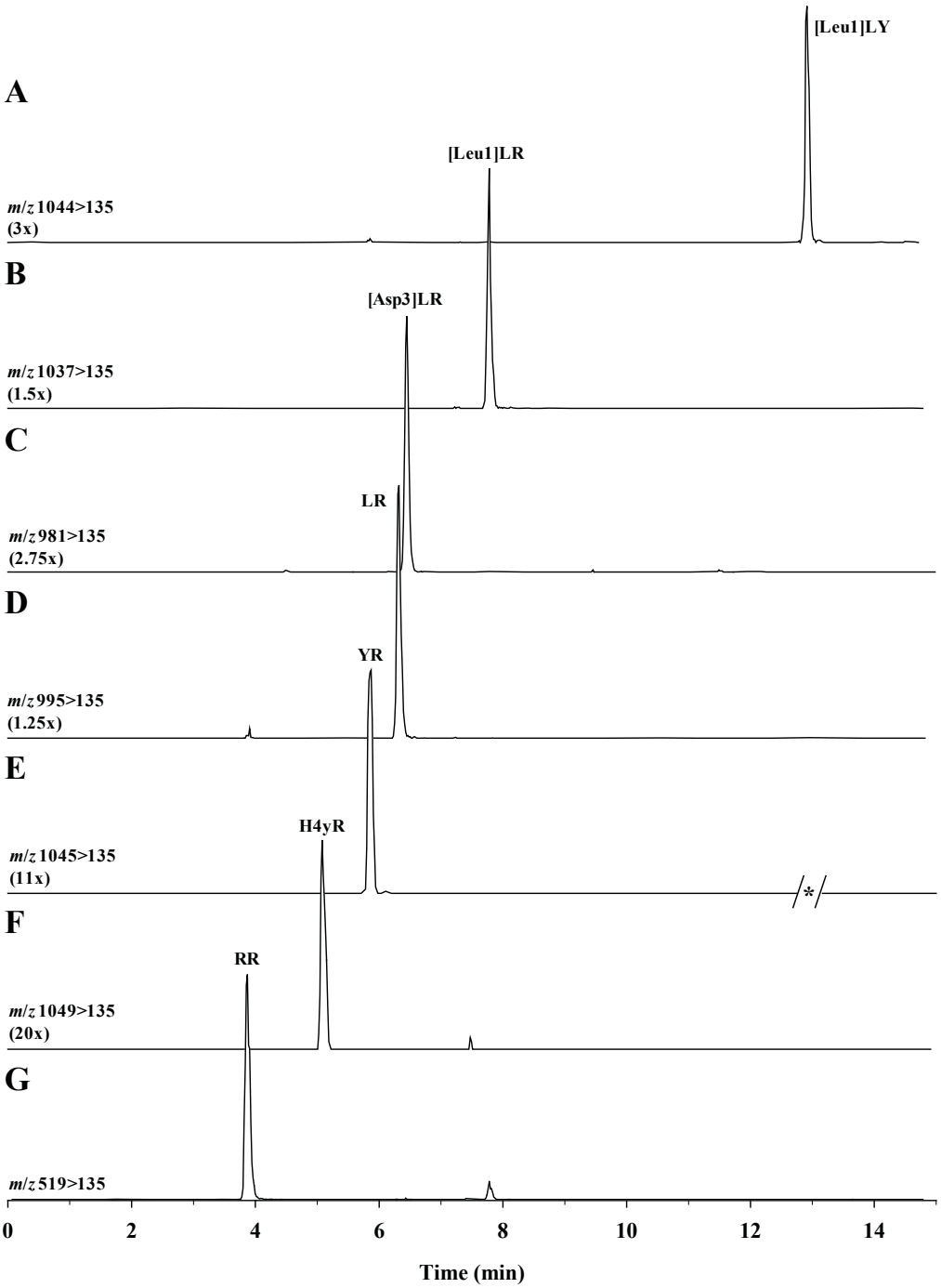

Figure 3.40: LC-MS/MS SRM chromatograms of: (A) [Leu1]-microcystin-LY ([Leu1]LY; (B) [Leu1]-microcystin-LR ([Leu1]LR; (C) [Asp3]-microcystin-LR ([Asp3]LR; (D) microcystin-LR (LR); (E) microcystin-YR (YR); (F) microcystin-H4yR (H4yR); (G) microcystin-RR (RR). Samples were separated on a Poroshell SB C18(2) column (150 mm x 2.1 mm) with gradient elution using a flow rate of 0.25 mL min^{-1}. '*' denotes an isotopic peak for [Leu]LY at [M+H] + 1 that was removed from the chromatogram.

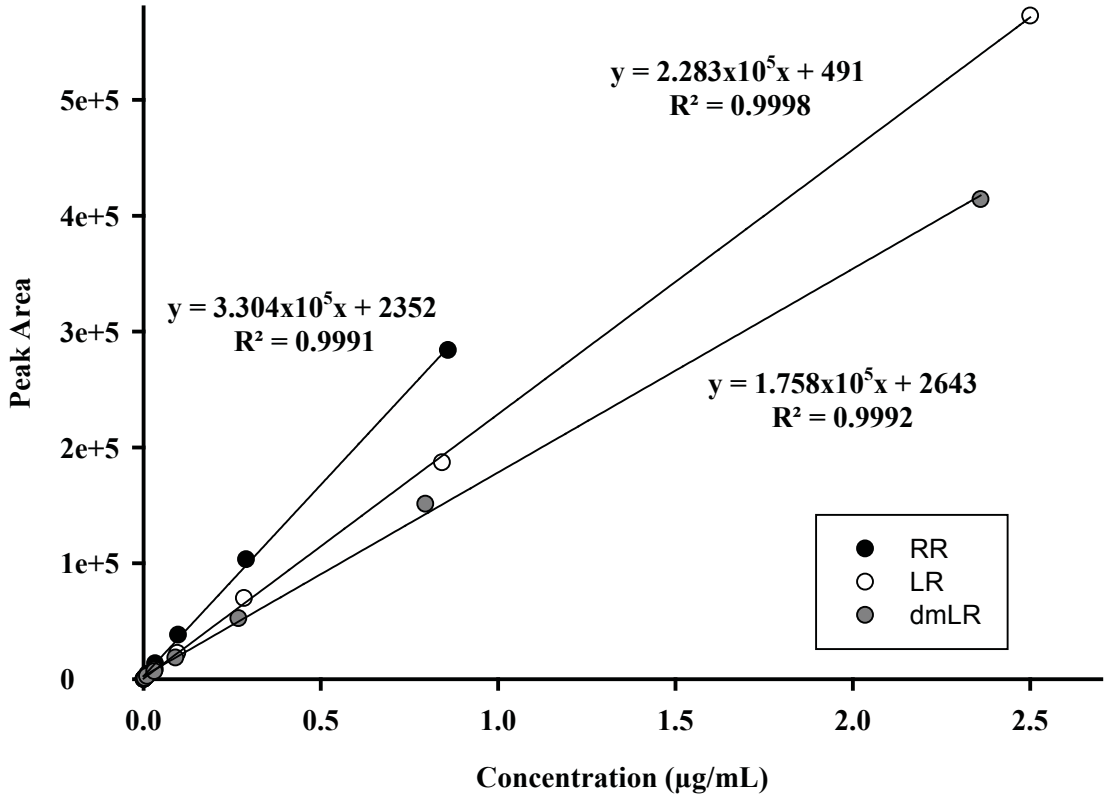

Figure 3.41: LC-MS/MS calibration curves of microcystin-RR (RR), microcystin-LR (LR) and dmLR constructed from dilution of standards. Samples were separated on a Poroshell SB C18(2) column (150 mm x 2.1 mm) with a gradient elution at a flow rate of 0.25 mL min^{-1}. Each plotted point represents the average of 4 replicates.

A slightly different retention time was observed while quantifying microcystins through LC-MS/MS when compared to LC-UVD, which was due to the different mobile phases run using LC-MS/MS. The LC-UVD method was changed slightly by using a different mobile phase (0.05% TFA in H_2O and MeCN). The TFA mobile phase was used instead of the ammonium formate mobile phase because TFA absorbs less at the detection wavelength (238 nm), resulting in less baseline drift during the gradient elution. Before analysis with LC-UVD, identities of the microcystins were first verified by using

the same Agilent 1200 binary pump on LC-UVD and LC-MS/MS to confirm identities of LC-UVD peaks (Figure 3.42).

A six point calibration curve for LC-UVD analysis was constructed using a mixture of the microcystin CRMs, microcystin-RR, microcystin-LR and dmLR. As shown in Figure 3.43, microcystin-RR is clearly resolved from other interferences in the LC-UVD chromatogram, while microcystin-LR and [Asp3]-microcystin-LR partially co-elute due to the structural similarities. Because of the co-elution of dmLR and microcystin-LR, their combined concentration was used for the calibration curve (Figure 3.43). Through LC-UVD calibration, the concentration of microcystin-RR was 481 ± 15 μg g^{-1} (6), while the combined concentration of microcystin-LR and [Asp3]-microcystin-LR was 880 ± 21 μg g^{-1} (6). While there was no [Asp3]-microcystin-LR standard available, the dmLR standard is very similar in structure and retention time, and was used as a standard for [Asp3]-microcystin-LR. Other microcystins in RM-BGA (including microcystin-(H4y)R, microcystin-YR, [Leu1]-microcystin-LR and [Leu1]-microcystin-LY) had concentrations of 193 ± 6, 267 ± 7, 1434 ± 24 and 630 ± 16 respectively (μg g^{-1}; n = 6). Comparison of the two quantitation methods for microcystins showed good agreement between the methods for toxins quantified with accurate CRM-based calibrants (Table 3.12).

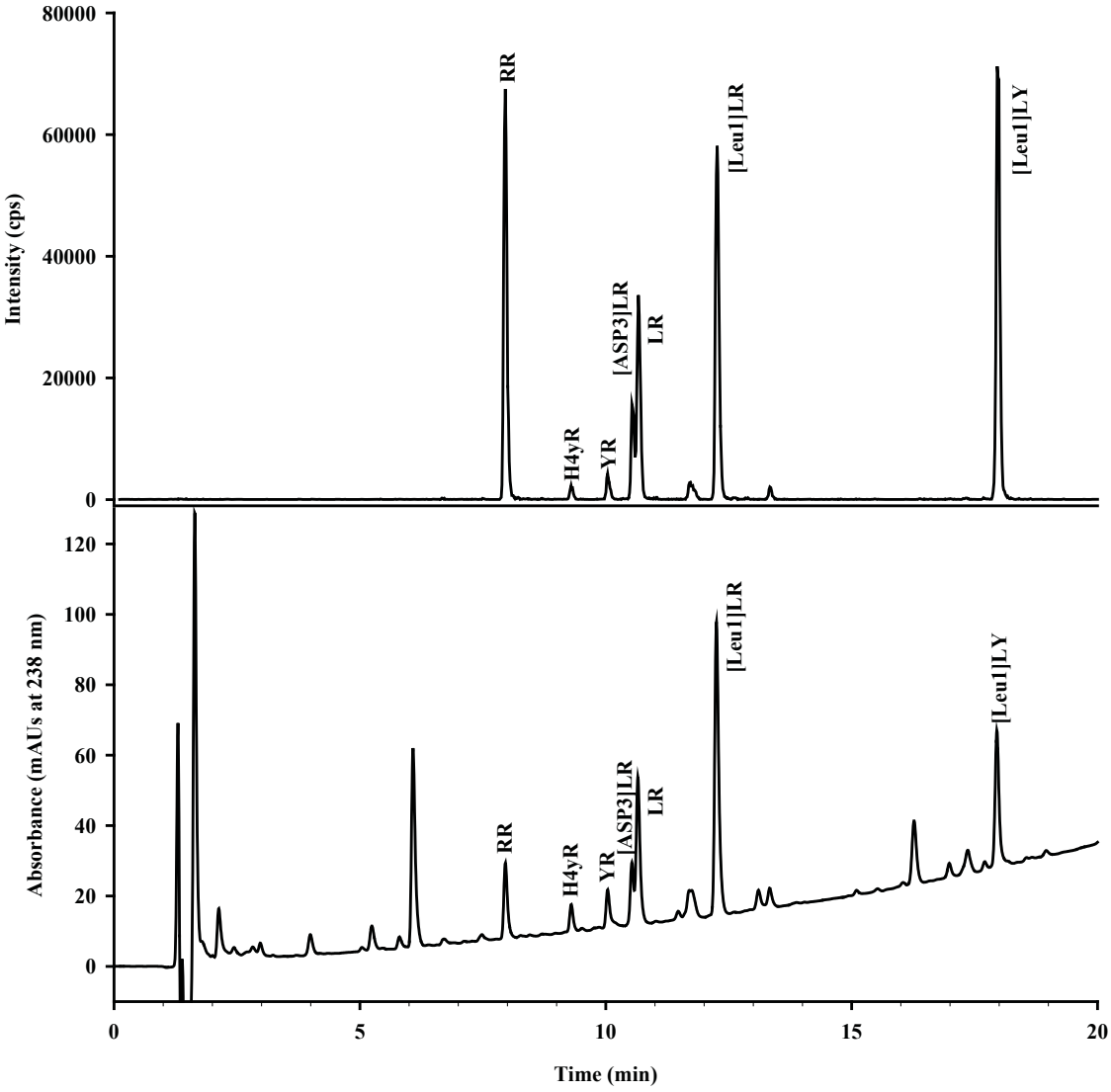

Figure 3.42: (Above) LC-MS/MS total ion chromatogram of microcystins in RM-BGA run on an Agilent 1200 binary pump. (Below) LC-UVD chromatogram of the same RM-BGA sample run on the same Agilent 1200 binary pump used for the LC-MS/MS chromatogram above. Both LC-MS/MS and LC-UVD peaks are labeled according to the microcystin eluted at the specific retention time. For both chromatograms the Poroshell SB C18(2) column (150 mm x 2.1 mm) was used with gradient elution at both chromatograms with a flow rate of 0.25 mL min^{-1}.

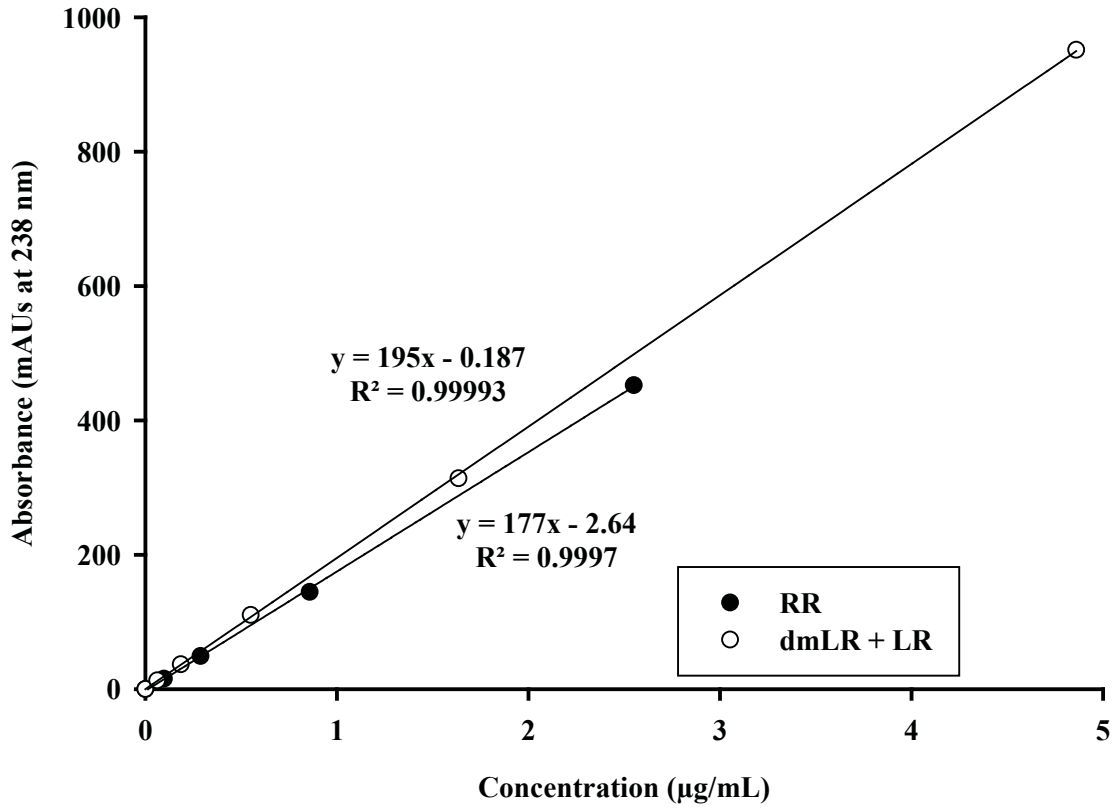

Figure 3.43: LC-UVD calibration curves; microcystin-RR (RR) and a mixture of dmLR and microcystin-LR (dmLR + LR) were used as calibrants. The method used the Poroshell SB C18(2) column (150 mm x 2.1 mm) with gradient elution at a flow rate of 0.25 mL min^{-1}. Each plotted point represents an average of 4 replicates.

Microcystins that showed the largest discrepancies between quantified values had their calibration based on microcystin-LR since accurate standards of those analytes were not available. Differences in response between structural analogues were expected in LC-MS due to differences in ionization efficiencies that commonly exist between different analytes. It was expected that LC-UVD response would be similar amongst some microcystins with very similar structures but many of the microcystin analogues in RM-BGA contain amino acids with an aromatic amino acid (Y = Tyrosine) that would affect

UV absorbance. This emphasizes the importance of matched accurate standards for quantitation purposes. Therefore concentration values in RM-BGA cannot be accurately assigned for microcystin-(H4y)R, microcystin-YR, [Leu1]-microcystin-LR or [Leu1]-microcystin-LY. Toxins with available standards (microcystin-RR, microcystin-LR and [Asp3]-microcystin-LR) were quantified using LC-UVD and LC-MS with results agreeing between the two methods.

Table 3.12: Quantitation results for microcystins using LC-MS/MS and LC-UVD when n=6. Available standards included microcystin-RR (RR), dmLR and microcystin-LR (LR)

	LC-MS/MS	LC-UVD
microcystin-RR	508 ± 21	481 ± 15
[Asp3]-microcystin-LR	305 ± 11	
microcystin-LR	579 ± 16	
[Asp3]-microcystin-LR + microcystin-LR	884 ± 24	880 ± 21
microcystin-(H4 y)R	15 ± 1	193 ± 6
microcystin-YR	64 ± 2	267 ± 7
[Leu1]-microcystin-LR	419 ± 14	1434 ± 24
[Leu1]-microcystin-LY	275 ± 14	630 ± 16

CHAPTER 4 CONCLUSIONS

A calibration solution reference material (RM-hATX) was developed for homoanatoxin-a. An efficient extraction was performed on an *Oscillatoria formosa* algal culture to isolate, purify, quantify and characterize the homoanatoxin-a used to produce RM-hATX. It was characterized by NMR, accurate mass analysis in a high resolution Orbitrap mass spectrometer, enhanced product ion analysis using a triple quadrupole mass spectrometer and LC-UVD. A toxin concentration of 20.2 ± 0.7 μM was determined in the RM using qNMR and CLND. RM-hATX was assessed for stability and found to be stable when stored at -80°C. Two compounds resulting from storage at high temperature (40°C) were noted as possible oxidation products. Dihydro and epoxy analogues of the two anatoxins were also produced to serve as qualitative standards for oxidized and reduced compounds.

A successful derivatization reaction for the anatoxins was established using dansyl chloride as a reagent. The reaction was optimized to be quick (10 min), low in volume (300 μL) and robust over a pH range of 8.9 to 9.6. A novel cleanup method using a Phenomenex Strata X-AW cartridge was used to remove excess derivatization reagent from the reaction mixture while retaining the derivatized analytes. This allowed for elution of salts by an aqueous wash and the derivatized analytes by organic elution. Over 98% of dansylated compound was recovered from the X-AW cartridge. The organic elution solvent allowed for easy evaporative pre-concentration of the eluted compounds, permitting trace level detection of analytes by LC-FLD and LC-MS/MS.

The DNS-LC-MS/MS method was first established for dansylated analytes with DP and CE setting optimization. Product ion spectra were acquired to establish the SRM transitions for monitoring the dansylated compounds. Relative molar responses between dansylated anatoxin-a (*m*/*z* 399→170) and homoanatoxin-a (*m*/*z* 413→170) were explored, with dansylated homoanatoxin-a having 89.1 ± 2.5% the response of dansylated homoanatoxin-a. Two internal standards, piperidine and pyrrolidine, were suitable internal standards, for quantitation of anatoxin-a and homoanatoxin-a, respectively. Validation established a linear range of 9.7 pg mL^{-1} to 42 ng mL^{-1} and a high degree of accuracy (94-102%) determined using spiked concentrations of anatoxin (6.6 - 1598 ng g^{-1}). LOD and LOQ of the method using dansyl-anatoxin-a standards were 20 ng L^{-1} and 60 ng L^{-1}, respectively. The established HILIC-MS/MS analysis of underivatized anatoxin-a had LOD and LOQ of 250 ng L^{-1} and 750 ng L^{-1}, respectively. The DNS-LC-MS/MS method was able to resolve anatoxin-a from its isobaric interference, phenylalanine, as well as the epoxy and dihydro analogues in a quick (8.5 min) analysis using a short column (50 mm x 2.0 mm) and a mobile phase flow rate of 0.2 mL min^{-1}. Six samples were analyzed for their anatoxin content via DNS-LC-MS/MS and compared with HILIC-MS/MS. The DNS-LC-MS/MS method agreed with the HILIC-MS/MS method within a 95% confidence interval for the analysis of anatoxin-a and homoanatoxin-a. The other analytes had close quantitation but had statistically significant differences likely due to the lack of quantitative standards.

An LC-FLD method was established to exploit the highly fluorescent properties of dansyl chloride. An acetonitrile mobile phase with formic acid modifier (pH 2.3) was selected to provide the best separation from reagent peaks and interferences. Despite

concerns with possible quenching of the analyte's fluorescence in the acidic mobile phase, dansyl-anatoxin was found to be strongly fluorescent. The method was optimized with a wide bore column (150 mm x 4.6 mm) that provided the required resolution of anatoxin analytes from reagent peaks and compatibility with the fluorescence detection cell volume. Method validation established a linear range of 1.6 ng mL^{-1} to 1.1 mg mL^{-1} using a dansyl anatoxin-a standard, with a LOQ of 1.6 ng mL^{-1}. The response of dansylated homoanatoxin-a to anatoxin-a was 134.0 ± 0.7 %, with intramolecular quenching believed to be responsible for the non-equal molar response. These findings determined that one quantitative standard cannot be used to quantify the anatoxin analogues. However, the method served as a viable method of quantitation when a standard was available. Quantitation of dansylated anatoxin-a and homoanatoxin-a was compared with HILIC-MS/MS analysis and was found to have no statistically significant difference within a 95% confidence interval for the three samples examined.

A previously established microcystin method [72] was modified for LC-MS/MS and LC-UVD analysis of microcystins. Validation of the LC-MS/MS method determined the LOQ to be 3.8 μg L^{-1} in the final extract. However, a pre-concentration step using an Oasis HLB column cartridge, which could recover 98% of the toxin, gave a thirty-fold concentration for quantitation of microcystins allowing microcystins to be detected at levels well below the New Zealand maximum allowable concentration of microcystins in water samples (1 μg L^{-1}). The linear range of the instrument was 3.8 to 2800 μg L^{-1}. Validation of the LC-UVD method established a LOQ of 97 μg L^{-1}, with a linear range of 97 – 2550 μg L^{-1}. Six algal nutritional supplement samples were examined, with all *A. flos-aquae* samples being found to contain some level of microcystin. It was shocking

and disturbing to find that the levels of toxins in some of the supplements were higher than regulatory limits established for protection of human health. The results of this study reiterated the need for regulation of the algal supplement industry.

Finally, algal cultures and samples were screened for their suitability for use in a freeze dried algal reference material. Cultures containing anatoxins and microcystins were selected based on toxin concentration and available biomass. A method for the production of RM-BGA was established, with moisture analysis monitored throughout the experiment to provide the best conditions for stability. Scanning electron microscopy was used as a qualitative check for homogeneity of particle size. Particle size analysis performed off-site indicated a relatively homogenous mixture with two major particle sizes corresponding to the cell size of the algal samples used. Short term (27 day) stability studies found the reference material to be sufficiently stable over short term storage under all temperatures tested (-20, 4, 23 and 40°C) for both microcystins and anatoxins. Quantitation was performed on anatoxin-a and homoanatoxin-a present within the RM-BGA using the three methods established in this project: HILIC-MS/MS, DNS-LC-MS/MS and DNS-LC-FLD. The concentrations determined for anatoxin-a and homoanatoxin-a agreed within the standard deviation of each method and were deemed to have no statistically significant difference within a 95% confidence interval. Microcystins were quantified by LC-UVD and LC-MS/MS; however, only those microcystins with available standards could be correctly quantified, molar responses between the different analytes varied in the two methods. Microcystin-RR, [Asp3]-microcystin-LR and microcystin-LR quantitation was achieved with no statistically significant difference between the two methods using a 95% confidence interval.

Future work will involve long term homoanatoxin-a stability studies to verify long term stability of the reference material, along with freeze-thaw experiments to see if this was a possible cause of decomposition for the -20°C samples. Accurate mass analysis of the homoanatoxin-a decomposition products will be performed to verify the elemental composition of these compounds. The epoxidation reaction for anatoxin-a and homoanatoxin-a will be further explored to prepare a dansylated epoxy analogue as a qualitative standard. Future work involving the RM-BGA will involve preparing a control sample that is negative for microcystin and anatoxin toxins, and will focus on isolating a tyrosine containing microcystin for better LC-UVD quantitation.

REFERENCES

1. Bláhová L, Babica P, Maršálková E, Maršálek B, Bláha L. (2007) Concentrations and Seasonal Trends of Extracellular Microcystins in Freshwaters of the Czech Republic – Results of the National Monitoring Program. Clean 35:348–354. doi: 10.1002/clen.200700010

2. Puschner B, Hoff B, Tor ER (2008) Diagnosis of Anatoxin-a Poisoning in Dogs from North America. Journal of Veterinary Diagnostic Investigation 20:89–92. doi: 10.1177/104063870802000119

3. Gugger M, Lenoir S, Berger C, Ledreux A, Druart JC, Humbert JF, Guette C, Bernard C. (2005) First report in a river in France of the benthic cyanobacterium Phormidium favosum producing anatoxin-a associated with dog neurotoxicosis. Toxicon 45:919–928. doi: 10.1016/j.toxicon.2005.02.031

4. Wood SA, Selwood AI, Rueckert A, Holland PT, Milne JR, Smith KF, Smits B, Watts LF, Cary CS. (2007) First report of homoanatoxin-a and associated dog neurotoxicosis in New Zealand. Toxicon 50:292–301. doi: 10.1016/j.toxicon.2007.03.025

5. Falconer IR (2005) Cyanobacterial toxins of drinking water supplies: cylindrospermopsins and microcystins. CRC Press

6. Azevedo SMF., Carmichael WW, Jochimsen EM, Rinehart KL, Lau S, Shaw GR, Eaglesham GK. (2002) Human intoxication by microcystins during renal dialysis treatment in Caruaru—Brazil. Toxicol. 181–182:441–446. doi: 10.1016/S0300-483X(02)00491-2

7. WHO | Toxic cyanobacteria in water: A guide to their public health consequences, monitoring and management. In: WHO. http://www.who.int/water_sanitation_health/resourcesquality/toxicyanbact/en/. Accessed 2 Feb 2013

8. Stanier RY, Bazine GC (1977) Phototrophic Prokaryotes: The Cyanobacteria. Annual Review of Microbiology 31:225–274. doi: 10.1146/annurev.mi.31.100177.001301

9. Krienitz L, Ballot A, Kotut K, Wiegand C, Pütz S, Metcalf JS, Codd GA, Pflugmacher S. (2003) Contribution of hot spring cyanobacteria to the mysterious deaths of Lesser Flamingos at Lake Bogoria, Kenya. FEMS Microbiol Ecol 43:141–148. doi: 10.1111/j.1574-6941.2003.tb01053.x

10. Stal LJ (2007) Cyanobacteria. Springer Netherlands, pp 659–680

11. Brock TD, Madigan MT (1991) Biology of microorganisms. Prentice Hall

12. Stal LJ (2001) Nitrogen Fixation in Cyanobacteria. eLS

13. Paul VJ (2008) Global warming and cyanobacterial harmful algal blooms. Adv Exp Med Biol 619:239–257. doi: 10.1007/978-0-387-75865-7_11

14. Mink farms likely polluted lakes, study finds - Nova Scotia - CBC News. http://www.cbc.ca/news/canada/nova-scotia/story/2012/04/02/ns-mink-farms-water-quality-lakes.html. Accessed 2 Feb 2013

15. Lakes in every province high in dangerous toxin: study. In: CTVNews. http://www.ctvnews.ca/health/lakes-in-every-province-high-in-dangerous-toxin-study-1.915502. Accessed 2 Feb 2013

16. Orihel DM, Bird DF, Brylinsky M, Chen H, Donald DB, Huang DY, Giani A, Kinniburgh D, Kling H, Kotak BG, Leavitt PR, Nielsen CC, Reedyk S, Rooney RC, Watson SB, Zurawell RW, Vinebrooke RD. (2012) High microcystin concentrations occur only at low nitrogen-to-phosphorus ratios in nutrient-rich Canadian lakes. Can J Fish Aquat Sci. 69:1457–1462. doi: 10.1139/f2012-088

17. Jochimsen EM, Carmichael WW, An J, Cardo DM, Cookson ST, Holmes CEM, Antunes MBC, Melo Filho DA, Lyra TM, Barreto VST, Aevedo SMFO, Jarvis WR. (1998) Liver Failure and Death after Exposure to Microcystins at a Hemodialysis Center in Brazil. N Eng. J Med 338:873–878. doi: 10.1056/NEJM199803263381304

18. Dillenberg HO, Dehnel MK (1960) Toxic Waterbloom in Saskatchewan, 1959. Can Med Assoc J 83:1151–1154.

19. Turner PC, Gammie AJ, Hollinrake K, Codd GA (1990) Pneumonia associated with contact with cyanobacteria. BMJ 300:1440–1441.

20. Griffiths DJ, Saker ML (2003) The Palm Island mystery disease 20 years on: a review of research on the cyanotoxin cylindrospermopsin. Environ Toxicol 18:78–93. doi: 10.1002/tox.10103

21. Long EG, Ebrahimzadeh A, White EH, Swisher B, Callaway CS. (1990) Alga associated with diarrhea in patients with acquired immunodeficiency syndrome and in travelers. J Clin Microbiol 28:1101–1104.

22. Long EG, White EH, Carmichael WW, Quinlisk PM, Raja R, Swisher BL, Daugharty H, Cohen MT. (1991) Morphologic and Staining Characteristics of a Cyanobacterium-like Organism Associated with Diarrhea. J Infect Dis 164:199–202. doi: 10.2307/30112898

23. MacKintosh C, Beattie KA, Klumpp S, Cohen P, Codd GA. (1990) Cyanobacterial microcystin-LR is a potent and specific inhibitor of protein phosphatases 1 and 2A from both mammals and higher plants. FEBS Lett 264:187–192.

24. Heussner AH, Mazija L, Fastner J, Dietrich DR (2012) Toxin content and cytotoxicity of algal dietary supplements. Toxicol Appl Pharmacol 265:263–271. doi: 10.1016/j.taap.2012.10.005

25. Vichi S, Lavorini P, Funari E, Scardala S, Testai E. (2012) Contamination by Microcystis and microcystins of blue–green algae food supplements (BGAS) on the italian market and possible risk for the exposed population. Food Chem Toxicol 50:4493–4499. doi: 10.1016/j.fct.2012.09.029

26. Francis G (1878) Poisonous Australian Lake. Nature 18:11–12. doi: 10.1038/018011d0

27. Nishiwaki-Matsushima R, Ohta T, Nishiwaki S, Suganuma M, Kohyama K, Ishikawa T, Carmichael WW, Fujiki H. (1992) Liver tumor promotion by the cyanobacterial cyclic peptide toxin microcystin-LR. J Cancer Res Clin Oncol 118:420–424.

28. Spencer PS, Nunn PB, Hugon J, Ludolph AC, Ross SM, Roy DN, Robertson RC. (1987) Guam amyotrophic lateral sclerosis-parkinsonism-dementia linked to a plant excitant neurotoxin. Science 237:517–522.

29. Cox PA, Banack SA, Murch SJ, Rasmussen U, Tien G, Bidigare RR, Metcalf JS, Morrison LF, Codd GA, Bergman B. (2005) Diverse taxa of cyanobacteria produce β-*N*-methylamino-L-alanine, a neurotoxic amino acid. PNAS 102:5074–5078. doi: 10.1073/pnas.0501526102

30. Duncan MW, Steele JC, Kopin IJ, Markey SP (1990) 2-Amino-3-(methylamino)-propanoic acid (BMAA) in cycad flour: an unlikely cause of amyotrophic lateral sclerosis and parkinsonism-dementia of Guam. Neurology 40:767–772.

31. Krüger T, Mönch B, Oppenhäuser S, Luckas B (2010) LC-MS/MS determination of the isomeric neurotoxins BMAA (beta-N-methylamino-L-alanine) and DAB (2,4-diaminobutyric acid) in cyanobacteria and seeds of Cycas revoluta and Lathyrus latifolius. Toxicon 55:547–557. doi: 10.1016/j.toxicon.2009.10.009

32. Replies to Lack of β-methylamino-l-alanine in brain from controls, AD, or Chamorros with PDC. http://www.neurology.org/content/65/5/768.abstract/reply. Accessed 28 Feb 2013

33. Montine TJ, Li K, Perl DP, Galasko D (2005) Lack of β-methylamino-l-alanine in brain from controls, AD, or Chamorros with PDC. Neurology 65:768–769. doi: 10.1212/01.wnl.0000174523.62022.52

34. Snyder LR, Cruz-Aguado R, Sadilek M, Galasko D, Shaw CA, Montine TJ. (2009) Parkinson-dementia complex and development of a new stable isotope dilution assay for BMAA detection in tissue. Toxicol Appl Pharmacol 240:180–188. doi: 10.1016/j.taap.2009.06.025

35. Quilliam MA (2003) The role of chromatography in the hunt for red tide toxins. J Chromatogr A 1000:527–548.

36. Falconer IR (1993) Algal toxins in seafood and drinking water. Academic Press

37. Turner PC, Gammie AJ, Hollinrake K, Codd GA (1990) Pneumonia associated with contact with cyanobacteria. BMJ 300:1440–1441. doi: 10.1136/bmj.300.6737.1440

38. Dawson RM (1998) The toxicology of microcystins. Toxicon 36:953–962.

39. Holstege CP, Kirk M, Sidell FR (1997) CHEMICAL WARFARE: Nerve Agent Poisoning. Critical Care Clinics 13:923–942. doi: 10.1016/S0749-0704(05)70374-2

40. BLAKE v. CELL TECH INTERNATIONAL INCORPORATED, 050403928; A135647., May 20, 2009 - OR Court of Appeals | FindLaw. http://caselaw.findlaw.com/or-court-of-appeals/1383117.html. Accessed 1 Mar 2013

41. Yoshizawa S, Matsushima R, Watanabe MF, Harada K, Ichihara A, Carmichael WW, Fujiki H. (1990) Inhibition of protein phosphatases by microcystis and nodularin associated with hepatotoxicity. J Cancer Res Clin 116:609–614. doi: 10.1007/BF01637082

42. Gilroy DJ, Kauffman KW, Hall RA, Huang X, Chu FS. (2000) Assessing potential health risks from microcystin toxins in blue-green algae dietary supplements. Environ Health Perspect 108:435–439.

43. Rawn DFK, Niedzwiadek B, Lau BPY, Saker M (2007) Anatoxin-a and its metabolites in blue-green algae food supplements from Canada and Portugal. J Food Prot 70:776–779.

44. Rellán S, Osswald J, Saker M, Gago-Martinez A, Vasconcelos V. (2009) First detection of anatoxin-a in human and animal dietary supplements containing cyanobacteria. Food Chem Toxicol 47:2189–2195. doi: 10.1016/j.fct.2009.06.004

45. Jiang Y, Xie P, Chen J, Liang G (2008) Detection of the hepatotoxic microcystins in 36 kinds of cyanobacteria Spirulina food products in China. Food Addit Contam Part A 25:885–894. doi: 10.1080/02652030701822045

46. Government of Canada HC (2004) Blue-Green Algae (Cyanobacteria) and Their Toxins - Drinking Water. http://www.hc-sc.gc.ca/ewh-semt/pubs/water-eau/cyanobacter-eng.php. Accessed 28 Feb 2013

47. Chan E, Rappaport LA, Kemper KJ (2003) Complementary and Alternative Therapies in Childhood Attention and Hyperactivity Problems. J Dev Behav Pediatr 24:4–8.

48. Devlin JP, Edwards OE, Gorham PR, Hunter NR, Pike RK, Stavric B. (1977) Anatoxin-a, a toxic alkaloid from Anabaena flos-aquae NRC-44h. Can J Chem 55:1367–1371. doi: 10.1139/v77-189

49. Koskinen AM, Rapoport H (1985) Synthetic and conformational studies on anatoxin-a: a potent acetylcholine agonist. J Med Chem 28:1301–1309.

50. Cadel-Six S, Iteman I, Peyraud-Thomas C, Mann S, Ploux O, Méjean A. (2009) Identification of a polyketide synthase coding sequence specific for anatoxin-a-producing Oscillatoria cyanobacteria. Appl Environ Microbiol 75:4909–4912. doi: 10.1128/AEM.02478-08

51. Carmichael WW (1992) Cyanobacteria secondary metabolites—the cyanotoxins. J Appl Microbiol 72:445–459. doi: 10.1111/j.1365-2672.1992.tb01858.x

52. Namikoshi M, Murakami T, Watanabe MF, Oda T, Yamada J, Tsujimura S, Nagai H, Oishi S. (2003) Simultaneous production of homoanatoxin-a, anatoxin-a, and a new non-toxic 4-hydroxyhomoanatoxin-a by the cyanobacterium Raphidiopsis mediterranea Skuja. Toxicon 42:533–538. doi: 10.1016/S0041-0101(03)00233-2

53. Viaggiu E, Melchiorre S, Volpi F, Di Corcia A, Mancini R, Garibaldi L, Crichigno G, Bruno M. (2004) Anatoxin-a toxin in the cyanobacterium Planktothrix rubescens from a fishing pond in northern Italy. Environ Toxicol 19:191–197. doi: 10.1002/tox.20011

54. Ballot A, Krienitz L, Kotut K, Wiegand C, Pflugmacher S. (2005) Cyanobacteria and cyanobacterial toxins in the alkaline crater lakes Sonachi and Simbi, Kenya. Harmful Algae 4:139–150. doi: 10.1016/j.hal.2004.01.001

55. Petersen JS, Fels G, Rapoport H (1984) Chirospecific syntheses of (+)- and (-)-anatoxin a. J Am Chem Soc 106:4539–4547. doi: 10.1021/ja00328a040

56. Fawell JK, Mitchell RE, Hill RE, Everett DJ (1999) The toxicity of cyanobacterial toxins in the mouse: II Anatoxin-a. Hum Exp Toxicol 18:168 –173. doi: 10.1177/096032719901800306

57. Stevens DK, Krieger RI (1991) Stability studies on the cyanobacterial nicotinic alkaloid anatoxin-A. Toxicon 29:167–179. doi: 10.1016/0041-0101(91)90101-V

58. James KJ, Sherlock IR, Stack MA (1997) Anatoxin-a in Irish freshwater and cyanobacteria, determined using a new fluorimetric liquid chromatographic method. Toxicon 35:963–971.

59. Tonk L, Visser PM, Christiansen G, Dittmann E, Snelder EOFM, Wiedner C, Mur LR, Huisman J. (2005) The Microcystin Composition of the Cyanobacterium Planktothrix agardhii Changes toward a More Toxic Variant with Increasing Light Intensity. Appl Environ Microbiol 71:5177 –5181. doi: 10.1128/AEM.71.9.5177-5181.2005

60. Bishop CT, Anet EF, Gorham PR. (1959) Isolation and identification of the fast-death factor in Microcystis aeruginosa NRC-1. Can J Biochem Phys 37:453.

61. Botes DP, Tuinman AA, Wessels PL, Viljoen CC, Kruger H, Williams DH, Santikarn S, Smith RJ, Hammond SJ. (1984) The structure of cyanoginosin-LA, a cyclic heptapeptide toxin from the cyanobacterium Microcystis aeruginosa. J Chem Soc, Perkin Trans 1 2311–2318. doi: 10.1039/P19840002311

62. Honkanen RE, Zwiller J, Moore RE, Daily SL, Khatra BS, Dukelow M, Boynton AL. (1990) Characterization of microcystin-LR, a potent inhibitor of type 1 and type 2A protein phosphatases. J Biol Chem 265:19401–19404.

63. Egloff M-P, Cohen PTW, Reinemer P, Barford D (1995) Crystal Structure of the Catalytic Subunit of Human Protein Phosphatase 1 and its Complex with Tungstate. J Mol Biol 254:942–959. doi: 10.1006/jmbi.1995.0667

64. Nishiwaki-Matsushima R, Nishiwaki S, Ohta T, Yoshizawa S, Suganuma M, Harda K, Watanabe MF, Fujiki H. (1991) Structure-Function Relationships of Microcystins, Liver Tumor Promoters, in Interaction with Protein Phosphatase. Jpn J Cancer Res 82:993–996. doi: 10.1111/j.1349-7006.1991.tb01933.x

65. Yu F-Y, Liu B-H, Chou H-N, Chu FS (2002) Development of a Sensitive ELISA for the Determination of Microcystins in Algae. J Agric Food Chem 50:4176–4182. doi: 10.1021/jf0202483

66. Furey A, Crowley J, Hamilton B, Lehane M, James KJ. (2005) Strategies to avoid the mis-identification of anatoxin-a using mass spectrometry in the forensic investigation of acute neurotoxic poisoning. J Chromatogr A 1082:91–97.

67. Sano T, Takagi H, Nishikawa M, Kaya K (2008) NIES certified reference material for microcystins, hepatotoxic cyclic peptide toxins from cyanobacterial blooms in eutrophic water bodies. Anal Bioanal Chem 391:2005–2010. doi: 10.1007/s00216-008-2040-x

68. Backer LC, McNeel SV, Barber T, Kirkpatrick B, Williams C, Irvin M, Zhou Y, Johnson TB, Nierenberg K, Aubel M, LePrell R, Chapman A, Foss A, Corum S, Hill VR, Kieszak SM, Cheng Y-S. (2010) Recreational exposure to microcystins during algal blooms in two California lakes. Toxicon 55:909–921. doi: 10.1016/j.toxicon.2009.07.006

69. Harada K, Matsuura K, Suzuki M, Watanabe MF, Oishi S, Dahlem AM, Beasley VR, Carmichael WW. (1990) Isolation and characterization of the minor components associated with microcystins LR and RR in the cyanobacterium (blue-green algae). Toxicon 28:55–64. doi: 10.1016/0041-0101(90)90006-S

70. Snyder LR, Kirkland JJ, Dolan JW (2010) Introduction to modern liquid chromatography. John Wiley and Sons

71. Wood SA, Holland PT, Stirling DJ, Briggs LR, Sprosen J, Ruck JG, Wear RG. (2006) Survey of cyanotoxins in New Zealand water bodies between 2001 and 2004. New Zeal J Mar Fresh Research 40:585–597. doi: 10.1080/00288330.2006.9517447

72. Dell'Aversano C, Eaglesham GK, Quilliam MA (2004) Analysis of cyanobacterial toxins by hydrophilic interaction liquid chromatography–mass spectrometry. J Chromatogr A 1028:155–164. doi: 10.1016/j.chroma.2003.11.083

73. Wood SA, Rasmussen JP, Holland PT, Campbell R, Crowe ALM. (2007) First report of the cyanotoxin anatoxin-a from *Aphanizomenon issatschenkoi* (cyanobacteria). J Phycol 43:356–365.

74. Pietsch J, Fichtner S, Imhof L, Schmidt H, Brauch J. (2001) Simultaneous determination of cyanobacterial hepato-and neurotoxins in water samples by ion-pair supported enrichment and HPLC-ESI-MS-MS. Chromatographia 54:339–344. doi: 10.1007/BF02492680

75. Spoof L, Vesterkvist P, Lindholm T, Meriluoto J (2003) Screening for cyanobacterial hepatotoxins, microcystins and nodularin in environmental water samples by reversed-phase liquid chromatography-electrospray ionisation mass spectrometry. J Chromatogr A 1020:105–119.

76. Neffling M-R, Spoof L, Meriluoto J (2009) Rapid LC-MS detection of cyanobacterial hepatotoxins microcystins and nodularins--comparison of columns. Anal Chim Acta 653:234–241. doi: 10.1016/j.aca.2009.09.015

77. Van Berkel GJ, Asano KG (1994) Chemical Derivatization for Electrospray Ionization Mass Spectrometry. 2. Aromatic and Highly Conjugated Molecules. Anal Chem 66:2096–2102. doi: 10.1021/ac00085a027

78. Negri A, Stirling D, Quilliam M, Blackburn S, Bolch C, Burton I, Eaglesham G, Thomas K, Walter J, Willis R. (2003) Three novel hydroxybenzoate saxitoxin analogues isolated from the dinoflagellate Gymnodinium catenatum. Chem Res Toxicol 16:1029–1033. doi: 10.1021/tx034037j

79. Robertson A, Stirling D, Robillot C, Llewellyn L, Negri A. (2004) First report of saxitoxin in octopi. Toxicon 44:765–771. doi: 10.1016/j.toxicon.2004.08.015

80. Furey A, Crowley J, Shuilleabhain AN, Skulberg OM, James KJ. (2003) The first identification of the rare cyanobacterial toxin, homoanatoxin-a, in Ireland. Toxicon 41:297–303.

81. Bernard C, Harvey M, Briand JF, Biré R, Krys S, Fontaine JJ. (2003) Toxicological comparison of diverse Cylindrospermopsis raciborskii strains: Evidence of liver damage caused by a French C. raciborskii strain. Environ Toxicol 18:176–186. doi: 10.1002/tox.10112

82. Zotou A, Jefferies TM, Brough PA, Gallagher T (1993) Determination of anatoxin-a and homoanatoxin in blue—green algal extracts by high-performance liquid chromatography and gas chromatography—mass spectrometry. Analyst 118:753–758. doi: 10.1039/AN9931800753

83. Takino M, Daishima S, Yamaguchi K (1999) Analysis of anatoxin-a in freshwaters by automated on-line derivatization-liquid chromatography-electrospray mass spectrometry. J Chromatogr A 862:191–197.

84. Kimothi SK (2002) The Uncertainty of Measurements: Physical and Chemical Metrology : Impact and Analysis. Asq Press

85. ISO Guide 35:1989 - Certification of reference materials -- General and statistical principles. http://www.iso.org/iso/catalogue_detail.htm?csnumber=19741. Accessed 1 Mar 2013

86. Roper P, Burke S, Lawn R, Barwick V, Walker R. Chapter 1. Introduction. Applications of Reference Materials in Analytical Chemistry. RSC Publishing, Cambridge, pp 1–7

87. Seafood and Freshwater Toxins - CRC Press Book.

88. Lajeunesse A, Segura PA, Gélinas M, Hudon C, Thomas K, Quilliam MA, Gagnon C. (2012) Detection and confirmation of saxitoxin analogues in freshwater benthic Lyngbya wollei algae collected in the St. Lawrence River (Canada) by liquid chromatography–tandem mass spectrometry. J Chromatogr A 1219:93–103. doi: 10.1016/j.chroma.2011.10.092

89. Burton IW, Quilliam MA, Walter JA (2005) Quantitative 1H NMR with external standards: use in preparation of calibration solutions for algal toxins and other natural products. Anal Chem 77:3123–3131. doi: 10.1021/ac048385h

90. Aráoz R, Nghiêm H-O, Rippka R, Palibroda N, Tandeau de Marsac N, Herdman M. (2005) Neurotoxins in axenic oscillatorian cyanobacteria: coexistence of anatoxin-a and homoanatoxin-a determined by ligand-binding assay and GC/MS. Microbiol 151:1263–1273. doi: 10.1099/mic.0.27660-0

91. James KJ, Crowley J, Hamilton B, Lehane M, Skulberg O, Furey A. (2005) Anatoxins and degradation products, determined using hybrid quadrupole time-of-flight and quadrupole ion-trap mass spectrometry: forensic investigations of cyanobacterial neurotoxin poisoning. Rapid Commun Mass Spectrom 19:1167–1175. doi: 10.1002/rcm.1894

92. Skulberg OM, Skulberg R, Carmichael WW, Andersen RA, Matsunaga S, Moore RE. (1992) Investigations of a neurotoxic oscillatorialean strain (Cyanophyceae) and its toxin. Isolation and characterization of homoanatoxin-a. Environ Toxicol Chem 11:321–329. doi: 10.1002/etc.5620110306

93. Kozikowski BA, Burt TM, Tirey DA, Williams LE, Kuzmak BR, Stanton DT, Morand KL, Nelson SL. (2003) The Effect of Freeze/Thaw Cycles on the Stability of Compounds in DMSO. J Biomol Screen 8:210–215. doi: 10.1177/1087057103252618

94. ISO Guide 35:2006 - Reference materials — General and statistical principles for certification http://www.iso.org/iso/catalogue_detail.htm?csnumber=39269. Accessed 1 Mar 2013

95. Gros C, Labouesse B (1969) Study of the Dansylation Reaction of Amino Acids, Peptides and Proteins. Eur J Biochem 7:463–470. doi: 10.1111/j.1432-1033.1969.tb19632.x

96. Lawrence JF, Frei RW (1972) Fluorigenic labelling of carbamates using dansyl chloride : II. Fluorescence phenomena of the derivatives. J Chromatogr A 66:93–99. doi: 10.1016/S0021-9673(01)82932-0

97. Drinking-water Standards for New Zealand 2005 (Revised 2008). In: Ministry of Health. http://www.health.govt.nz/publication/drinking-water-standards-new-zealand-2005-revised-2008-0. Accessed 25 Aug 2012

98. McCarron P, Giddings SD, Miles CO, Quilliam MA (2011) Derivatization of azaspiracid biotoxins for analysis by liquid chromatography with fluorescence detection. J Chromatogr A 1218:8089–8096. doi: 10.1016/j.chroma.2011.09.017

99. Holmes-Farley SR, Whitesides GM (1986) Fluorescence properties of dansyl groups covalently bonded to the surface of oxidatively functionalized low-density polyethylene film. Langmuir 2:266–281. doi: 10.1021/la00069a002

100. Strauss UP, Vesnaver G (1975) Optical probes in polyelectrolyte studies. II. Fluorescence spectra of dansylated copolymers of maleic anhydride and alkyl vinyl ethers. J Phys Chem 79:2426–2429. doi: 10.1021/j100589a017

101. Barbosa J, Sanz-Nebot V, Toro I (1996) Solvatochromic parameter values and pH in acetonitrile-water mixtures optimization of mobile phase for the separation of peptides by high-performance liquid chromatography. J Chromatogr A 725:249–260. doi: 10.1016/0021-9673(95)00851-9

102. Barbosa J, Beltrán JL, Sanz-Nebot V (1994) Ionization constants of pH reference materials in acetonitrile—water mixtures up to 70% (w/w). Analytica Chimica Acta 288:271–278. doi: 10.1016/0003-2670(94)80140-1

103. Pan C-P, Barkley MD (2004) Conformational Effects on Tryptophan Fluorescence in Cyclic Hexapeptides. Biophys J 86:3828–3835. doi: 10.1529/biophysj.103.038901

104. Dietrich D, Hoeger S (2005) Guidance values for microcystins in water and cyanobacterial supplement products (blue-green algal supplements): a reasonable or misguided approach? Toxicol Appl Pharmacol 203:273–289. doi: 10.1016/j.taap.2004.09.005

105. May JC (2010) Regulatory Control of Freeze-Dried Products: Importance and Evaluation of Residual Moisture, Freeze Drying/Lyophilization of Pharmaceutical and Biological Products, Informa Healthcare. http://informahealthcare.com/doi/abs/10.3109/9781439825761.011. Accessed 28 Mar 2013

106. Mazur-Marzec H, Browarczyk-Matusiak G, Forycka K, Kobos J, Pliński. (2010) Morphological, genetic, chemical and ecophysiological characterisation of two Microcystis aeruginosa isolates from the Vistula Lagoon, southern Baltic. Oceanol Acta 52(1):127-146

107. Gibson CE (1975) Cyclomorphosis in natural populations of Oscillatoria redekei Van Goor. Freshwater Biol 5:279–286. doi: 10.1111/j.1365-2427.1975.tb00141.x

APPENDIX

$$U = k \cdot \bar{x} \cdot \sqrt{\left(\frac{SD_1}{x_1}\right)^2 + \left(\frac{SD_2}{x_2}\right)^2}$$

Equation.1: Calculation of uncertainty for RM-hATX, where k represents expansion factor (k = 2 in this case), $\bar{x}$ represents the average of analyses, and SD and x represent the standard deviations and averages of the two methods, respectively.